KONINKLIJK NEDERLANDS METEOROLOGISCH INSTITUUT

MEDEDELINGEN EN VERHANDELINGEN

No. 92

C. J. E. SCHUURMANS

THE INFLUENCE OF SOLAR FLARES ON THE TROPOSPHERIC CIRCULATION

(Statistical indications, tentative explanation and related anomalies of weather and climate in Western Europe)

1969

Prijs f. 19,00

STAATSDRUKKERIJ / 'S-GRAVENHAGE

THE INFLUENCE OF SOLAR FLARES ON THE TROPOSPHERIC CIRCULATION

(Statistical indications, tentative explanation and related anomalies of weather and climate in Western Europe)

KONINKLIJK NEDERLANDS METEOROLOGISCH INSTITUUT

MEDEDELINGEN EN VERHANDELINGEN

No. 92

C. J. E. SCHUURMANS

THE INFLUENCE OF SOLAR FLARES ON THE TROPOSPHERIC CIRCULATION

(Statistical indications, tentative explanation and related anomalies of weather and climate in Western Europe)

1969

STAATSDRUKKERIJ/'S-GRAVENHAGE

PUBLIKATIENUMMER K.N.M.I. 102-92

U.D.C.: 551.510.52:
551.513:
551.583.1:
551.590.21:
519.2:

PREFACE

The first essential for long-range forecasting of the behaviour of the atmosphere is to know which physical processes are involved and to what extent. One of the factors which is insufficiently understood is the influence of solar activity.

There has been for many years at the Royal Netherlands Meteorological Institute special interest in research into the influence of solar activity on the weather. In this connection particular mention can be made of the studies of Dr. S. W. VISSER and Dr. H. P. BERLAGE.

The present publication is the outcome of an investigation into the relation between the eruptions on the sun and the circulation in the upper air. The results are very interesting and present a new light on some of the earlier established solar-weather relationships. Moreover, the author has been succesful in deriving a theory, which offers a possible physical explanation of the way in which the influence of the sun is effected.

This study has been accepted also by the Faculty of Natural Sciences of the University of Utrecht as a thesis for the degree of doctor.

The Director in Chief of the

Royal Netherlands Meteorological Institute

M. W. F. SCHREGARDUS

VOORWOORD

Om het gedrag van de atmosfeer op lange termijn te kunnen voorspellen is het in de eerste plaats nodig om te weten welke fysische processen, en in welke mate, hierbij een rol spelen. Een van de factoren waarvan nog onvoldoende bekend is in hoeverre en op welke wijze hij van invloed is, is de activiteit van de zon.

Het onderzoek naar de invloed van de activiteit van de zon op het weer heeft op het K.N.M.I. reeds vele jaren in de belangstelling gestaan. In dit verband mogen worden genoemd de studies van Dr. S. W. VISSER en Dr. H. P. BERLAGE.

De publikatie die hier voor ons ligt is het resultaat van een onderzoek waarin verband wordt gezocht tussen uitbarstingen op de zon en de luchtstroming in de bovenlucht. De resultaten zijn bijzonder interessant en werpen een nieuw licht op enige reeds bekende zon-weer relaties. De auteur is er bovendien in geslaagd om uit de resultaten een theorie af te leiden die een mogelijke verklaring inhoudt van de wijze waarop de zonne-invloed tot stand komt.

Deze studie werd door de Faculteit der Wiskunde en Natuurwetenschappen van de Rijksuniversiteit te Utrecht aanvaard als dissertatie.

De Hoofddirecteur van het

Koninklijk Nederlands Meteorologisch Instituut

M. W. F. SCHREGARDUS

CONTENTS

page

11 I **Introduction**

11 1 The earth's atmosphere
11 2 Long-term weather anomalies and their possible cause

13 II **Solar activity as a cause of long-term weather anomalies**

13 1 Solar activity: essential features
14 2 Solar-weather relationships
15 3 Solar flares and their relation to upper-atmospheric phenomena
18 4 The search for the influence of solar flares on the troposphere and lower stratosphere

22 III **Statistical study of the tropospheric flare effect in the IGY/IGC period**

22 1 Short outline
24 2 Data: sources and handling
27 3 The height changes of the 500 mbar level after a solar flare
41 4 The vertical profile of height changes after a flare
43 5 Variations in height of pressure levels in the troposphere from 2 days before up to 5 days after a flare
47 6 Temperature changes related to the height changes after a solar flare
49 7 Dependence of the tropospheric flare effect on the initial atmospheric conditions

55 IV **A chain of events offering a possible explanation of the tropospheric flare effect**

55 1 The causing agent: corpuscular radiation rather than UV-radiation
62 2 The possible interaction between energetic solar protons and ozone in the lower stratosphere
78 3 Radiational temperature changes due to ozone removal in the lower stratosphere, especially during moist and cloudy conditions in the upper troposphere
83 4 Model of a heat sink at the tropopause as a possible explanation of the observed height changes in the troposphere

10

91 V **The tropospheric flare effect as a possible factor in the occurrence of long-term weather anomalies**

91 1 The flare effect in an individual case

93 2 Increased frequency of meridional circulation types over Western Europe as a result of the flare effect

100 3 Some indications of a relationship between the yearly amplitude and the month-to-month persistence of monthly mean temperatures at De Bilt and sunspot variability

107 4 The 80-90 year period in sunspot variability and its related climatic cycle

113 **Summary**

119 **References**

I. INTRODUCTION

I.1 The earth's atmosphere

At a mean distance of 150.000.000 km our planet Earth is continuously irradiated by the sun at a rate of 1,400 J/m^2 sec. Nevertheless the earth is able to retain an atmosphere of appreciable depth, due to its comparatively high escape velocity. Atmospheric pressure, which measures about 1000 mbar at the earth's surface decreases gradually upward, thus balancing the earth's gravity. So far the earth's atmosphere is a system at rest.

However, two external forces, related to the earth's rotation and to the differential heating of the earth's surface by the sun, are at work on this system. These forces keep the atmosphere in motion against the fricitional dissipation of energy, particularly at the surface. In the ideal hypothesis of a globe with a smooth, homogeneous surface and with no lateral differences in atmospheric properties, atmospheric movement would be quite regular, the mode of circulation depending only on the ratio of the two external forces. In fact, however, the circulation is far from systematic.

On a small scale the moving system is severely disturbed by radiational and thermodynamic processes, which are brought about by the properties of some of the constituent gases of the atmosphere. Another important source of disturbance is found in the interaction of the moving air with the earth's surface, mainly through friction and the exchange of sensible heat. Most sources and sinks of heat of the nature just discussed are randomly distributed and may cover a wide range of scales in area and time. Each of them causes horizontal and vertical pressure gradients and gives rise to a characteristic scale of motion. Movements on different scales interact with each other and with the global circulation in an often very complex manner.

The complexity of the synoptic circulation pattern, as discussed above, gives way to a much simpler pattern when the flow is averaged over a period of time. However, long-period averages still reveal substantial deviations from symmetry, which are obviously attributable to the topography of the earth's surface and the distribution of land and sea.

I.2 Long-term weather anomalies and their possible cause

In view of the foregoing considerations, it is not surprising that a wide range of weather conditions occur in our atmosphere. The question arises whether the observed deviations of the weather from normal (long-term average) are not merely the variations to be expected from the random occurrence of variations of shorter period. An answer to this crucial question has been given by CRADDOCK (1957), who was able to demonstrate that the contribution to the variance in temperature and pressure by variations over periods longer than 30 days is greater than could be expected on statistical grounds. His findings strongly suggest that longterm weather anomalies

such as the cold winters and wet summers in middle latitudes require an explanation which is not to be found in the occurrence of short spells of cold or wet weather.

In the search for causes of long-term weather anomalies one is restricted formally to the following categories:

1 irregular extra-terrestrial effects such as solar activity and variations in cosmic radiation;

2 interactions with the atmospheric environment; conditions at or near the earth's surface especially, may change according to the frequency of volcanic eruptions, slowly moving currents in the deep ocean and the area covered by ice and snow;

3 internal mechanisms of the atmosphere; this category of causes assumes the conditions at the upper boundary as well as at the surface or lower boundary to be constant; any weather anomalies occurring are simply to be considered as members of a large family of circulation modes, which the atmosphere is able to sustain under the influence of one and the same stimulus.

At the present time the relative importance of the three contributory factors is still virtually unknown.

By investigating the possible influence of the sun's activity on earth's weather, this publication will try to make a contribution to the solution of this difficult problem. At the end of the next chapter the aim of this study will be described more precisely.

II. SOLAR ACTIVITY AS A CAUSE OF LONG-TERM WEATHER ANOMALIES

II.1 Solar activity: essential features

Solar activity is the collective name for all features related to the appearance and disappearance of large magnetic fields at the solar surface. The best-known features of inconstant behaviour of the sun are the sunspots. The number of spots is highly variable, but their individual appearance and mean location on the solar disc also vary with time. Variations in sunspot frequency show a periodicity of about 11 years. A long-term period of 80-90 years has also been established.

In modern times a large number of additional activity phenomena have been discovered, most of them only observable by refined instrumental techniques. One of these newly explored features is the explosion-like phenomenon called solar flare; flares are only rarely observable in the visible part of the spectrum.

During the past few decades heliophysicists have devoted much time to investigating the coherence between the different solar phenomena. As an indication of the coherence the term "active region" has found acceptance. In such a region, chromospheric flare outbursts may occur, coronal radiation may enhance, while in the photosphere the center of activity is characterized by the development of one or more dark spots surrounded by bright areas, called photospheric faculae. In fact all layers of the solar atmosphere take part in the activity phenomenon, of which the origin is to be sought in the circulation of the deeper layers.

The regions just below the visible photosphere (down to about 10^5 km) are not in radiative equilibrium; energy transfer taking place to a large extent by convective motion. Partial suppression of this convection by local disturbances of the solar magnetic field is the most plausible explanation of the relatively dark appearance of sunspots. Apart from that, the solar magnetic field is believed to play an extremely important role in the whole complex of solar activity. As a matter of fact, the 11-year cycle referred to above may be considered as exactly half the physical solar activity cycle because of the reversal of the polarity of sunspot group magnetic fields between alternate sunspot maxima.

The lifetime of the active regions varies from a few days to several months. The regions usually show a fairly regular sequence of growth, maximum and decline. Their motion is determined to a large extent by the rate of rotation of the sun, which is highest at the equator (rotation period about 27 days) with uniform diminution towards the poles.

In considering the sun's activity from the point of view of energy release, it is interesting to note that by far the greatest variability is found in the extremities of the spectrum, i.e. the far ultraviolet and X-ray part and, at the other end, the region of radio waves. Opinions are still divided regarding the variability in the visible part of

the spectrum. Apart from those in the electro-magnetic radiation, large variations occur in the corpuscular radiation of the sun. These variations range from a more or less regular fluctuation of the continuous particle stream, called solar wind, which consists of low energy protons and electrons (with proton energies up to 10 keV), to the sudden releases of very energetic particles to hundreds of MeV and on occasions even to 10 GeV during solar flare outbursts.

Estimates of the total amount of energy contained in these sudden releases reveal that the energetic importance of solar activity as a producer of energy is slight compared with the sun's normal energy output (ELLISON, 1963). In spite of this now commonly known fact, much effort is still being made to show that solar activity is connected with our weather and climate.

II.2 Solar-weather relationships

The search for solar-weather relationships began less than half a century after GALILEO'S first instrumental observation of sunspots in 1610. Scientists at that time must have suspected intuitively that the sun's radiation constituted the ultimate driving force of all atmospheric motion; and having no explanation for the large variability in weather and climate, they understandably tried to attribute these changes to sunspot variations. Unfortunately, in these early days instrumental records of weather elements did not exist and consequently their work was confined to mere speculation.

In a later age, when observational data were gradually being amassed, an extensive study was made of the statistical correlation between mean temperatures or amounts of precipitation at a particular location and sunspot frequency. On some occasions rather high correlation coefficients happened to appear which, during the first half of this century, created some optimism among meteorologists as to the existence and usefulness of solar-weather relationships (VISSER, 1946). Unfortunately, for some reason, these high correlations were not normally found to persist when observational data of later years were incorporated. Some correlations were even found to change from a plus value to a minus, or vice versa. It was this that made meteorologists wary of the subject of the influence of solar activity on the weather. A recent article by LAWRENCE (1965), in which he postulates that solar-weather relationships are subject to changes according to the amplitude of the sunspot cycle will probably not alter the situation very much.

So in spite of the more optimistic views on the subject in earlier times, C. W. ALLEN in the 10th Report on Solar-Terrestrial Relations (1964) felt it necessary to state that "at present no widespread conclusions about solar activity influences on the bottom layers of the earth's atmosphere are generally accepted". However, ALLEN ends his review with the remark that "the matter cannot be considered to be fully explored". The challenge of the problem therefore remains.

II.3 Solar flares and their relation to upper-atmospheric phenomena

The strong solar flare stands out among the various manifestations of solar activity as a spectacular, clearly distinguishable and well-defined phenomenon. For other reasons too, these flare outbursts may be considered as a promising parameter in solar-weather research. In the first place it is known that flare radiation — both the ultraviolet or X-ray part and the corpuscular part — greatly affects the structure and properties of the uppermost layers of the atmosphere. Secondly, solar physicists maintain an almost continuous watch on solar flares.

Solar flares are sometimes called chromospheric eruptions, a name indicating their explosive nature and location of origin. Flares are only rarely visible in white light

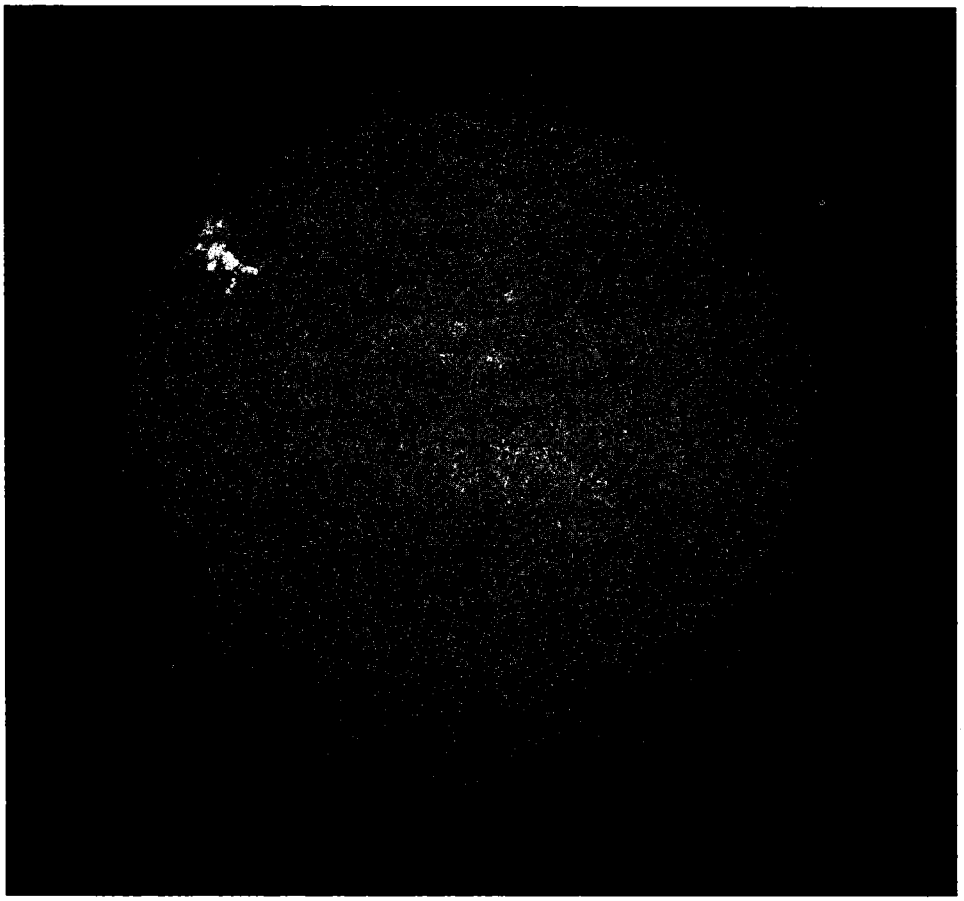

Fig. 1 Photograph of solar flare outburst on June 1, 1960, taken with the Lyot-filter (Hα-filter with $\Delta\lambda = 0.75$ Å) of the Utrecht Observatory. The photograph was taken approximately at the time of the maximum of the flare.

and are best observed in the spectral lines of hydrogen or calcium. (Hα = 6563 Å, Ca II (H) = 3934 Å, Ca II (K) = 3968 Å). Figure 1 shows a picture of the flare of June 1, 1960, taken with a Hα filter, at the Utrecht Observatory. One of the common characteristics of flares is their sudden increase to maximum brightness, mostly within a few minutes, followed by a gradual decline to normal light intensity.

Flares differ largely in the level of maximum brightness, the area covered and their duration. According to these differences the classification used before 1966 was into three groups of importance, namely 1 (lowest), 2 and 3. Subdivisions of these groups are indicated by + following the number.

Active flares are mainly those of importance 2^+ or higher, which means that they cover a portion of the visible solar disk of more than 10^{-3} and have a duration of over half an hour.

Solar flares, especially the stronger ones which we are considering here, are accompanied by several phenomena both in the solar atmosphere and at the fringe of the earth's atmosphere. A few of these phenomena are the activation of certain types of prominence and the occurrence of radio bursts in the solar atmosphere, while in the high atmospheric layers and magnetosphere of the earth the sudden ionospheric disturbances and geomagnetic storms have long been attributed to certain energy releases in solar flares.

In recent decades our knowledge about the energy release in flares has grown enormously, both through the heliophysical and geophysical studies concerning flare phenomena, and in later years by direct observations of the flare radiation in extraterrestrial space. A full account of the present state of knowledge about solar flares has recently been given by H. and E. SMITH (1963). We shall not dwell on the subject as a whole, but confine ourselves to summarizing the aspects which are pertinent to our study.

Generally speaking, earlier views on the subject have been confirmed in that it has been shown that most of the stronger flares emit wave radiation as well as particle radiation. More interesting, however, are the details which have become available about both types of radiation. During flares augmentation of wave radiation occurs over practically all wave lengths of the spectrum from the short wave length X-rays through the long radio waves. In the X-ray region strong emission has been observed in the 1—10 Å band, which penetrates the earth's atmosphere to a height of about 70 km. The augmentation in the far ultraviolet region, where the Lyman-α (1215 Å) is the most important emission line, is found to be of the order of less than 10% of the non-flare level. The increased D-region ionisation (ionized portion of the earth's atmosphere below 80 km) which gives rise to certain anomalies in radio wave transmission and reflection, referred to as sudden ionospheric disturbances (SID), is at present generally attributed to the excess X-ray flux, in spite of the fact that the normal D-region ionisation is caused primarily by Lyman-α radiation.

The sudden ionospheric disturbances are mostly confined to the sunlit portion of the earth. Forced induction currents are believed to flow owing to the sudden increase in electric conductivity of the sunlit part of the ionosphere. These currents cause variations of the geomagnetic field, which are known as the geomagnetic solar flare effect.

Little is known about the flare's emission in the near-ultraviolet region (1700—3000 Å). One of the principal absorbers in this spectral region is atmospheric ozone. In the literature many constructive suggestions have been made on the possible role of ozone as an intermediary agent between the supposed excessive UV-radiation of flares and the circulation of the lower atmospheric layers. Apart from the slight influence of ozone-layer heating on the pressure distribution at ground level (WEXLER, 1950), it still remains uncertain to what extent the UV-radiation during flares is augmented.

During flares the augmentation of the visible part of the solar spectrum is known to be very small. On the basis of the intensity increase of the emission lines and of the continuum (for strong flares the Hα intensity increase amounts to a factor of about 2), ELLISON (1963) has given an estimate of the total wave energy released by a strong flare. This value, 1.3×10^{25} J, is about 1/30 of the total radiant energy emitted by the sun in 1 second.

Finally, the radio-wave emission accompanying flares, although unimportant in connection with the earth's atmosphere, is found to provide a very rich source of information on the flares' corpuscular emission.

The information is such as to offer very stringent conditions for a "radio"-flare to cause the ejection of particles in a certain energy range. Leaving the matter at this point and turning to the question of the flares' particle radiation, we find that it covers a very wide range of energies, at least from energies less than 10 keV up to relativistic energies of more than 10^3 MeV. Usually this wide range of energies is subdivided into 3 classes, according to the observed effects in the earth's neighbourhood. The first class are particles, generally moving as clouds of plasma, with a velocity of the order of 1000 km/s. The plasma consist mainly of protons and electrons, their respective energies being of the order of 10 keV and 10 eV. The incidence of these clouds on the earth's magnetosphere gives rise to geomagnetic storms about 1 day after the occurrence of the flare. Associated with these geomagnetic storms decreases of 1—10% sometimes occur in the ground-level cosmic radiation intensity. The latter effect is known as a Forbush-decrease. Furthermore, the arrival of the plasma cloud by some still unknown mechanism gives rise to the precipitation of electrons into the high atmospheric layers. The interactions of these electrons with the atmospheric constituents cause the well-known auroras. Although auroral phenomena may occur at all levels between 80 and 600 km, they are mainly confined to those between 100 and 200 km.

A second class of particles released during solar flare outbursts is formed by the

streams of fast-moving corpuscules (mainly protons) which reach the earth in a few hours. The energies of these protons range from about 1—10^3 MeV. Because of their extremely low density these particles do not disturb the geomagnetic field, but each particle follows a Störmerian orbit along a magnetic field line. According to Störmerian theory, which will not be treated here, the geomagnetic latitude at which the particles penetrate the earth's atmosphere depends on their kinetic energy. The cut-off latitude, being the latitude nearest to the equator at which a charged particle can penetrate the earth's atmosphere, lies, for protons, in the specified energy range generally poleward of 55° geomagnetic latitude. In this region, the so-called polar cap, the protons penetrate the atmosphere to a level between 15 and 50 km above the earth's surface. At this level the protons cause strong ionisation of the air. Both the penetrating protons themselves and the intense low-altitude ionisation have been observed quite frequently. The absorption of radio waves to which the low-altitude ionisation gives rise is known as Polar Cap Absorption. A detailed description of this phenomenon is given by BAILEY (1964), who was actually the first to discover it.

The third class, the high energy solar particles, consist of protons of relativistic energies. These particles, which are called solar cosmic rays, reach the earth's surface, especially at the higher geomagnetic latitudes, in about 10 minutes after the start of the flare. Flares which produce relativistic protons are rather rare; only a dozen cases were observed during the last two sunspot cycles (1944—1964).

II.4 The search for the influence of solar flares on the troposphere and lower stratosphere

In the present state of knowledge concerning the interactions between the upper and lower layers of the atmosphere, it is difficult to infer any solar flare influence on the lower atmospheric layers from the known influence op the top layers. Unfortunately, this applies even more if one inquires into the effects of the specific flare radiations which enter our atmosphere. We know that the excess ultraviolet radiation is probably absorbed by the ozone layer, mainly at the sub-polar point, but our knowledge of the interaction of particles — ranging in energy from the slow-moving auroral particles to the very fast-moving solar cosmic ray particles — with the atmospheric constituents is extremely poor.

In view of this a number of people have attacked the problem through a statistical study; thus a large sample of flares was selected and their mean after-effects in the atmosphere were investigated. Notable contributions on the subject have been made by DUELL and DUELL (1948), VALNÍČEK (1952, 1953), NORDØ (1953), PALMER (1953), ATTMANNSPACHER (1955), HARTMANN (1963), KUBISHKIN (1966), TAKAHASHI (1966) and STOLOV and SPAR (1968). Others who have studied the subject are SHAPIRO (1956), RIEHL (1956), ROBERTS and MACDONALD (1960), TWITCHELL (1963), WILLETT and PROHASKA (1964), GNEVYSHEW and SAZONOV (1964), MUSTEL (1966) and BAUR (1967).

The above publications have been divided into two groups according to their approach to the problem. In selecting a sample of flares for studying their possible effect on the lower atmosphere, the first group considers the flare outburst itself to be indicative of the flare event, while the second group considers the flare event to be characterized by the occurrence of geomagnetic disturbances or auroras, which usually follow a flare. Although it may be argued that the latter procedure is preferable since it starts from the prior existence of a solar influence on the earth's atmosphere, this approach also has a serious disadvantage, namely the difficulty in the interpretation of the results. In general, geomagnetic disturbances are not attributable exclusively to extra-terrestrial influences, and consequently a statistical relationship between geomagnetic disturbances and some weather element does not necessarily imply that the weather element is influenced by extra-terrestrial factors.

For this reason we shall only consider here the results of the studies of the first group, in which the flare event is defined purely by the observation of the flare outburst itself. Since these studies differ greatly in their characteristics (number of flares, atmospheric parameter, geographical extent, etc.) a general conclusion cannot be drawn from them. Moreover, in only two of these studies (NORDØ (1953), STOLOV and SPAR (1968)) have the necessary statistical checks been made. The characteristics and the results of the various studies are summarized in Table I.

In the present study the influence of solar activity on the lower layers of the earth's atmosphere has also been investigated by means of a statistical method. For reasons already given in the review chapter the observation of a strong solar flare has been chosen as an index of solar activity.

The statistical study is based upon a sample of 81 flares, which all occurred during the period July 1957 through December 1959 (IGY/IGC-period). The investigation concerns the response to solar flares of contour heights of several constant pressure levels between the ground and the 50 mbar level. For one level (500 mbar), the investigation covers the whole northern hemisphere north of 10° N and the southern hemisphere south of 20° S. A description of the results and the statistical check is given in Chapter III. Part of the results have been published already in a separate paper (SCHUURMANS and OORT, 1969).

In Chapter IV a physical theory is presented, which makes it possible to give a quantitative explanation of the influence of solar flares on the tropospheric circulation.

Finally, in Chapter V, an estimate is given of the importance of the tropospheric flare effect on the weather and climate in Western Europe.

TABLE I.

author	No. of flares	period	atmospheric parameter	geographical region	results
DUELL and DUELL (1948)	51	1936—41	500 mbar heights	European-Atlantic region between 45°—60°N and 5°W—25°E	mean height rise of the 500 mbar level (max. +1 gpdm over the North Sea and adjacent areas) from the day before the flare to the day of the outburst.
DUELL and DUELL (1948)	51	1936—41	sea level pressure	3 stations in Central Europe	maximum of interdiurnal pressure change between 2—4 days after a flare; maximum of pressure itself 4—6 days after a flare.
VALNÍČEK (1952)	69	1936 (33) 1947 (36)	pressure and temperature at ground level	Eastern Atlantic and Europe	SE-ward displacement of the polar front, 2—5 days after a flare, displacement being accompanied by a change in circulation regime from zonal to meridional.
VALNÍČEK (1953)	53	1949—50	500 mbar heights	Eastern Atlantic and Europe	mean height rise of the 500 mbar level (max. + 5 gpdm over North Sea-southern Scandinavia) between the fifth day before the flare to the day of the flare outburst.
NORDØ (1953)	115	July 1935 — June 1952	sea level pressure	Oslo (Norway)	significantly positive 24-hour pressure tendencies during the first day after strong isolated flares, occurring in winter at night time. (in NORDØ's opinion the evidence is not convincing).
PALMER (1953)	?	March through May 1951	temperatures in the lower stratosphere	equatorial regions (Marshall Islands)	temperature rise of about 7 °C per day at a level close to the tropopause, with a delay of less than 36 hours after a flare.

ATTMANNSPACHER (1955)	30	Jan. 1951 — June 1952	temperature at 96, 41 and 15 mbar	Berlin	temperature rise during the first 24 hours after a flare of the order of 1 °C, increasing with increasing height of the pressure level.
HARTMANN (1963)	1	June 1, 1960	temperature of the 500 mbar level	whole northern hemisphere	temperature rise (area-mean of the hemisphere) of 4 °C from June 1 to June 2.
KUBISHKIN (1966)	41	1956—61	ground level pressure	94 northern hemisphere stations (43 in USSR) and 9 stations in Angola (Africa)	pressure reaches an extreme on the third to fourth day after a flare, the sign of the extreme depending on the location of the station.
TAKAHASHI (1966)	54	1957—63	amount and frequency of occurrence of precipitation	5 Japanese stations	increase of precipitation on the day of the flare outburst.
STOLOV and SPAR (1968)	41*	1956—61	ground level pressure	31 stations in North America	no statistical significant pressure departures following the flares.

* KUBISHKIN's list of flares.

III. STATISTICAL STUDY OF THE TROPOSPHERIC FLARE EFFECT IN THE IGY/IGC-PERIOD

III.1 Short outline

This study starts from the assumption that a solar flare alters the height of the constant pressure levels in the troposphere and lower stratosphere. The heights H of the 500 mbar level over the northern hemisphere (north of 10° N) have therefore been investigated. The height of a given pressure level (say, 500 mbar) at a given location P is subject to variations of both a regular and an irregular nature. The former are the diurnal and annual variations, due to diurnal and annual variations in solar insolation. The irregular variations are caused by the passage of synoptic circulation patterns, ridges of high pressure and troughs of low pressure embedded in the main zonal airflow. At the approach of a ridge the pressure levels will rise for a few days, while in the rear of the ridge and in front of the trough the levels will fall. The rise or fall in an interval of, say, 24 hours may be large compared with the annual height variation and will usually far exceed the diurnal height variation.

In the following we shall study the height changes due to irregular variations for a fixed interval of 24 hours. At most of the aerological stations observations are made every 12 hours, at 00h and 12h GMT, but for the present purpose an interval of 24 hours was selected in order to eliminate the effect of the diurnal variation. The 24-hour height changes are denoted by ΔH.

In view of the nature of the irregular height variations we may expect that the mean $\mu = \varepsilon(\Delta H)$ of a very large number (i.e. the population) of ΔH's, well distributed over the year (ΔH relating to a certain pressure level at a certain location) will be zero. If, however, a systematic effect is superimposed upon the ΔH's, due perhaps to the (still hypothetical) influence of solar flares, then by averaging over a large number of ΔH's, the $\overline{\Delta H}$ will be essentially different from zero.

Solar flares occur at random intervals and their duration ranges between a fraction of an hour and several hours. Their influence on the height of pressure levels, if it exists at all, will be caused through the intermediary of excess ultraviolet radiation or of very energetic particle radiation, the latter being the more likely, as we shall see later. Therefore, the search for an effect superimposed upon the normal ΔH's may be restricted to a short time interval (say, a day or so) after the flare. As an arbitrary choice we have undertaken the study of the $\Delta H_{n=1}$ (see Fig. 2), being the difference in height between the first aerological observation after a flare and the observation made 24 hours earlier.

Thus $\Delta H_{n=1} = H(t_1) - H(t_1 - 24h)$, where t_1 is the moment of the first aerological observation after a flare.

A brief description of the method of analysis is given below. First we selected a sample of flares (see next section). The time of maximum brightness is known for

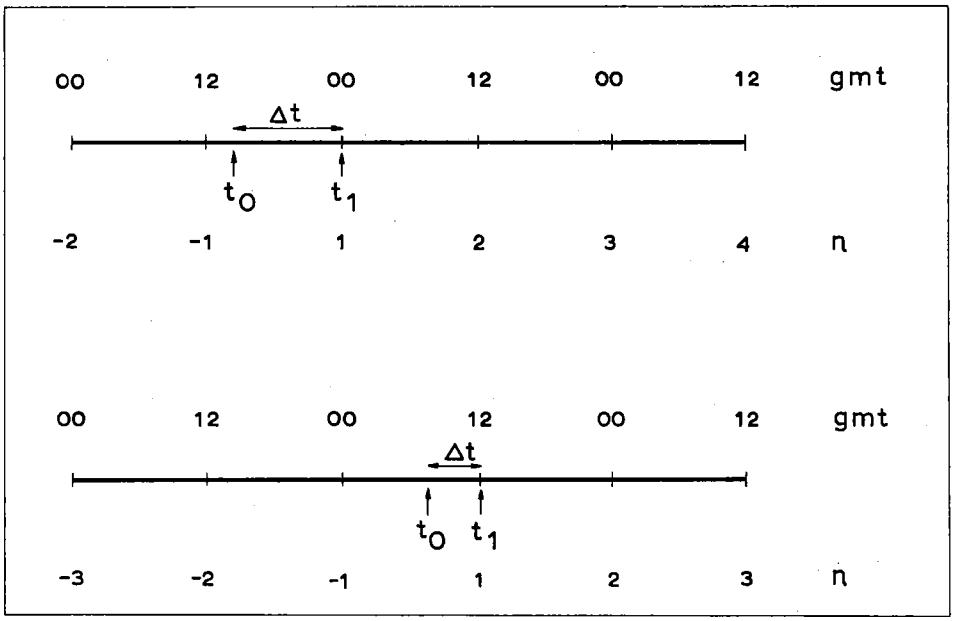

Fig. 2 Time axis illustrating the analysing method. The moment of flare maximum is denoted by t_0; the moment of the first aerological observation thereafter by t_1. The numbering of successive aerological observations before or after the flare is indicated by n.

each flare; this moment is denoted by t_0. Then the date and time of the first aerological observation after t_0 are indicated for each flare. This results in a list of t_1's on the basis of which the $\Delta H_{n=1}$'s have been calculated. This may be done for any point in the (x, y, p)-space for which height data are available. Having a sample of N flares available, one thus gets a series of N $\Delta H_{n=1}$'s for that particular point. This series of N values of $\Delta H_{n=1}$ may be averaged to give $\overline{\Delta H}_{n=1}$.

We intended to give a description of $\overline{\Delta H}_{n=1}$ as a function of (x, y, p). The following maps and cross-section were constructed for the purpose:

a a horizontal hemispheric map of $\overline{\Delta H}_{n=1}(x, y)$ at 500 mbar for the northern and southern hemispheres separately;

b a vertical cross-section versus longitude of $\overline{\Delta H}_{n=1}(x, p)$ along the Atlantic sector of roughly the 60 °N parallel.

In order to get an idea about the variation in time of $\overline{\Delta H}$ at a certain point, we also constructed a cross-section of $\overline{\Delta H}(p, t)$ for one aerological ocean station, namely Ship B. This was done by calculating the 24-hour height change at succesive steps of 12 hours after and also before t_1. For the time of 12 hours after t_1, this

moment being the second aerological observation after the flare, $\overline{\Delta H}$, which again refers to a 24 hours change, is denoted by $\overline{\Delta H}_{n=2}$; 24 hours after t_1 gives $\overline{\Delta H}_{n=3}$ etc.

The horizontal map covers the northern hemisphere north of 10° N. The cross-sections extend vertically from the ground up to the 50 mbar level. The cross-section versus time ranges from an average of 54 hours before the flare ($n = -5$) up to 54 hours after the flare ($n = +5$).

In addition to the computation of the mean height changes $\overline{\Delta H}$, the 24 hour temperature changes $\overline{\Delta T}(p)$ for $n = 1$ were computed at a few stations. Despite the fact that the height of a constant pressure level is related to the vertical temperature distribution through the hydrostatic equation, a separate study of the temperature changes is not superfluous, since temperature is a more directly measured element than height. The coherence between the 24 hour height change ΔH of the pressure levels p_1 and p_2 and the change in (virtual) temperature, ΔT, of the layer between is given by the following formula:

$$\Delta H_1 - \Delta H_2 = \frac{R}{g} (ln\, p_2 - ln\, p_1)\, \Delta T_{12}$$

where R = gas constant of dry air and g = acceleration of gravity. The reason why the study as a whole was not based on temperature changes instead of on height changes, is merely that changes in the circulation pattern are more readily inferred from height (i.e. pressure) distributions than from temperature distributions. Finally, the possible dependence of the occurrence of a tropospheric flare effect on the initial atmospheric conditions was investigated.

A large part of this chapter is devoted to the statistical checking of the results. Since we selected a statistical approach (for reasons expressed in II.4) to studying the possible influence of solar flares on the tropospheric circulation, this matter requires the fullest attention here. In some relevant cases we compared our results with those of other statistical studies summarized in Table I.

III.2 Data: sources and handling

The sample of solar flares used in this investigation was selected from the IGY Solar Activity Report Series Nos. 15 and 17 (High Altitude Observatory, Boulder, Colorado).

The selection was made on the basis of the following criteria:

1 the importance of the flare should be classified as 2^+ or higher (the scale of flare importance runs from 1^- up to 3^+);

2 the flare should be isolated from others of a similar importance by at least 48 hours.

The first criterion was chosen because only intense flares are generally followed

by important geomagnetic disturbances and other effects in the high atmosphere. The second criterion was a compromise between the necessity of avoiding overlapping and the statistical necessity of including as many flares as possible.*

In the period July 1957 through December 1959, 81 flares qualified in accordance with the criteria stated above; a complete list of the flare sample, together with some of their characteristics, is presented in Table II.

The average time interval Δt between the moment of maximum brightness of the flare t_0 and the time of the first aerological observation after the flare t_1 (taken as occurring at exactly 00 or 12h GMT) in this sample is 5h53m. This means that the epoch $n = 1$, defined above as the first aerological observation after the flare has an average value of nearly 6 hours after the flare.

The values of the atmospheric parameters (height and temperature) of several constant pressure levels used in this study were obtained from the following sources:

A Northern Hemisphere Grid Point Data, National Weather Records Center, U.S. Weather Bureau;**

B Northern Hemisphere Data Tabulations, Daily Series, Part II, U.S. Weather Bureau;

C Daily Aerological Record, Meteorological Office, London;

D Southern Hemisphere Maps and Data, Notos South African Weather Bureau.

From the first source the 500 mbar height data for the northern hemisphere have been used. The grid is diamond shaped with a total number of 1020 grid points, north of approximately 10° N.

All data north of 35° N (425 grid points) were used, while a selection of 104 points was made from the remaining points south of 35° N. The average distance between grid points north of 35° N is of the order of 500 km and of 1000 km in the latitude belt 10° —35° N. The smoothing effect of using grid point data from analysed maps as compared with station values proved to be negligible, as will be shown later on.

For the construction of the vertical cross-section of the height tendencies (and temperature changes) we used data from the sources B and C at the pressure levels 1000, 850, 700, 500, 400, 300, 250, 200, 150, 100 and 50 mbar.

The southern hemisphere 500 mbar grid point height data were taken from source D. The grid is determined by the normal geographic network. Height values are given at every 5th degree of latitude from 20° S onwards up to 65° S at 36 grid points (10 degrees of longitude apart); poleward of 65° they are given at a gradually diminishing number of grid points per latitude circle.

In our investigation we only used height data of grid points on the 20°, 30°, 40° etc. to 90° S latitude circles. Thus a total number of 217 grid points was used. Since the

* Criterion (2) reduces the number of flares available by a factor of about 2/3.

** The grid point data were kindly supplied to us by G. P. Cressman of the U.S. Weather Bureau.

TABLE II. *The flare sample*

No.	$t(n=1)$	Δt	I
	1957		
1	3 July, 12	4 15	3
2	22 July, 12	2 05	3
3	25 July, 00	5 33	2+
4	29 July, 00	9 58	2+
5*	1 Sept., 00	10 48	3
		3 20	2+
6	4 Sept., 00	9 32	3
7	6 Sept., 00	2 35	3
8	15 Sept., 12	7 32	2+
9	23 Sept., 00	3 52	3
10	27 Sept., 00	4 08	3
11	1 Oct., 00	6 55	3
12	6 Oct., 00	11 05	2+
13	13 Oct., 12	6 21	2+
14	16 Oct., 12	10 08	3
15	23 Oct., 12	5 32	3
16	10 Nov., 12	5 39	2+
17	29 Nov., 12	9 47	3+
18	13 Dec., 00	5 54	2+
19	15 Dec., 00	11 10	3
20	19 Dec., 12	3 59	2+
21	22 Dec., 00	1 09	3
	1958		
22	16 Jan., 00	7 18	3
23	25 Jan., 12	2 00	3
		1 53	3
24	1 Feb., 00	11 36	2+
25	11 Feb., 12	3 37	2+
26	1 Mar., 12	2 43	3
27	3 Mar., 12	1 40	3
28	5 Mar., 12	6 20	3
		5 51	3
29	7 Mar., 12	10 45	3
30	15 Mar., 00	8 53	2+
		1 56	3+
31	23 Mar., 12	1 50	3+
		1 42	2+
32	25 Mar., 12	6 30	2+
		5 57	2+
33	28 Mar., 00	2 03	2+
34	5 May, 12	7 45	2+
35	4 June, 00	8 48	2+
36	15 June, 12	11 31	2+
37	26 June, 12	8 53	2+
38	7 July, 12	10 47	3
39	11 July, 12	3 28	2+
40	20 July, 00	4 52	2+

TABLE II. *The flare sample (continued)*

No.	$t(n=1)$	Δt	I
	1958 (continued)		
41	4 Aug., 12	7 25	3
42	8 Aug., 00	8 52	3+
43	16 Aug., 12	7 21	3
44	20 Aug., 12	11 16	2+
45	23 Aug., 00	8 54	3
		1 11	2+
46	26 Aug., 12	11 33	3+
47	3 Sept., 00	2 55	2+
48	8 Sept., 00	9 10	2+
49	18 Sept., 12	3 35	2+
50	15 Oct., 12	11 53	3
51	22 Oct., 00	0 30	2+
	25 Oct., 00	9 10	2+
52		8 59	2+
53	25 Nov., 00	5 39	3
54	3 Dec., 12	4 55	2+
55	12 Dec., 00	2 10	2+
56	23 Dec., 00	8 48	2+
	1959		
57	1 Jan., 00	6 57	3
58	15 Jan., 00	9 50	2+
59	22 Jan., 00	6 51	3
60	9 Feb., 12	2 05	2+
61	13 Feb., 00	0 35	3
62	19 Mar., 12	1 17	2+
63	24 Mar., 12	4 23	2+
		1 45	3
64	29 Mar., 00	2 34	3
65	8 Apr., 12	2 40	3
66	10 Apr., 12	1 20	2+
67	9 May, 00	1 09	2+
68	17 May, 12	6 33	2+
69	3 June, 00	5 36	2+
70	12 June, 12	3 30	2+
71	18 June, 12	0 15	3+
72	10 July, 12	9 30	3+
73	17 July, 00	7 44	3
		2 28	3+
74	28 July, 00	2 45	3
75	30 July, 00	2 40	2+
76	19 Aug., 00	13 30	3
		6 35	2+
77	25 Aug., 00	1 20	2+
78	17 Nov., 12	11 12	2+
79	26 Nov., 12	2 23	2+
80	5 Dec., 00	5 37	2+
81	10 Dec., 12	6 42	2+

$t(n=1)$ Date and time (GMT) of the first aerological observation after the flare.
Δt Time interval (in hours and minutes) between the moment of maximum brightness of the flare and $t(n=1)$.
I Importance of the flare.

* Flares occurring in the same 12-hour interval between two successive aerological observations have been treated as one flare case; however, the individual characteristics (Δt, I) are indicated for each flare separately.

height data for certain large areas of the southern hemisphere are not very reliable (TALJAARD and VAN LOON (1964)) we do not believe that the use of a denser grid would have added much to the significance of the results. For the southern hemisphere 500 mbar height data were only available for the period July 1957 through December 1958.

Computations and analysis in this investigation have been done partly by computer.*

III.3 The height changes of the 500 mbar level after a solar flare

III.3.1 For the sample of 81 flares a map of $\overline{\Delta H}_{n=1}$ at 500 mbar for the northern hemisphere was prepared, following the method outlined in section III.1. The quantity $\overline{\Delta H}_{n=1}$ is therefore the mean height change (of 81 cases) of a certain atmospheric pressure level, at a particular location, between the first aerological observation after a solar flare and the aerological observation 24 hours earlier. In the foregoing section we have seen that for this particular flare sample the first aerological observation after the flare took place after an average interval of nearly 6 hours.

The map of $\overline{\Delta H}_{n=1}$ for 500 mbar is shown in Fig. 3. The individual grid point values of $\overline{\Delta H}_{n=1}$ (529 in number) have not been entered. The map as a whole shows a rather chaotic pattern of areas of mean height rise and areas of mean height fall. This alternating character is especially marked in the latitude belt 40—60° N. In polar regions a mean drop in height prevails, whereas in the subtropical belt there are both plus and minus mean height changes.

With regard to the magnitudes of the mean values, it is clear that the largest deviations from zero mean are found in middle to high latitudes.

The crucial question about the map of $\overline{\Delta H}_{n=1}$ is obviously whether it does show, by the magnitude of the mean values or by its geographical pattern, an influence of solar origin. This question will be considered in detail in the following sub-section.

First, however, we shall draw a comparison between our results and those of DUELL and DUELL and of VALNÍČEK, for the European-Eastern Atlantic region. In our map this region is dominated by a large cell of mean height rise with a maximum of + 1.5 gpdm over the North Sea. This is in perfect agreement with the results of the above authors (see Table I). However, in VALNÍČEK's study there is a lack of certainty about the time interval between the flare and the aerological observation on the day of the flare outburst. DUELL and DUELL, who only took into account flares observed between 9h and 15h GMT, most likely used aerological data of 15h GMT (instead of 03h GMT), although in their publication this is not explicitly stated.** This would mean

* The use of the computer facilities at the Geophysical Fluid Dynamics Laboratory (E.S.S.A.) is kindly acknowledged. The programming was carried out by A. H. Oort.

** In the relevant period (1936—41) routine upper-air observations were performed at 03h and 15h GMT. Since June 1957 daily aerological observation times have been at 00h and 12 h GMT.

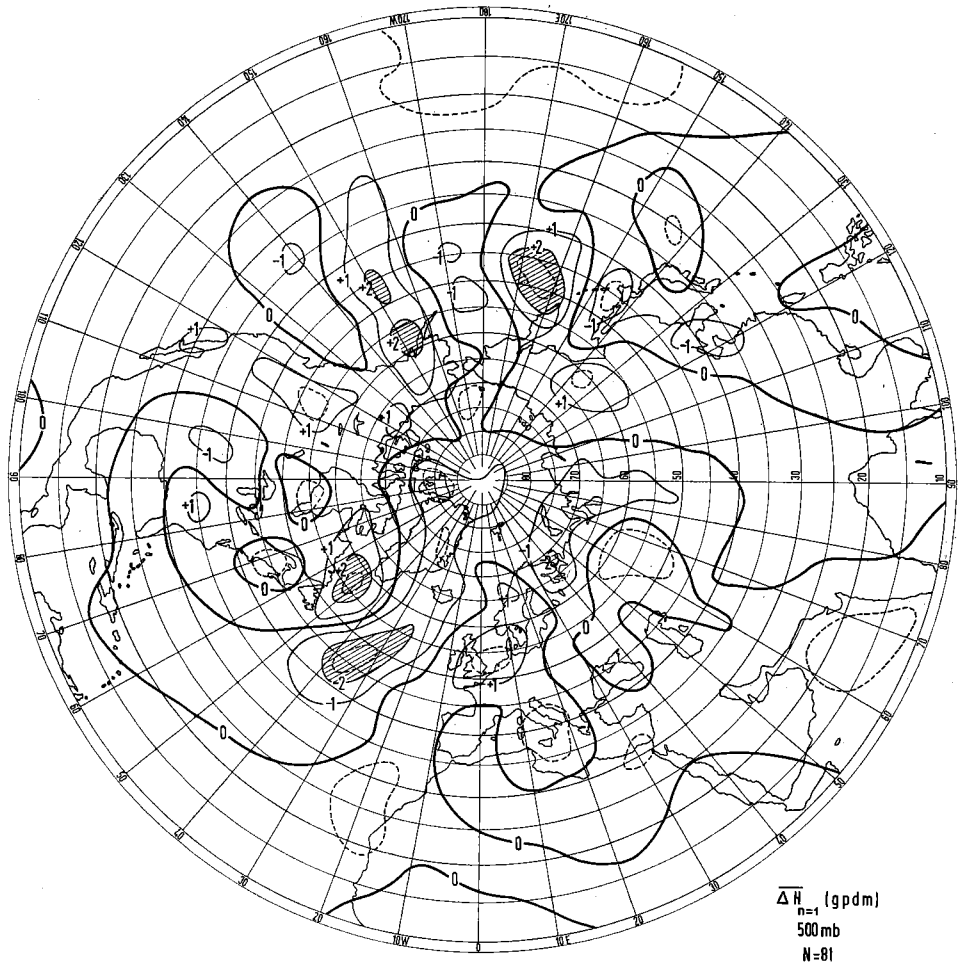

Fig. 3 A northern hemisphere map of the 500 mbar height changes after a solar flare (mean of 81 cases of the difference in height between the first aerological observation after a flare and the observation 24 hours earlier).

that the time interval between the flare outburst and the first aerological observation thereafter ranges from 0 to 6 hours, which is considerably shorter than the time interval in our study. In spite of this inconsistency we may consider the work of DUELL and DUELL and the present investigation as fairly similar analyses applied to independent data material. From this point of view the nice agreemeent between the results, as clearly shown by Fig. 4, at least forms a preliminary indication of a real solar flare effect.

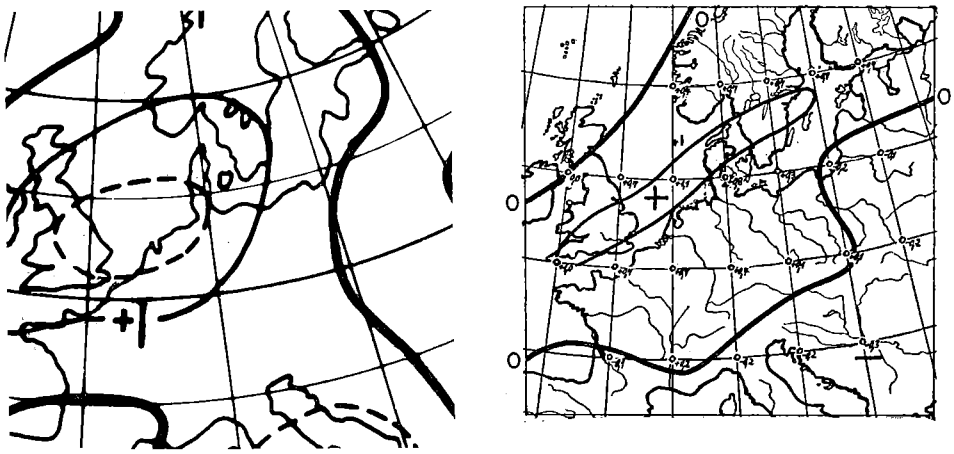

Fig. 4 Part of the map of mean height changes of the 500 mbar level after a solar flare, shown in Fig. 3, compared with the mean height changes of the 500 mbar level after a flare, as published by Duell and Duell (1948).

III.3.2 Statistically speaking the ΔH's at a given geographical location, for a given constant pressure level, taken throughout the year, during a very long period of years and regardless of whether a flare occurred or not, constitute a population with a mean $\mu = 0$ and a standard deviation σ. Taking at random only one sample of N elements from this population, with sample mean $\overline{\Delta H}$ and sample standard deviation s (being estimates of μ and σ), then this $\overline{\Delta H}$ will generally not be zero. Drawing new samples of N repeatedly, the $\overline{\Delta H}$ values will constitute a population with a mean $\mu' = \mu = 0$ and a standard deviation $\sigma' = \sigma/\sqrt{N}$. If the ΔH-population is normal or not too skew and if N is sufficiently large, then 95% of all $\overline{\Delta H}$'s will lie within the range $-1.96\ \sigma/\sqrt{N}$ to $+1.96\ \sigma/\sqrt{N}$ and 99% within $\pm 2.58\ \sigma/\sqrt{N}$ (usually rounded off to 2.0 and 2.6). In other words: the ratio $q = \overline{\Delta H}/\sigma'$ satisfies a standard normal distribution (with mean $\mu_q = 0$ and standard deviation $\sigma_q = 1$).* This q-distribution gives a means of testing the statistical significance of a calculated $\overline{\Delta H}$ value. If σ (or s) is known and q, based on 81 flare ΔH values at a given grid point, turns out to lie outside the 95% range for q, then we may conclude that $\mu \neq 0$ (in so concluding we know we are making an error of the first kind, namely an error of rejecting a true hypothesis, but the probability of this error is only 0.05). Then the interpretation is: the selected ΔH-population (selected because the ΔH's belong to flares) possesses a mean differing from zero.

* If s is used instead of σ, then the ratio $t = \overline{\Delta H}/s \,.\, N^{\frac{1}{2}}$ follows the Student or t-distribution with N—1 degrees of freedom. Then q is situated with a 0.95 chance between $\pm t_{0,95}$, where $| t_{0,95} | > 2.0$, although for $N > 30$ the difference between t and 2.0 is negligible.

If one could draw 100 independent random samples of 81 flares from the flare-population, then in the mean 95 of these 100 samples would lead to a $\overline{\Delta H}$-value at a given station within the range $\pm 2\,\sigma/81^{\frac{1}{2}}$ Unfortunately, this is impossible, but we can also consider 100 stations (or grid points), at each of which the same 81 flares give a sample of 81 ΔH-values. At station $j = 1$ the 81 ΔH-values possess a mean $\overline{\Delta H}_1$, and a standard deviation s_1, (being estimates of $\mu_1 = 0$ and σ_1), at station $j = 2$ $\overline{\Delta H}_2$ and s_2 (estimates of $\mu_2 = 0$ and σ_2), etc. Then if the 100 samples (100 stations) are independent, 95 of the 100 ranges $\pm \sigma_j/81^{\frac{1}{2}}$ ($j = 1, 2, \ldots, 100$) will contain $\overline{\Delta H}j$.

Having computed the standard deviations of the ΔH's at each of the 529 grid points used in the construction of Fig. 3, we calculated 529 values $q_j = \overline{\Delta H}_j/\sigma_j 81^{-\frac{1}{2}}$ ($j = 1, 2, \ldots, 529$) and verified whether $26 = 0.05 \times 529$ of these q-values lie outside the range $\pm 2\,\sigma_j 81^{-\frac{1}{2}}$. A map of the quantity q is given in Fig. 5.

It was found that at 44 of the 529 grid points the value of q exceeded 2.0. So instead of 5%, we have $44/5.29 = 8.3\%$ of the grid point values with $\overline{\Delta H}/\sigma\ N^{-\frac{1}{2}} > 2$. This 8.3% seems to be rather high compared with the 5% produced by chance. In fact, the number of significant points in a map of 529 grid points is a stochastic quantity, which follows a binomial distribution with $\mu = 529 \times 0.05 = 26$ and standard deviation $\sigma = (529 \times 0.95 \times 0.05)^{\frac{1}{2}} = 5.1$. We see that the number of 44 significant points deviates from the expected number 26 by $44 - 26 = 3.54\,\sigma$, which in terms of a standard normal distribution means a chance of only 0.0004 that the effect is spurious.

However, we have to remember that the 5%-rule as outlined above, is only valid if the stations or grid points are independent. In our case the requirement of independence is certainly not met, since it is well-known that the height changes of constant pressure levels are spatially correlated.

Tests were performed in order to find out whether the large number of significant q-values in Fig. 5 (large compared with the expected number) is merely due to the influence of the spatial correlation. First, an analysis exactly the same as was done in the construction of Fig. 3 and 5, was made of a sample of 81 key dates chosen at random from the period July 1957 through December 1959. The work was in fact done for 3 random samples. A series of random sampling numbers from a statistical handbook was used to select the random days. Afterwards the random samples (RI, RII, RIII) were combined so as to give a fourth random sample RIV, which is based on $3 \times 81 = 243$ key dates. The reason for computing a fourth sample was to get a better estimate of the standard deviation of the number of significant points (grid points with $|\,q\,| \geqslant 1.96$) for the random case. In view of the large amount of

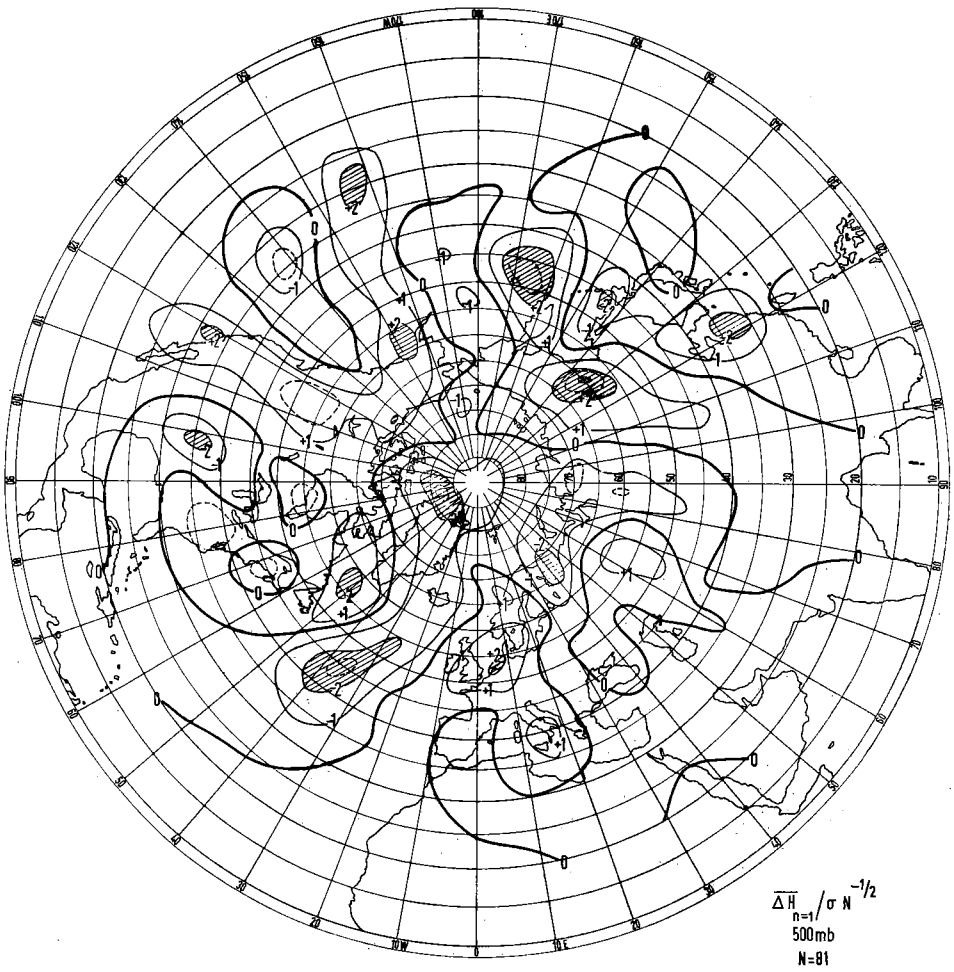

Fig. 5 A northern hemisphere map of the mean 500 mbar height difference between the first aerological observation after a flare and the observation 24 hours earlier, divided by the standard error of the mean.

work involved the calculations were performed by computer. Once having the computer program available, maps of $\overline{\Delta H}$ and $\overline{\Delta H}/\sigma\ 81^{-\frac{1}{2}}$ were also calculated for the flare sample for epochs $n = -1$ and $n = +2$. 500 mbar height data for all 1020 grid points were used in the computations. Since in the original analysis of the maps shown in Figs. 3 and 5, a less dense network was used for latitudes $\emptyset < 35°$ N, $\overline{\Delta H}_{n=1}$ and $\overline{\Delta H}/\sigma\ 81^{-\frac{1}{2}}$ were re-calculated for the flare sample, using the total number of 1020 grid points.

The number and percentage frequency of occurrence of grid point values $|q| \geqslant 1.96$ (5% significance level) and $|q| \geqslant 2.58$ (1% significance level) for each of the samples are given in Table III.

As shown by this table the differences in total number (or percentage frequency of occurrence) of significant points between the random samples on the one hand and the flare sample at the epochs $n = 1$ and $n = 2$ on the other are considerable.
While for the flare sample at the epochs $n = 1$ and $n = 2$ the numbers are far in excess of the expectation, for the random samples they vary from slightly below to slightly above the expected number for 5%-points and are generally equal to or below the expectation for the 1%-points.

Of course, the flare sample for the epoch $n = -1$ may also be considered as a random sample. Curiously enough, the number of significant points in this sample deviates more from the expected number than is the case with any of the true random samples. Possibly this is not just an accidental effect, since the flare sample for $n = -1$ is the only random sample which is completely free from flare cases (because of the isolation of flare cases by at least 48 hours). The random samples R I to R IV contain 3, 7, 2 and 12 flares respectively.

The standard deviation of the number of significant points ($|q| \geqslant 1.96$) for the random samples R I to R IV proves to be 14.8. This means that the number of significant points for the flare sample at $n = 1$ (84) minus the expected number (51) is more than twice the standard deviation, namely 84—51/14.8 = 2.23, which means that the difference is statistically significant (according to the standard normal distribution, at 2.23 σ the chance of the effect being not real is only 0.0258).
Though by comparison with the random samples we can see that the number of q's in the flare sample at $n = 1$ (and at $n = 2$) where $|q| \geqslant 1.96$ and even more so where $|q| \geqslant 2.58$ is significantly in excess of the expected number, we want to know something more about the influence of the spatial correlation on the number of significant points.

TABLE III

		number of q's where $\|q\| \geqslant 1.96$ (5% level)		number of q's where $\|q\| \geqslant 2.58$ (1% level)	
sample	epoch	number	%	number	%
R 1		45	4.4	7	0.7
R II		71	7.0	10	1.0
R III		38	3.7	4	0.4
R IV		60	5.9	10	1.0
Flares	n = —1	26	2.6	1	0.1
Flares	n = 1	84	8.2	23	2.3
Flares	n = 2	82	8.0	18	1.8
Expectation		51	5.0	10	1.0

We therefore tried to eliminate the spatial correlation by widening the network in successive steps, so as to cover the original area (northern hemisphere, north of 10° N) with 1020, 521, 262, 128 and 66 points respectively. The spatial correlation in the height patterns is probably eliminated altogether in the case of the coarsest grid. The grid distance is in this case of the order of 3000 km, which is generally larger than the wave-length of the synoptic disturbances. The result of applying the above procedure to the maps of q ($= \overline{\Delta H}/\sigma\ 81^{-\frac{1}{2}}$) for the random samples R I, R II and R III, and for the flare sample ($n = 1$) is given in Table IV.

TABLE IV *Percentages of grid points where* $|q| \geqslant 1.96$ *(5% level) for various network densities.*

N_t = number of grid points	R I	R II	R III	R I + R II + R III	Solar flares
1020	4.4	7.0	3.7	5.0	8.2
521	4.6	7.5	4.0	5.4	8.4
262	3.4	7.2	3.8	4.8	8.0
128	5.6	5.2	3.9	4.9	7.3
66	6.1	5.0	5.6	5.6	8.6

In the random samples the percentages tend to approach the expected value (5%) with decreasing density of grid points. There is virtually no such tendency in the flare sample. The percentages in the sum of the three random samples remain very close to five, for all densities applied.

The results of the tests show that:

1 a comparison between random samples and the flare sample gives a strong indication that the excess number of significant points is meaningful and not due to pure chance.

2 the spatial correlation of the height changes cannot account for the excess number of significant points in Fig. 5.

In other words, it seems probable that by our analysis we have isolated an effect associated with strong solar flares from synoptic "noise" at the atmospheric level concerned.

III.3.3 Though on the basis of the above we may say that solar flares have an effect on the height of constant pressure levels in the troposphere, we still lack a clear description of what the effect really looks like. We shall therefore consider the geographical pattern shown in Figs. 3 and 5.

We have already noted that this reaction pattern shows a cellular character, espe-

cially at the mid-latitudes (30—70° N). However, this character is also found to be an essential feature of the $\overline{\Delta H}$-patterns for each of the random samples, though here the patterns as a whole are much more chaotic in nature than the flare reaction pattern. The last statement can be illustrated quantitatively by considering the difference in total number of isolated cells exceeding a certain value of q ($= \overline{\Delta H}/\sigma\ 81^{-\frac{1}{2}}$) on each map. For instance, in each of the patterns for the random samples the number of closed cells where $| q | > 1$ is found to be nearly twice as large as in the flare reaction pattern.

Further examination of the flare reaction pattern reveals that although cells of

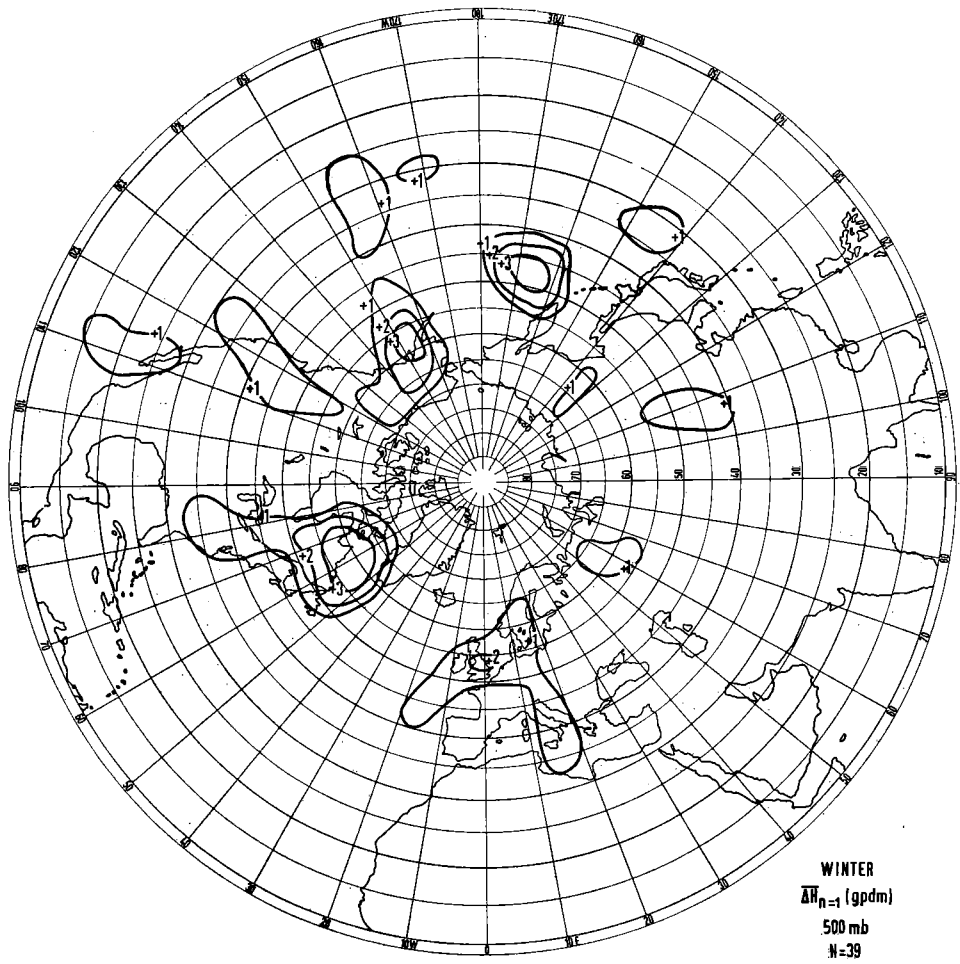

Fig. 6 Cells of mean 500 mbar height rise after a solar flare greater than 1 gpdm, for the winter half-year.

height rise alternate with cells of height drop, the cells of height rise are predominant. This is not the case with the random samples, as will be shown later on.

Another interesting feature of the reaction pattern was found by dividing the flare sample into two nearly equal subsamples (42 flares occurring in the summer half-year and 39 in the winter half-year) and constructing a map of $\overline{\Delta H}_{n=1}$ for each sample. It appeared not only that the cells of height rise were predominant, but furthermore that these cells are located at nearly the same place in the two maps (see Figs. 6 and 7 in which only the cells where $\overline{\Delta H} > +1$ gpdm have been reproduced). The last feature will be discussed in more detail in section IV.2.4.

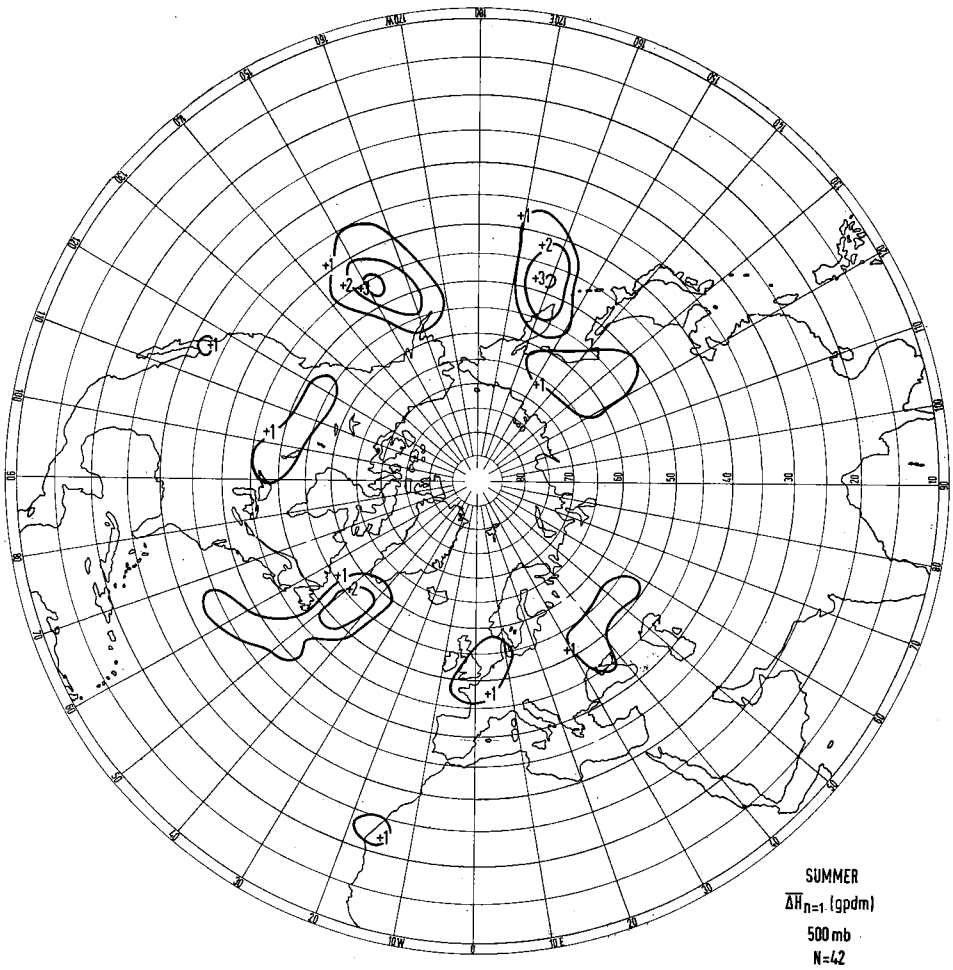

Fig. 7 Cells of mean 500 mbar height rise after a solar flare greater than 1 gpdm, for the summer half-year.

In order to investigate the predominance of the height rises at the mid-latitudes more thorougly, we computed zonal averages of the mean height changes. This was done by reading off interpolated values of $\overline{\Delta H}_{n=1}$ in Fig. 3 at each 10th meridian along the latitude circles 25° N, 30° N, ... 90° N. Averages were first plotted for the 4 quadrants, 10° E — 80° W, 80° — 170° W, 170° W — 100° E and 100° — 10° E, separately (Fig. 8). Each of the curves shows more or less the same tendency: height rises at the mid-latitudes and height drops in the polar regions. A complete hemispheric zonal average profile is depicted in Fig. 9. Zonally averaged mean height changes, denoted by $[\overline{\Delta H}]$, amount to about 4 geopotential meters per day at latitudes 55 and 60° N; north of 65° N values become gradually more negative, with a maximum of — 10 gpm at the pole. Viewed in the mean over a latitude circle, the predominance of the positive height changes proves to occur in a relatively narrow

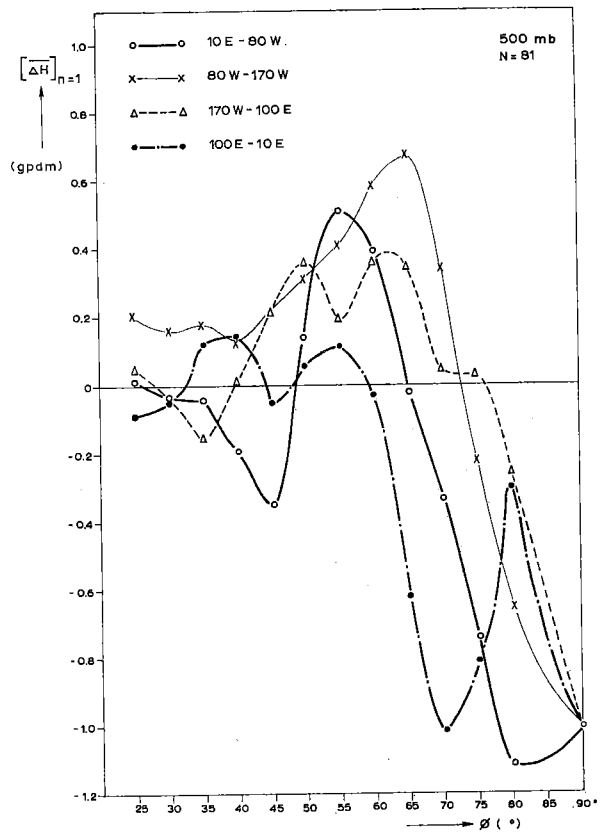

Fig. 8 Zonal averages of the pattern of 500 mbar height changes shown in Fig. 3, as a function of latitude for four separate quadrants of the northern hemisphere.

zone between 50° and 60° N. The statistical significance of this predominance has been tested by means of the analysis of variance. In the mid-latitude zone between 30—70° N the standard deviation of the ΔH's is approximately the same. Consequently, this also holds for the standard deviation of the $\overline{\Delta H}$'s in this zone. The latitudinal means $[\overline{\Delta H}]$ between 30—70° N, therefore, may be considered as the means of independent samples of $\overline{\Delta H}$'s taken from the same population of $\overline{\Delta H}$'s. The analysis of variance method (also called F-test), extensively described by BROOKS and CARRUTHERS (1953), now has been applied to the means of the grid point values in the latitude belts 30—40° N, 40—50° N, 50—60° N and 60—70° N. The number of grid points in these groups is respectively 170, 140, 92 and 65. The group means for the flare sample, being — 0.02, + 0.04, + 0.43 and + 0.08 respectively, were found to be statistically different, as can be shown in the following way.

The F-ratio, being the ratio of the between-group to within-group variance, was computed for the total of 467 grid point values. The within-group variance is taken about the mean of each group (the 4 latitude belts) and the between-group variance is that of the group means about the total mean. The significance level of the F-ratio is computed on the basis of n—r (here = 463) and r—1 (here = 3) degrees of freedom where n is the total number of grid points considered and r is the number of groups. The F-ratio found was 4.17/0.72 = 5.77. Since the 5% and 1% levels of significance are 2.62 and 3.83 respectively, the null-hypothesis that the 4 groups are not statistically different must be rejected. In other words, we may conclude that the predominance of

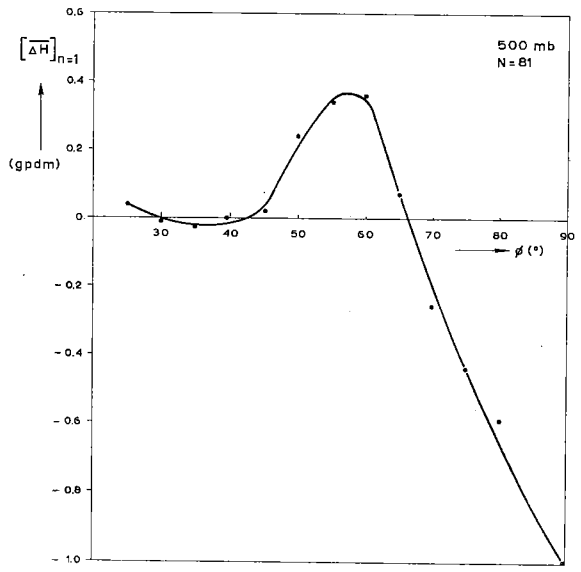

Fig. 9 Zonal averages of the pattern of 500 mbar height changes shown in Fig. 3, as a function of latitude for the whole northern hemisphere.

the height rises in the belt 50—60° N is real. The group means for the random samples, as defined above, were generally small, their highest positive and negative values being + 0.06 and — 0.17. For none of the random samples were the 4 group means found to be statistically different.

At this stage it is useful to draw attention to the fact that several classical studies on the relation between the 11-year sunspot cycle and pressure variations at the ground (WEXLER (1950), RAMAMURTI (1953), WILLETT (1965)), have produced results which are compatible with the tropospheric flare effect; namely, an increase in pressure in the latitude belt 50°—70° during years of maximum sunspot activity (as compared with years of minimum sunspot activity). This point will be considered in furhter detail in the last chapter.

We shall also discuss, in this connection, the controversial question whether solar activity favours zonality or meridionality of the atmospheric flow pattern. Indications of an increase in the zonal wind after solar events were found by TRENKLE (1957) for instance, while the development of meridional flow patterns, or even blocking, during high solar activity conditions has been advocated by VALNÍČEK (1952), BORISOVA and KHESINA (1963), and others.

The change in zonal circulation rate may be calculated from Fig. 9, using the geostrophic wind equation:

$$U_g = -\frac{g\,\partial[\overline{\Delta H}]}{f\,\partial y}$$

where

U_g = geostrophic wind in the direction west to east;
g = acceleration of gravity;
f = $2\,\Omega \sin\phi$, Ω being the earth's rotation and ϕ the geographic latitude;
y = distance in the direction south to north.

Northward of 55° N (see Fig. 9) $\frac{\partial[\overline{\Delta H}]}{\partial y}$ is negative, which means a general acceleration of the geostrophic wind in the higher mid-latitude and polar regions. The acceleration is greater between 60° N and 75° N, than it is at higher latitudes (due to large $\frac{\partial[\overline{\Delta H}]}{\partial y}$ and relatively small f). In this latitude belt the zonal mean westerlies at 500 mbar increase by nearly 0.5 m/s in 24 hours. A deceleration of the westerlies occurs in the latitudinal zone between 55° N and 45° N; it amounts to nearly 0.4 m/s per 24 hours.

Though this indicates an increased zonality of the atmospheric circulation at 500 mbar, the existence of alternative cells of height rise and height drop (see Fig. 3) could imply an increased tendency to meridionality. As will be shown in the last

chapter, an increased frequency of meridional circulation types (Grosswetterlagen) in the Eastern Atlantic-European area was indeed found to occur, especially on the second and third day after a flare.

So in combining the above arguments we are inclined to think that the ultimate effect of a flare will be the intensification of the meridional circulation, probably through the intermediary of an initially increased zonal flow aloft. The vertical distribution of the tropospheric flare effect, to be discussed in the next section, amply supports this suggestion.

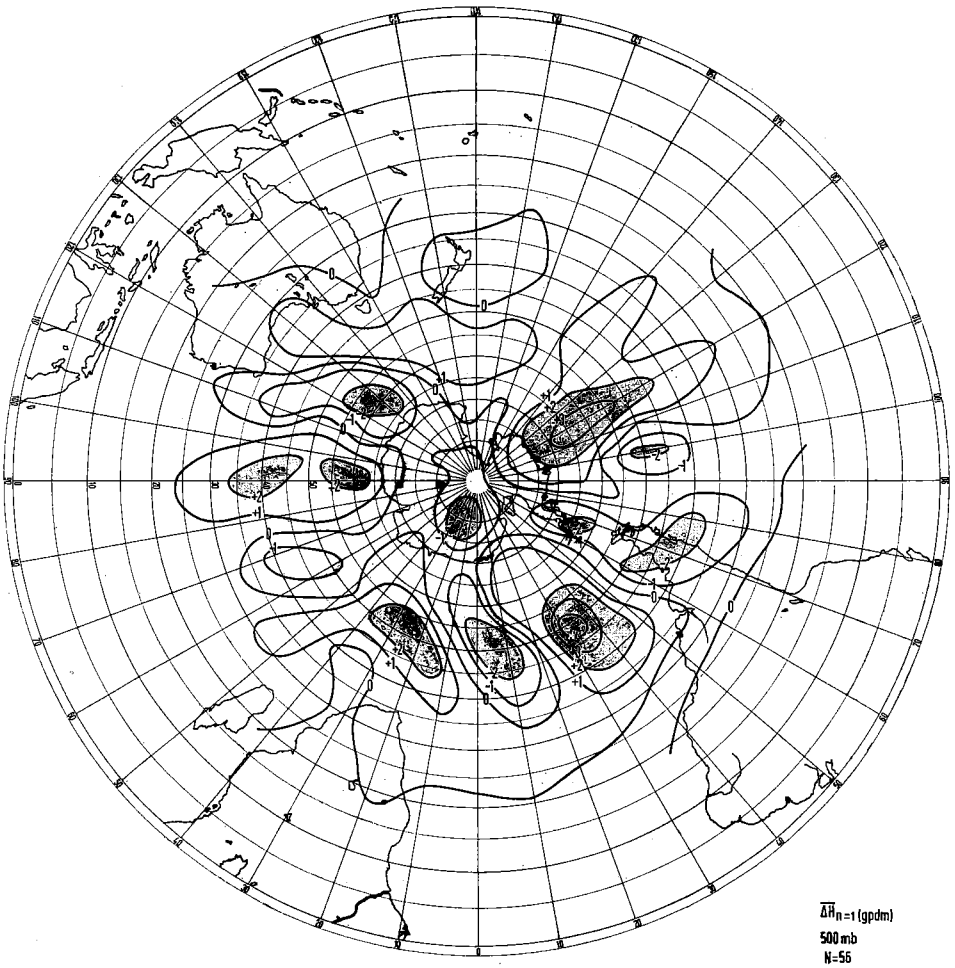

Fig. 10 A southern hemisphere map of the difference in height of the 500 mbar level between the first aerological observation after a flare and the observation 24 hours earlier (mean of 56 cases).

III.3.4 It would have been interesting and valuable, and to a certain extent also a matter of verification, to perform the same investigation for the southern hemisphere as has been done for the northern hemisphere. This could not be done, however, because of non-availability of aerological data and the known unreliability of available 500 mbar data for certain regions (see III.2). We therefore decided to construct a map of $\overline{\Delta H}_{n=1}$ at 500 mbar and to determine the zonal average $[\overline{\Delta H}]$ of this map only. Since the 500 mbar data for 1959 have so far not been at our disposal, we could only use the first 56 flares of our sample. It is only in the number of flares on which it is based that the construction of the map of $\overline{\Delta H}_{n=1}$ at 500 mbar for the southern hemisphere differs from the one for the northern hemisphere.

On the whole the pattern of $\overline{\Delta H}_{n=1}$ in the southern hemisphere, presented in Fig. 10, showns the same characteristics as the distribution in the northern hemisphere (Fig. 3). The mean values in the southern hemisphere map are somewhat higher. Also the zonal averages, shown in Fig. 11, have higher values than for the corresponding latitudes in the northern hemisphere. This might be due to the greater uniformity of the surface and atmospheric conditions in the southern hemisphere. However, the shapes of the zonal average profiles for the two hemispheres are similar to a degree that makes it very unlikely that the effect is accidental.

Thus the tropospheric flare effect, consisting of negative height changes at the polar regions and positive height changes at the mid-latitudes, appears to be a

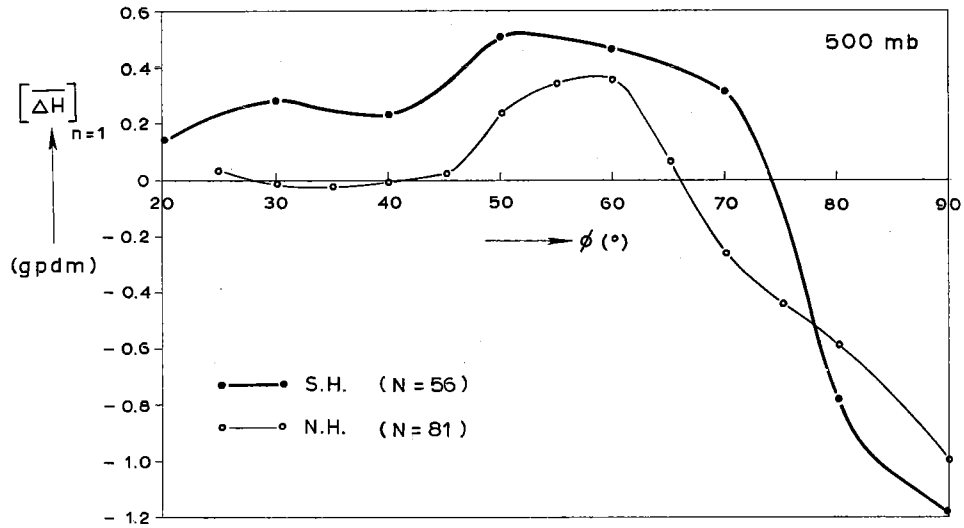

Fig. 11 Zonal averages of the pattern of 500 mbar height changes shown in Fig. 10, as a function of latitude for the southern hemisphere (the curve for the northern hemisphere is given for comparison).

world-wide phenomenon. Since the positive height changes at the mid-latitudes are predominant and since they take place over a much larger area than the negative changes in the polar regions, the height rises will be considered to be the primary effect from now on.

III.4 The vertical profile of height changes after a solar flare

As a next step it was thought worth while to investigate the vertical distribution of the tropospheric flare effect. The best way of doing this would be to study maps of $\overline{\Delta H_{n=1}}$ for selected pressure levels, e.g. 700, 300, 200 mbar etc.

In view of the considerable amount of work involved in constructing such maps, however, we chose an alternative approach, and constructed a vertical cross-section of $\overline{\Delta H_{n=1}}$ for the atmospheric layer between 1000 and 50 mbar. This cross-section lies along the Atlantic section of the 60 °N parallel and is based upon aerological data supplied by the stations Fort Chimo (58°06′ N, 68°26′ W), Ship B (56°30′ N, 51°00′ W), Ship I (59°00′ N, 19°00′ W) and Lerwick (60°08′ N, 01°11′ W). The

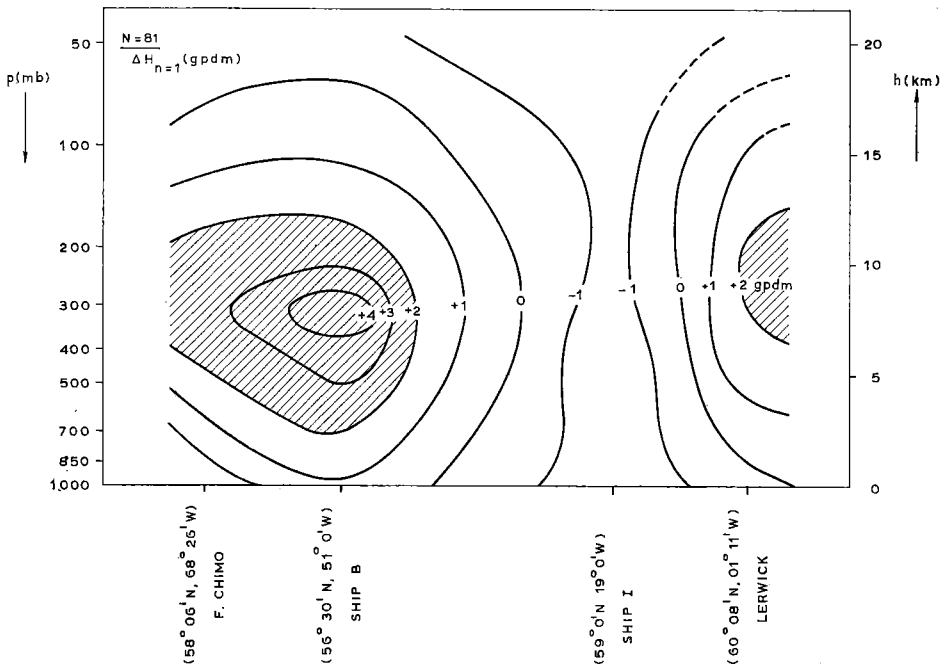

Fig. 12 Mean difference in height of constant pressure levels from the surface up to 50 mbar between the first aerological observation after a flare and the observation 24 hours earlier, at four stations located along the latitude circle 60° N.

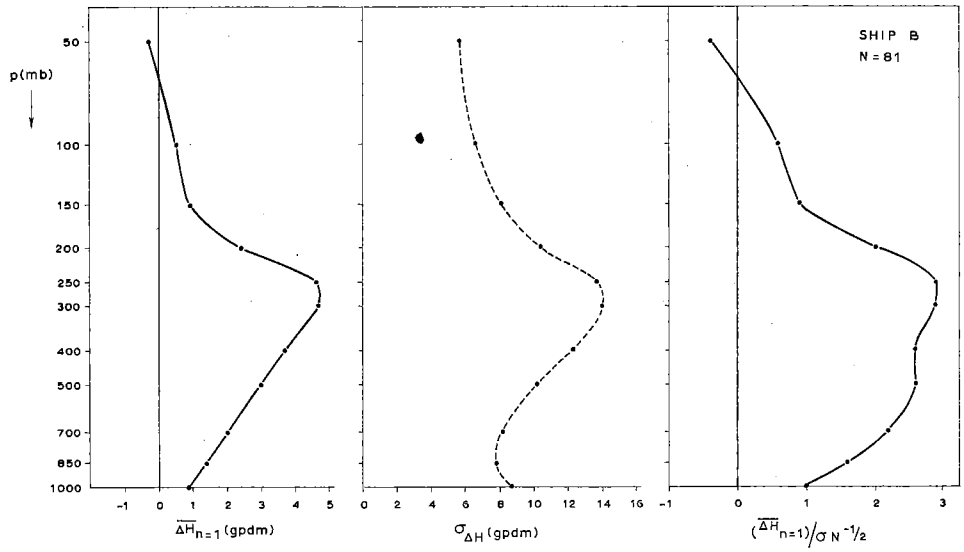

Fig. 13 Vertical distribution of (a) the mean differences in height of constant pressure levels from the surface up to 50 mbar between the first aerological observation after a flare and the observation 24 hours earlier, (b) the standard deviation of these height differences and (c) the ratio of the mean height differences and the standard error of the mean, at the aerological station Ship B.

analysis is based upon height data from the pressure levels 1000, 850, 700, 500, 400, 300, 200, 100 and 50 mbar.

In the cross-section shown in Fig. 12 isolines have been drawn for every geopotential decametre. In the case of Lerwick and Ship I the radio soundings often failed to reach the 50 mbar level. This resulted in less reliable mean values at the stratospheric levels; for this reason isolines in the relevant region are shown by a broken line. Regions with mean values higher than 2 gpdm have been hatched in. From Fig. 12 one may infer that the height rise tends to be greatest at or near the 300 mbar level, i.e. close to the tropopause level, at both the eastern and western part of the Atlantic. In the mid-Atlantic area of height drop any extremity in the vertical is virtually absent. Further, there appears to be no obvious shift from plus to minus of the height changes in the vertical, at least below 100 mbar.

A significance test on the height changes at different pressure levels has only been applied to the data from Ship B. In addition to the pressure levels used in Fig. 12 the 250 and 150 mbar level have been taken into account. Fig. 13 shows the mean height changes $\overline{\Delta H}_{n=1}(p)$, the standard deviation of the height changes $\sigma_{\Delta H}(p)$ and the vertical distribution of the ratio $\overline{\Delta H}_{n=1}/\sigma N^{-\frac{1}{2}}$ in the case of Ship B. From

the latter profile one can easily see that the mean height rises reach or exceed the 5% level of significance in the layer between 700 and 200 mbar; the 1% level is reached or exceeded in the layer between 500 and 250 mbar.

If we define that the maximum of the effect is located at the level where the above ratio has the highest value, then we may conclude that, at least at Ship B, this maximum occurs about the 300—250 mbar level.

Since the negative height changes are the same at all levels (which has been verified also for the polar station Alert), the occurrence of a maximum of positive height changes at the 300—250 mbar level causes the increase of the zonal westerlies between 55° and 75° N to reach a maximum at the same level.

At these high levels, just beneath the tropopause where a wind maximum is frequently observed, acceleration and deceleration effect are common phenomena. The recognition that these effects, with their strong bearing on the development of the pressure pattern at the ground, are due, at least in part, to the influence of solar activity, might be considered as an important result of this study.

III.5 Variations in height of pressure levels in the troposphere from 2 days before up to 5 days after a flare

So far we have considered only the height variations for the epoch $n = 1$ after a flare. It would be interesting to have similar maps and cross-sections as discussed in the foregoing sections for the epochs $n = 2$, 3 etc. after a flare. Furthermore, it would be worth while to extend the study to epochs before the flare, in order to obtain an idea of the mean height changes which occur without flare effect.

However, the preparation of all this material is too time consuming and we have therefore restricted ourselves to a study of $\overline{\Delta H}\ (p, t)$ at Ship B for the same pressure levels as used in Fig. 12 and for the epochs $n = -5$ through $n = +5$ (the meaning of the epochs is explained in section III.1). At each n, the corresponding time t with respect to the moment of the flare outburst is indicated in Fig. 14, showing the cross-section. The method by which Fig. 14 was obtained is known as "superposed epoch method" in the literature on the subject.

The cross-section of $\overline{\Delta H}\ (p)$ with time shows a succession of alternate spells of height drop and height rise throughout the whole layer between 1000 and 50 mbar. The mean values of the height change are generally small, except for the epoch $n = 1$. This is the only epoch for which the mean values reach or exceed the 5% level of significance, as may be deduced from a comparison between Fig. 14 and the vertical profile of $\sigma_{\Delta H}$ in Fig. 13. (For comment on the large, but not statistically significant, negative cell at $n = -3$, see note at the end of IV.2.4.)

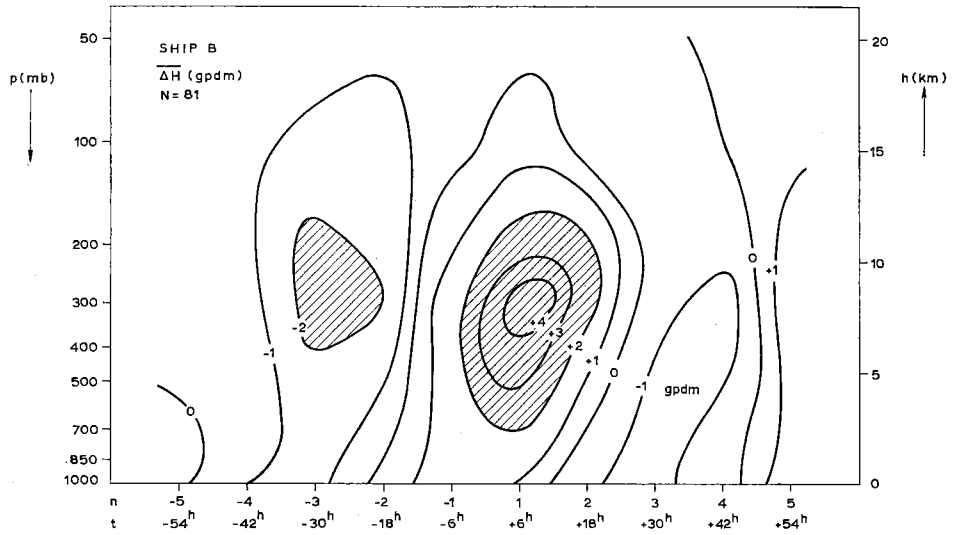

Fig. 14 Mean 24-hour height changes of constant pressure levels from the surface up to 50 mbar for the indicated hours, from roughly two days before till two days after a flare, at the aerological station Ship B.

An obvious method of testing the time cross-section is to divide the sample of 81 flare days into two equal parts and to construct a cross-section for the two sub-samples. In view of the uniformity in the vertical of the mean height changes, it will be sufficient to make the sub-division for only one pressure level. Fig. 15 shows the result for the 300 mbar level where the maximum effect is encountered. The sub-samples contain 40 and 41 flares respectively; they were selected from the original sample completely at random. In the figure the thin horizontal lines indicate the 5% level of significance, which is reached by both curves, but only at the epoch $n = 1$. This result furnishes new and independent evidence that the effect is real. Furthermore, the impression already gained from Fig. 14 that the effect is rather short-lived, is confirmed by both sub-samples. The height rises which are greatest at $n = 1$ become zero at $n = 3$, or rather give way to a height drop. This probably means that the duration of the solar influence is of the order of 24 hours, which of course does not imply that after this time interval the effect on the tropospheric circulation is completely lost.

In order to investigate the possible prolongation of the effect after $n = +5$, the cross-section shown in Fig. 14 has been extended up to $n = +11$ (+ 5d 6h after the flare).

To avoid overlapping, the extension demanded an isolation of the flares to at least 5 days apart. From the list comprising all flares of importance 2^+ or higher for

the IGY/IGC period, it was found that only 22 flares, a rather small number, fulfilled this condition.

$\overline{\Delta H}$ in this sample of 22 flares was calculated for 1000, 500 and 300 mbar pressure levels at Ship B and for $n = -2$ up to $n = +11$. As Fig. 16 clearly shows, at the higher levels (500 and 300 mbar) the only significant effect takes place close to the moment of the flare outburst. (Significant values appearing at $n = -1$ could perhaps be explained by the fact that 5 out of the 22 flares have a Δt greater than 11h, while for the sample of 81 flares there are only 8 cases where $\Delta t \geqslant 11$h; the influence of flares where $\Delta t \geqslant 11$h might well have been traced in the aerological observation at epoch $n = -1$). At 1000 mbar, however, the mean height changes, though in phase

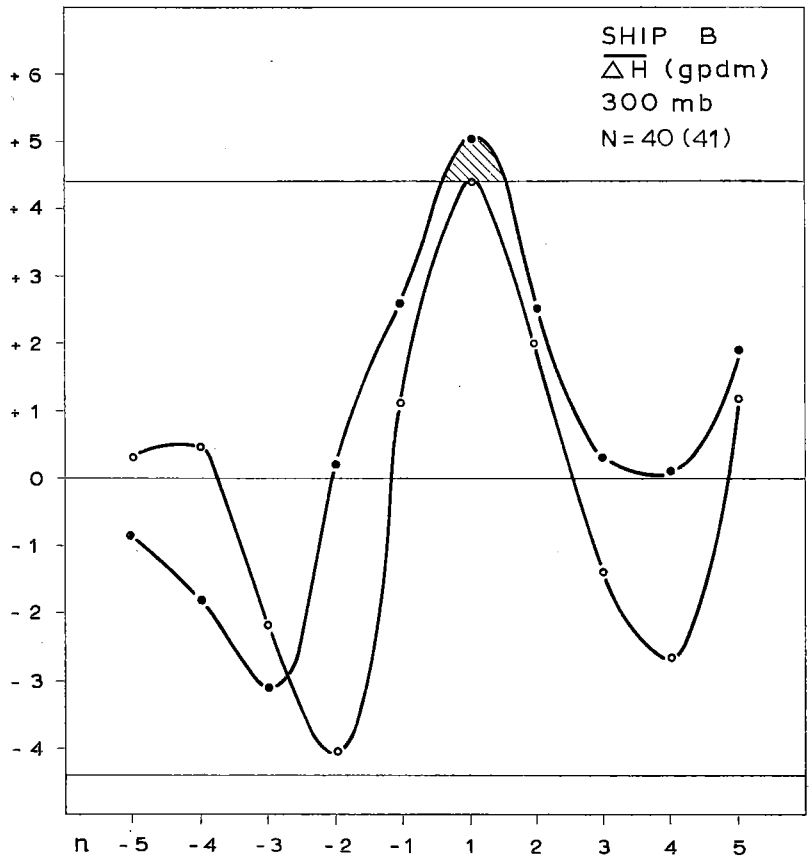

Fig. 15 Mean 24-hour height changes of the 300 mbar level for the indicated hours, from roughly two days before till two days after a flare, at the aerological station Ship B. Curves relate to two sub-samples selected at random from the original flare sample. The 5% significance limits are indicated by thin horizontal lines.

with the changes in the higher layers, reach their largest amplitude in the negative and do not exceed the 5% significance level until $n = +7$, corresponding to $t = +3$d 6h. This may be regarded as a very interesting result. In the first place the time interval of about 3 days tallies completely with the reported effects on sea level pressure (viz. DUELL and DUELL (1948), VALNÍČEK (1952) and KUBISHKIN (1966) in Table I). Secondly, this result confirms our tentative view that the solar influence has its effect in the high tropospheric layers, from where it works down to the earth's surface.

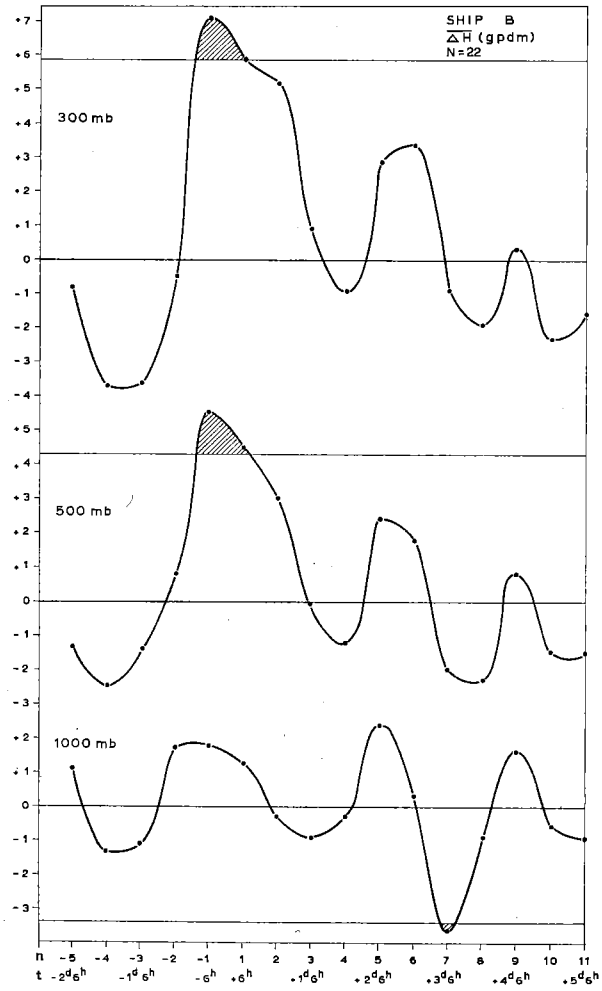

Fig. 16 Mean 24-hour height changes of the 1000, 500 and 300 mbar levels for the indicated hours, from roughly two days before till five days after a flare, at the aerological station Ship B. The 5% significance limits are indicated by thin horizontal lines.

III.6 Temperature changes related to the height changes after a solar flare

As mentioned earlier (p. 24), height changes and temperature changes in the atmosphere are not independent. Nevertheless we have made a separate study of the mean temperature changes at the two stations Ship B (56°30′ N, 51°00′ W) and Alert (82°30′ N, 62°20′ W) after a solar flare. In Fig. 3 Ship B is located in an area of height rise, Alert in an area of height drop. For Ship B Fig. 17 shows the vertical profile of $\overline{\Delta T}_{n=1}$, $\sigma_{\Delta T}$ and $\overline{\Delta T}_{n=1}/\sigma N^{-\frac{1}{2}}$.

Positive mean temperature changes are found over the whole tropospheric layer; in the layer between 700 and 500 mbar the rise in temperature is significant at the 5% level. The large drop in temperature occurring at the 250—200 mbar level is significant beyond the 1% level. This notwithstanding the fact that the standard deviations of ΔT at these heights are very great (due to large variations in the height of the tropopause, which is frequently located at or near the 250—200 mbar level).

In the lower stratosphere the values of $\overline{\Delta T}_{n=1}$ are low, but due to small variability the ratio $\overline{\Delta T}_{n=1}/\sigma\ N^{-\frac{1}{2}}$ maintains a value which at 100 mbar approximates the 5% significance level.

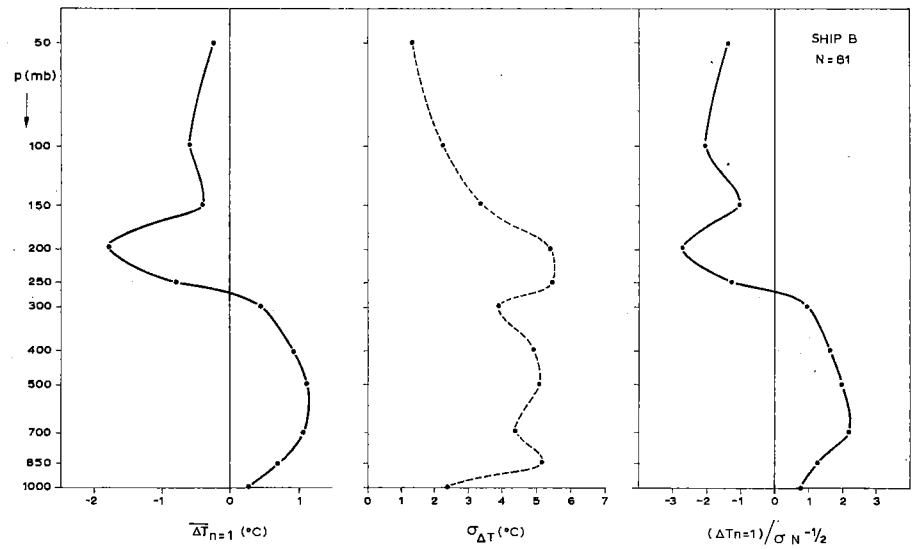

Fig. 17 Vertical distribution of (a) the mean temperature differences at constant pressure levels from the surface up to 50 mbar between the first aerological observation after a flare and the observation 24 hours earlier, (b) the standard deviation of the temperature differences and (c) the ratio of the mean temperature differences and the standard error of the mean, at the aerological station Ship B.

The vertical profile of $\overline{\Delta T}_{n=1}$ at Alert is given in Fig. 18. The profile is, at least in the troposphere and near the tropopause level, completely the reverse of the profile at Ship B. The cooling at the 850 mbar level amounting to a value of over 1° C in 24 hours just reaches the 5% level of significance; the rise in temperature at the 250 mbar level does not. In the lower stratosphere a slight cooling prevails, as was also found at Ship B.

The cooling in the 250—200 mbar layer at Ship B and the reverse temperature change at the 250 mbar level at Alert suggest that in both cases these temperature changes are related to variations in tropopause height, namely an increase of the tropopause height in the former case and a decrease in the latter. As far as this could be verified from the available aerological data, the anticipated tendency of the tropopause height was indeed found. Furthermore, a glance at Fig. 3 confirms that Alert is located in an area of height drop at 500 mbar, whereas Ship B is located in an area of height rise.

It will be shown that the observed mean temperature variations correspond fairly closely to the variations which are to be expected from the observed mean height variations. Applying the relation (p. 24) between ΔT and ΔH to the $\overline{\Delta H}_{n=1}(p)$ profile for Ship B, we find the following values for $\overline{\Delta T}_{n=1}(p)$ (see Table V).

From the available observations of ΔH and ΔT which are in all respects consistent, it seems to be quite impossible to find any evidence regarding the initial disturbance of the solar effect. However, some tentative inferences may be drawn from the fact that the largest effects occur at or below 200 mbar, in the case of both height and temperature variations. A direct propagation of the effect from the upper stratosphere to tropospheric levels, as happens in sudden mid-winter warmings, is therefore unlikely. Not only from observational experience regarding sudden warmings, but also from numerical experiments (BERKOFSKY and SHAPIRO, 1965), we know that a downward propagation of some upper-stratospheric disturbance is rather a slow process, which would take at least a few days to reach the troposphere. Therefore, it seems a more probable assumption that the sizeable effect near the tropopause level is a remnant of an initial disturbance in situ. The nature of this initial effect might well be a disturbance of the heat balance through diabatic cooling or heating in the layer concerned.

Finally, a brief comparison had to be made of our results on atmospheric temperature changes after solar flares with those obtained by other authors. (See Table I). It was found that HARTMANN's report of a hemispheric mean temperature rise at 500 mbar after a flare agrees with our results indicating a mean increase in height of the upper-tropospheric levels over most of the hemisphere.

The considerable temperature rise near the tropical tropopause, as found by

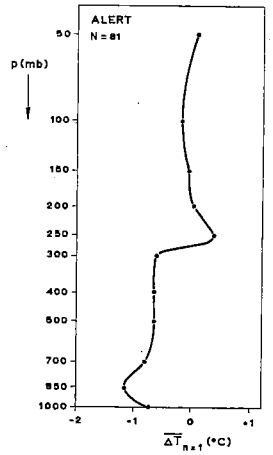

Fig. 18 Mean temperature difference at constant pressure levels from the surface up to 50 mbar, between the first aerological observation after a flare and the observation 24 hours earlier, at the aerological station Alert.

PALMER, is certainly not confirmed by our study, which shows the flare effect at lower latitudes to be fairly small. Nor are the temperature increases in the lower and middle stratosphere found by ATTMANNSPACHER confirmed by our results, at least up to the 50 mbar level.

III.7 Dependence of the tropospheric flare effect on the initial atmospheric conditions

It has frequently been supposed that the occurrence of a solar-atmospheric effect might depend on the initial conditions of the atmosphere (see RIEHL (1956), KRAUS

TABLE V

mbar	$\overline{\Delta H}_{n=1}$ (obs)	$\overline{\Delta T}_{n=1}$ (computed)	$\overline{\Delta T}_{n=1}$ (obs)
1000	0.9 gpdm	—	0.24 °C
850	1.4	1.06 °C	0.71
700	2.0	1.03	1.07
500	3.0	1.04	1.12
400	3.7	1.13	0.90
300	4.7	0.65	0.43
250	4.6	—1.93	—0.81
200	2.4	—2.46	—1.79
150	0.9	—0.93	—0.42
100	0.5	—0.37	—0.58
50	—0.3	—	—0.27

(1965)). Such suppositions mostly arise from stability considerations. It is felt that an outside influence, assumed to be small, is most likely to be effective when the atmospheric circulation is at a critical stage. At such a time a small additional force may be able to push the system over some threshold of instability.

In order to verify the possible difference in tropospheric flare effect for different states of the atmosphere, it was decided as a first step to study the flare effect for individual seasons. A first impression gained from Figs. 6 and 7 is that the difference in flare effect in the winter and summer half years is not large. Nevertheless, the original flare sample was subdivided, according to the meteorological seasons, into four sub-samples of 18 (winter), 16 (spring), 25 (summer) and 22 (autumn) flares. Maps of $\overline{\Delta H}_{n=1}$ (500 mbar), northern hemisphere, were constructed for each of the seasonal samples.

To save space the maps themselves are not shown here, but only the profiles of the zonal average $[\overline{\Delta H}]_{n=1}$ (Ø). (See Fig. 19). The predominance of the tropospheric flare effect in winter is very noticeable. The summer curve, on the contrary, is rather weak and differs in shape from the others, which show more or less the same profile as $[\overline{\Delta H}]_{n=1}$ (Ø) for the whole sample. (Fig. 9).

In view of the relatively small number of flares in each of the seasonal sub-samples, detailed conclusions with regard to the curves in Fig. 19 (for instance the difference in latitude of the maximum of height rise) will not be drawn. Rather, with the help of the data of the southern hemisphere, we shall try to verify the observation that the tropospheric flare effect is strongest in winter. Since these data refer to a much shorter period than our northern hemisphere data we have not attempted an investigation for four separate seasons, but only for two: winter (April—September) and summer (October—March). The winter sample in this case contains 27 flares, the summer sample 29 flares. The 500 mbar zonal average profiles of $\overline{\Delta H}_{n=1}$ are given in Fig. 20.

We see that the conclusion drawn for the northern hemisphere is confirmed by the southern hemispheric data: in winter the effect is strong and the latitudinal curve resembles the profile for the original sample (Fig. 11) very closely, whereas in summer the effect is weak and shows practically no resemblance to the profile in Fig. 11.

What conclusion should be drawn from the indication that the tropospheric flare effect is strongest in winter? We know that winter conditions at the earth's surface and in the atmosphere are extreme in many respects. As an initial condition for the occurrence of the flare effect, however, one aspect may be of particular importance, namely the intensity of the atmospheric circulation, which reaches its yearly maximum in winter.

To show that the intensive winter circulation is responsible for the strong flare effect in the winter season is not an easy task. First, we need an index of atmospheric

circulation. For our purpose we have calculated the zonal index at 500 mbar between 55° and 75° N for the half-hemisphere from 30° E westward to 150° W. This was done by reading off grid point values from 500 mbar maps analysed and published by the Deutscher Wetterdienst. The zonal indices, referred to below as I 55—75, pertaining to the last epoch of aerological observations before each flare outburst, were taken as a measure of the initial circulation condition for the tropospheric flare effect which might follow.

Having at our disposal an index of atmospheric circulation, a second problem now presents itself, namely how to connect the intensity of the flare effect with the intensity

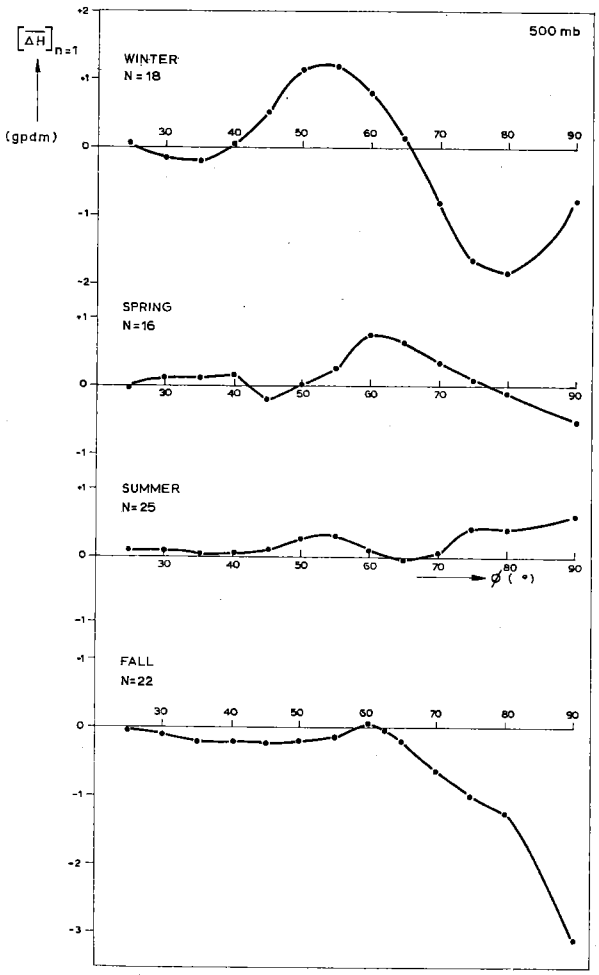

Fig. 19 Zonal averages of the seasonal patterns of the mean 500 mbar height changes after a flare (northern hemisphere).

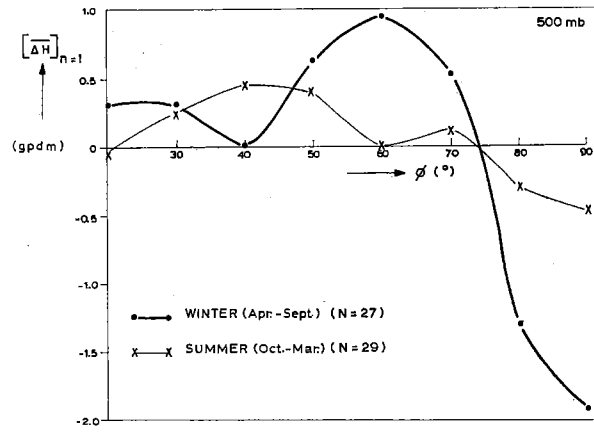

Fig. 20 Zonal averages of the seasonal (winter and summer half-year) patterns of mean 500 mbar height changes after a flare (southern hemisphere).

of the atmospheric circulation. The problem arises from the fact that there is a strong overall correlation between I 55—75 and the season of the year, high values of I 55—75 occurring almost exclusively in the winter season. Consequently, a simple sub-division of the flare sample in two or three groups according to the strength of I 55—75 would lead to useless results, since the group with the largest I 55—75 values, containing practically all winter cases, would show the largest flare effect. And this is what we know already.

It is necessary to approach the problem by making a sub-division according to I 55—75 for the winter cases only. However, the winter sample contains only 18 cases, which makes a separation into two classes rather illusory. We have therefore restricted ourselves to the calculation of the correlation-coefficient between I 55—75 and $\overline{\Delta H}_{n=1}$ at the Fort Chimo, Ship B, Ship I and Lerwick stations for the winter cases. In all these cases and for all pressure levels tested, the correlation is found to be positive, i.e. $\overline{\Delta H}_{n=1}$, tends to be more positive (or less negative) for higher values of I 55—75.

At Lerwick and Ship I the correlation coefficients are fairly low (near zero to + 0.20); at Fort Chimo and Ship B, both being located about the centre of the region to which I 55—75 pertains, they are generally higher. An example for Ship B is given in Table VI.

As we see from the Table, the correlation coefficient between $\overline{\Delta H}_{n=1}$ (300 mbar) at Ship B and I 55—75 is + 0.54. We know from statistical theory that according to

the null-hypothesis (two variables are simultaneously normally distributed without correlation ($\rho = 0$)), the sample correlation coefficient r is symmetrically distributed about a mean zero, with standard deviation $\frac{1}{\sqrt{N-1}}$, where N indicates the sample size (number of pairs). Provided that N is sufficiently large the null-hypothesis ($\rho = 0$) may be rejected at the 5% level as soon as $|r| > \frac{2}{\sqrt{N-1}}$. Here $N = 18$, $\frac{2}{\sqrt{N-1}} = 0.49$, $r = 0.54 > 0.49$, so that H_0 must be rejected.

From the above investigation we, therefore, may conclude that the initial state of the atmosphere has a strong influence on the intensity of the tropospheric flare effect. That more specifically the rate of the atmospheric circulation is involved in this

TABLE VI. *Mean 24-hour height changes after a flare and the zonal circulation index (winter cases only).*

Flare case, t(n = 1)	$I_{55-75°N}$(500 mbar) (in gpdm)	$\Delta H_{n=1}$(300 mbar) at Ship B (in gpdm)
1957		
13 Dec., 00	24	5.9
15 Dec., 00	28	— 3.4
19 Dec., 12	24	29.6
22 Dec., 00	30	41.8
1958		
16 Jan., 00	34	31.8
25 Jan., 12	6	— 7.6
1 Feb., 00	27	8.9
11 Feb., 12	12	— 2.5
3 Dec., 12	29	30.5
12 Dec., 00	1	3.1
23 Dec., 00	5	— 7.2
1959		
1 Jan., 00	31	9.4
15 Jan., 00	2	21.8
22 Jan., 00	7	0.1
9 Feb., 12	14	13.1
13 Feb., 00	28	5.7
5 Dec., 00	21	2.9
10 Dec., 12	7	— 13.1
Mean	18.3	9.5
σ	11.1	15.2

Correlation coefficient r(I, ΔH) = + 0.54.

influence, confirms KRAUS' (1965) ideas that the dynamical instability of the flow is of great importance in establishing a solar-atmospheric effect. Furthermore, these results support our views concerning the flare effect and its subsequent influence on sea-level pressure, given in section III.4.

IV. A CHAIN OF EVENTS OFFERING A POSSIBLE EXPLANATION OF THE TROPOSPHERIC FLARE EFFECT

IV.1 The causing agent: corpuscular radiation rather than UV-radiation

IV.1.1 As to the working agent which might establish a flare influence on the troposphere, opinions have thus far been divided. Many authors believe that the UV-radiation or (more likely from the heliophysical point of view) the X-radiation of the flare, through the intermediary of atmospheric ozone or otherwise, must be held responsible for a flare effect on the troposphere (e.g. DUELL and DUELL (1948), PALMER (1953)). Others, e.g. WILLETT (1952) and MUSTEL (1966), suggest that, through some still unknown mechanism, the flare's particle radiation should be regarded as the most likely origin of a tropospheric flare effect.

If a choice between wave-radiation or particle radiation is to be made on the basis of the characteristics of the flare effect described in the previous chapter, there are, in our opinion, at least two features that suggest that the particle radiation must be the ultimate cause.

These features are:

1 the fact that considerable height changes of the 500 mbar level, only occur at middle to high latitudes;

2 the fact that the maximum response, which we believe to be caused in situ, occurs as low as the tropopause level.

Two further arguments for a corpuscular cause of the flare effect are brought forward here:

3 the interval between the flare outburst and the maximum tropospheric flare effect is longer for flares occurring on the eastern hemisphere of the sun than for flares occurring on the western hemisphere.

It is a frequently observed fact that the delay of the onset of solar corpuscular effects after a solar flare depends on the heliographic longitude of the source flare. The relation is such that for flares on the western hemisphere of the sun the delays (in the case of particles in the relevant energy range — see section IV.1.2) are shorter by several hours than for flares on the eastern hemisphere (OBAYASHI, 1964a). The asymmetry is generally attributed to the configuration of the interplanetary magnetic field. This field is assumed to rotate with the sun up to a certain distance from it.

The fact that the tropospheric flare effect takes a shorter time to make itself felt in the case of western flares than in the case of eastern flares is a most interesting discovery and one that offers conclusive evidence in favour of the assumed particle

cause. This result, for Ship B, is shown in Fig. 21. In view of the fact that the aerological observations are 12 hours apart, a precise estimate of the time-difference in maximum tropospheric flare effect for E and W flares cannot be given.

4 the atmospheric reaction pattern is more symmetrical with respect to the geomagnetic than with respect to the geographic pole.

Since solar particles are most probably electrically charged, their region of entry into the earth's atmosphere will be determined by the earth's magnetic field. Therefore, the patterns of $\overline{\Delta H}_{n=1}$ (500 mbar), shown in Figs. 3 and 10, have been studied to

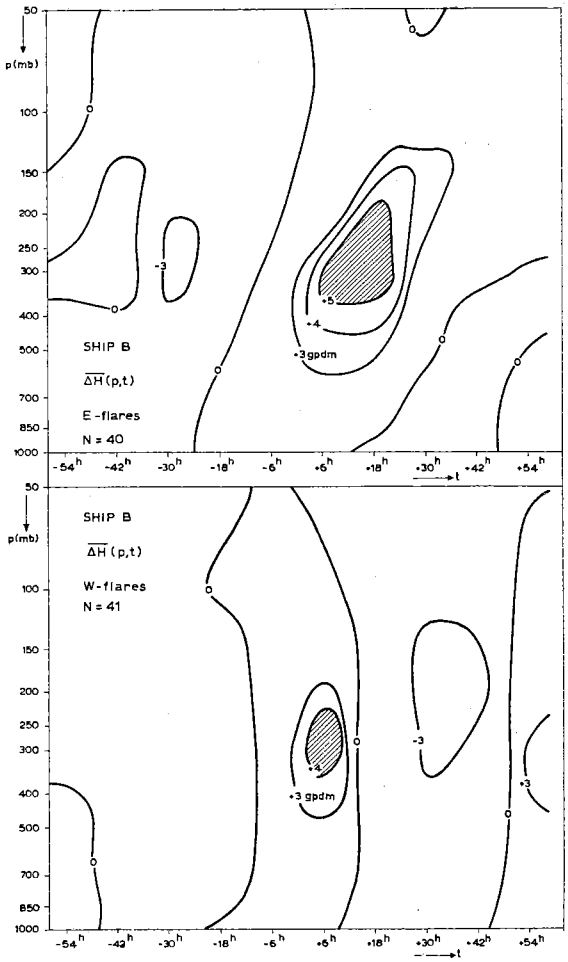

Fig. 21 Mean 24-hour height changes of constant pressure levels from two days before till two days after a flare, for flares which occurred on the eastern and western side of the solar disk separately.

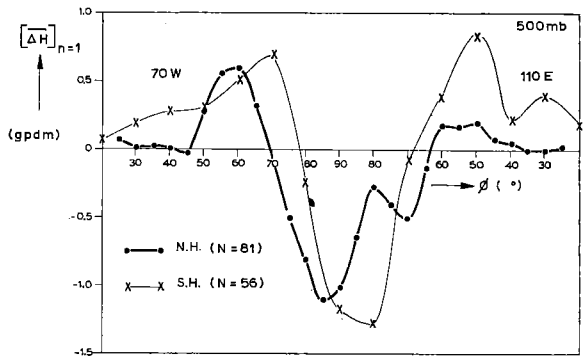

Fig. 22 Half-hemispheric (180°) zonal averages of the pattern of 500 mbar height changes shown in Figs. 3 and 10; the half hemispheres are centered in the meridian through the geographic and geomagnetic poles.

find their symmetry with respect to the geomagnetic dipole-poles, which are located at 78°.5 N and S, and 69° W and 111° E in the northern and southern hemispheres respectively. Slightly greater symmetry with respect to the geomagnetic poles than with respect to the geographic poles seems to be present, as may be concluded from Fig. 22 in which half-hemispheric geographical zonal averages $[\overline{\Delta H}]_{n=1}$ (500 mbar) are shown for both hemispheres of the globe. The half-hemispheres are centred in the great circle through the geographic and geomagnetic poles. As can easily be seen, the curves shift with respect to the geographic pole (90°) in the direction of the geomagnetic dipole-poles; the shift is less clearly indicated for the northern hemisphere curve than for the southern hemisphere curve.

Taken together, the above four arguments form a fairly strong basis for the assumption that the influence on the troposphere is caused by the flare's particle radiation.

IV.1.2 We shall now try to identify the energy range of the particles which could be held responsible for the flare effect. From the three main components of the flare's particle radiation we may ignore the slowest component, since its influence on the earth's atmosphere is delayed by at least 24 hours. The fastest particles may also be left out of consideration since, as we have seen, only very few flare events are accompanied by a measurable flux of high energy particles. The only class of particles left consists of protons (and some heavier particles) of moderate energy, which reach the earth in a few hours after the flare outburst (known as sub-relativistic particles). In the following we shall tentatively assume that this class of particles causes the tropospheric flare effect.

As a further approximation, we shall consider this class of particles to consist of protons only. In the introductory paragraphs it was stated that the energy of these protons ranges from 1 to 10^3 MeV. Concise information on the intensity, the spectral

distribution and the time duration of the proton precipitation is given by WHITTEN and POPPOFF (1965). The integral intensity J, which is the number of protons cm^{-2} sec^{-1} $sterad^{-1}$ with energy greater than E, is often given in the form of a power law of energy:

$$J = A\,E^{-n}, \text{ where } A \text{ is a constant.}$$

From balloon observations near the geomagnetic pole it has been found that $n = 4$ for protons between 85 and 300 MeV. n increases gradually up to a value of 7 for energies between 2 and 15 BeV. Peak proton intensities ($E > 10$ MeV) as observed by direct measurements with balloons or satellites, or estimated from polar cap absorption, vary from $J = 10^2 - 10^4$ protons cm^{-2} $sec^{-1}sterad^{-1}$. The duration of particle precipitation is also somewhat variable; a typical sequence is a rise time of a few hours, a peak value for 5—10 hours, followed by a slow decay of the flux over at least 1 day.

Solar protons of the energies in question cannot penetrate the earth's magnetic field except for a region of high geomagnetic latitudes. Assuming the earth's magnetic field to be a simple dipole field, the relation of the cut-off latitude $\varnothing_c$ to the proton energy is expressed by the following formula (HAKURA, 1964):

$$\cos^4 \varnothing_c = \frac{4a^2}{M} P$$

where

a = the earth's radius,
M = the magnetic moment of the earth's dipole,
P = the so-called rigidity, which determines the extent to which a particle is deflected by a magnetic field.
$P = \frac{mv}{eZ}$, where mv is the momentum of the particle and eZ is its charge.

P is normally expressed in volts and is related to the energy of the particle in the following way:

$$P = \frac{1}{eZ}(E^2 + 2\,m_0C^2\,E)^{\frac{1}{2}}$$

m_0C^2 = the rest energy of the particle.

Fig. 23 shows a graph of the cut-off latitude as a function of proton energy. Thus, protons cannot penetrate to latitudes lower than those indicated by the curve. However, from both satellites and ground-based observations it has become clear that the cut-off latitudes as inferred from Fig. 23 only give a rough estimate of the actual cut-off latitude, especially in geomagnetically disturbed conditions.

If, in view of these known deviations, we allow for a 5° equatorward shift of the cut-off boundaries in Fig. 23, which seems to be a reasonable value (ROSE and ZIAUDDIN,

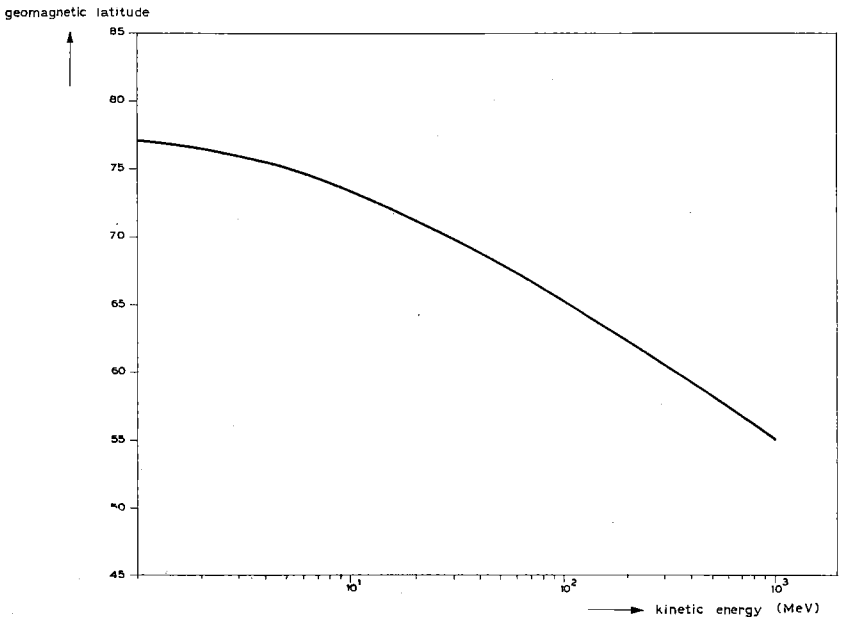

Fig. 23 Geomagnetic cut-off latitudes for protons in the 1-1000 MeV range.

1962), we may conclude that the cut-off latitudes for 1--10^3 MeV protons range from about 72°.5 to 50° geomagnetic latitude. Thus, penetration of solar particles into the earth's atmosphere at a geomagnetic latitude lower than 50° occurs only when the particle stream contains protons with an energy higher than 10^3 MeV.

Since the flux of protons of such high energies is usually very small, we can probably ignore them in explaining the tropospheric flare effect.

We have tried to compare the results explained above with the pattern of height changes of the 500 mbar level after solar flares reproduced in geomagnetic coordinates.

From the geomagnetic transforms of Fig. 3 and Fig. 10 we determined the geomagnetic zonal averages $[\overline{\Delta H}]_{n=1}$. (Fig. 24). The profiles in both hemispheres are alike in showing positive values of $[\overline{\Delta H}]_{n=1}$ equatorward of 70° and negative values at the poleward side of this (geomagnetic) latitude. A brief comparison with the similar curves given in Fig. 11 as a function of geographic latitude shows that for the southern hemisphere the amplitude is greater in geomagnetic than in geographic coordinates; for the northern hemisphere the opposite is true. In both hemispheres, however, relatively high values of $[\overline{\Delta H}]_{n=1}$, positive or negative, are only found poleward of 50° geomagnetic latitude, which is well in accordance with the suggestion that solar protons of less than 10^3 MeV are the causing agent.

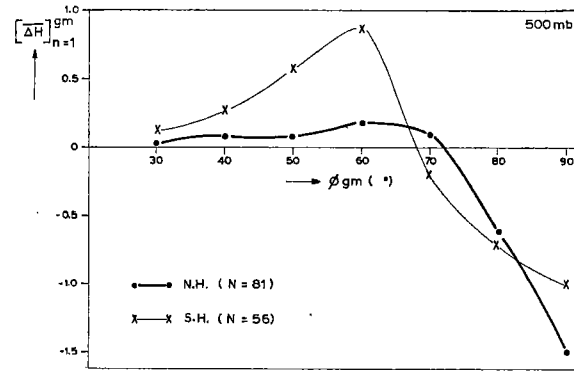

Fig. 24 (Geomagnetic) latitudinal profiles of the pattern of 500 mbar height changes shown in Figs. 3 and 10; zonal averages have been taken according to geomagnetic latitude circles.

IV.1.3 A lower limit for the energy range of the protons responsible for the flare effect has been obtained in the manner described below.

Solar flare protons with energies between 5 and 300 MeV are known to be responsible for the Polar Cap Absorption events. According to WARWICK and WOOD (1961), 26 out of the 45 PCA events between 1953 and 1960 were preceded within 6 hours by solar flares of importance greater than 2. Only 6 of the remaining 19 PCA's were not preceded within 14 hours by a flare or by solar radio bursts; only 3 were not connected with any observed flare activity phenomenon. In a later publication by ŠVESTKA (1966) the relation PCA-flare is found to be even stronger. The reverse relation between flare and PCA occurrence is rather weak: only half of the strong flares were accompanied by a PCA event. In the case of our flare sample given in Table II the correlation is even less: only 20 out of 81 flares were followed by a principle PCA event (See Table VII). A catalogue published by BASLER and OWREN (1964) was used to select the PCA's.

We shall now examine the tropospheric flare effect for PCA flares and for non-PCA flares separately.

The map of $\overline{\Delta H}_{n=1}$ at 500 mbar for the 20 PCA flares (not shown here) shows the same characteristics as the map of $\overline{\Delta H}_{n=1}$ for the whole flare sample (Fig. 3). Subtracting the first map from the second and taking the zonal averages $[\overline{\Delta H}]_{n=1}$ for the flare-PCA and flare-non-PCA cases (Fig. 25), we observe that the height rises of the 500 mbar level in the 55—65° latitude belt are about equal in the two cases, but the magnitude of the height drop poleward of 65° N differs substantially for the two sub-samples. In view of the smallness of the flare-PCA sample it is rather dangerous to draw detailed conclusions from this difference, though the comparison does seem to indicate that the occurrence of the tropospheric flare effect is not restricted to flares in connection with which a principal PCA-sequence has been reported.

TABLE VII. *List of flare-PCA cases*

No.	$t(n=1)$	Δt	PCA-onset (earliest and latest reported onset)
	1957		
1	3 July, 12	4 15	3 July, 08 15 — 11 00
2	25 July, 00	5 33	25 July, 00 00 — 01 00
3	29 July, 00	9 58	28 July, 15 00 — 21 00
4	1 Sep., 00	10 48	31 Aug., 13 40 — 15 30
5	4 Sep., 00	9 30	3 Sep., 15 00
6	27 Sep., 00	4 08	26 Sep., 21 00 — 23 15
	1958		
7	25 Jan., 12	2 00	25 Jan., 16 00
8	15 Mar., 00	8 53	14 Mar., 15 00 — 22 00
9	23 Mar., 12	1 50	23 Mar., 18 30
10	25 Mar., 12	6 30	25 Mar., 03 00 — 15 45
11	4 June, 00	8 48	3 June, 23 00 — 08 15 (4 June)
12	7 July, 12	10 47	7 July, 01 00 — 06 00
13	16 Aug., 12	7 21	16 Aug., 06 00 — 12 00
14	23 Aug., 00	8 54	22 Aug., 14 00 — 16 00
15	26 Aug., 12	11 33	26 Aug., 01 00 — 03 00
	1959		
16	13 Feb., 00	0 35	13 Feb., 09 00
17	12 June, 12	3 30	13 June, 08 00
18	10 July, 12	9 30	10 July, 04 00 — 08 00
19	17 July, 00	7 44	17 July, 02 00 — 06 00
		2 28	
20	19 Aug., 00	6 35	19 Aug., 09 00 — 10 00

$t(n=1)$ Date and time (GMT) of the first aerological observation after the flare.

Δt Time interval in hours and minutes between the moment of maximum brightness of the flare and $t(n=1)$.

PCA — onset times in hours and minutes GMT.

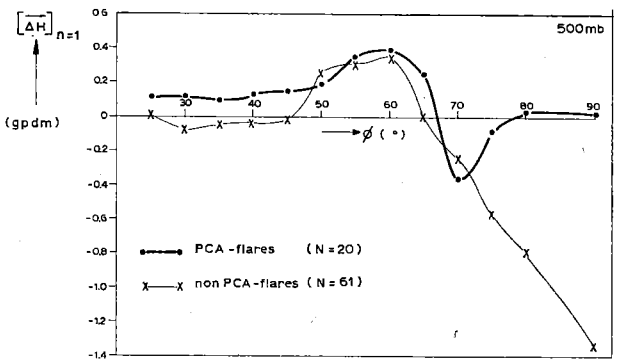

Fig. 25 Zonal averages of the pattern of mean 500 mbar height changes after a flare, for flares with and without subsequent PCA event.

This result justifies the conclusion that energies not falling within the indicated 5—300 MeV range must mainly be held responsible for the tropospheric flare effect; otherwise the effect would be greater in conjunction with PCA than without it. Since energies below 5 MeV may safely be ignored, the only possibility left is that protons with energies higher than 300 MeV are the causing agencies.

Combined with the upper limit derived in the foregoing section, the energy range of the protons responsible for the tropospheric flare effect may be tentatively specified as 300—1000 MeV.

IV.2 The possible interaction between energetic solar protons and ozone in the lower stratosphere

IV.2.1 The first question to be answered is how far protons in the energy range 300—1000 MeV penetrate the earth's atmosphere.

After deflection by the earth's magnetic field these particles enter the high latitude atmosphere, and on their way down dissipate their energy by electronic and nuclear collisions with the air. According to SCHIØTT (1966) the electronic stopping power (excitation and ionization of the air) is completely dominating, the nuclear stopping being 10^3 times smaller than electronic stopping for particle velocities

$$v > \frac{2\pi e^2}{h \varepsilon_0} Z^{2/3}$$

where

Z = the atomic number,

e = the electronic charge,

h = the Planck constant,

ε_0 = the permittivity of vacuum.

For protons ($Z = 1$) of energies of the order of 1 keV this condition is already fulfilled, so for MeV-protons we may safely assume that the total range of penetration is determined exclusively by electronic stopping.

However, the computation of the stopping power (energy loss per unit path length) of a gas over an incident beam of protons still remains very complicated, for several reasons. Therefore, laboratory measurements of stopping powers or range-energy relations are mostly used for practical purposes.

Experimental data relating to protons in air (or in N_2 and O_2) have been summarized by DALGARNO (1961).

Range-energy relationships are more readily used than stopping powers for calculating the depth of penetration of protons into the atmosphere.

Penetration depths for 1—100 MeV protons have been calculated by BAILEY (1967) using the measurements published by LIVINGSTONE and BETHE in 1937 for proton

ranges. The penetration depths have also been computed for proton ranges by BATES (1953), who based his calculations on the measurements of proton ranges in air, made by COOK, JONES and JORGENSON in 1953. Though BAILEY and BATES used quite different model atmospheres, their curves of penetration depths against proton energy prove to be substantially in agreement.

Approximate heights in the atmosphere to which vertically incident protons penetrate are given in Table VIII.

TABLE VIII.

Proton energy (MeV)	Altitude (km)
1	90
10	65
100	30

Unfortunately, experimental data on stopping power or particle ranges are not readily available for energies higher than 100 MeV. If nevertheless we have to make an estimate of the penetration depth of high energetic protons, the best approach seems to be a comparison of some of the existing approximations.

1 According to LINGENFELTER and FLAMM (1964) measurements on protons in nitrogen lie roughly along a line of constant attenuation length (range over which the energy is degraded to $\frac{1}{e}$ of the initial energy) of about 125 g cm^{-2} for proton energies above 100 MeV.

2 In first approximation, cosmic ray physicists sometimes use the rule: the energy loss of high energy protons in air is 2 MeV per g cm^{-2}.

3 For proton energies outside the laboratory range DALGARNO (1961) refers to a formula of the stopping power, derived by BETHE:

$$-\frac{dE}{dx} = 3.46 \times 10^{-12} \quad \frac{N}{E} \ln\left(\frac{2.18\ E}{I}\right) \text{eV cm}^2,$$

where $\frac{dE}{dx}$ is the energy loss per unit path length, in a gas at standard temperature and pressure,

N is the concentration of the absorber,

I has the significance of an average excitation energy, being about 94 eV for air,

E is the proton energy in keV.

By integration of these formulas (the last one numerically) we have obtained the penetration depths in g/cm^2 as a function of the energy of the incident proton.

The integrals between E and 100 MeV have been computed for each energy, i.e. the range of a proton necessary to lower its energy from the initial value E to 100 MeV was estimated. In accordance with the data given in Table VIII a range of 10 g/cm^2 has been assumed in each case for the dissipation of the remaining 100 MeV (the atmospheric mass above 30 km is approximately 10 g/cm^2).

The curves of the penetration depths for each of the three formulas are given in Fig. 26. The curves show a considerable spread, the curve relating to the simplest estimate of the stopping power having a course in between the other two curves over the whole range of energies. However, a point of intersection of the three curves is found at E, equal to 525 MeV, where a penetration depth of 220 g/cm^2 is found.

The main conclusion to be drawn from the figure is that protons with $E > 300$ MeV enter the lower stratosphere, while at still higher energies ($E > 700$ MeV) they reach the tropospheric layers. This conclusion remains approximately the same when instead of Fig. 26 the tables of proton ranges in air are used, which have been published quite recently by BARBAS and BERGER (1964) and WILLIAMSON (1966).

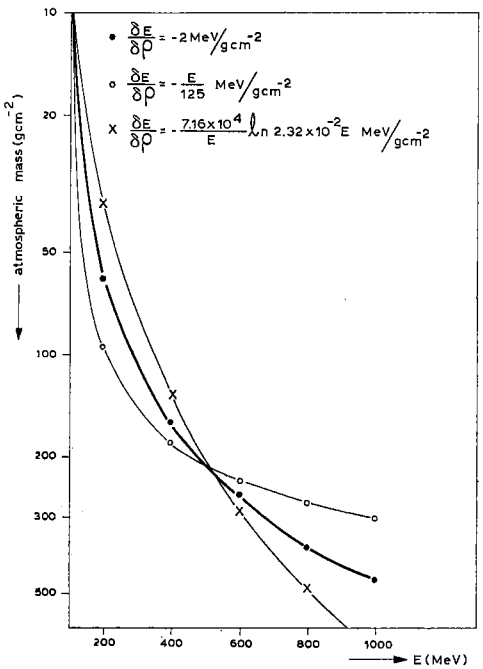

Fig 26 Penetration depth of protons of energy E for three different energy loss functions.

These tables, which are based on modified versions of the Bethe-formula, give generally somewhat smaller penetration depths, especially at the lower energies. In view of the power law spectrum of the protons (see section IV.1.2) the number of particles which enter the troposphere is only a small fraction of the total number of particles passing the 100 mbar level. For an exponent $n = 4$ in the power law, which is a rather conservative value, we can easily calculate that the flux of protons with $E > 700$ MeV is only about 4% of the flux in the 300—700 MeV range.

We may therefore conclude that the bulk of the protons lie in the 300—700 MeV range and are consequently stopped in the lower stratosphere between the 100 mbar level and the tropopause.

IV.2.2 The most crucial question to be answered now is how the solar protons which dissipate their energy in the lower stratosphere may give rise to the observed tropospheric flare effect. To formulate the problem more specifically let us for a moment re-examine section III.6 in which the vertical distribution of temperature changes after a solar flare was discussed. It was suggested there that the considerable cooling effects near the tropopause level observed in the regions of height rise of the 500 mbar level might be caused by diabatic cooling in situ. Though as a whole the arguments for an initial disturbance at tropopause level are not particularly strong, the results of the foregoing section indicating that the source protons are in fact capable of reaching the lower stratospheric region lend considerable support to this suggestion. The problem to be solved may therefore be stated as follows: what mechanism can account for the creation of a diabatic heat sink by penetrating solar protons.

In the earth's atmosphere the main cooling mechanism is the loss of heat by radiation. The most promising approach to the problem would therefore be the investigation of a possible interaction of the solar protons with one of the radiative constituents of the lower stratosphere. Since there are indications that the atmospheric ozone content decreases after a solar flare (see next section), the probability of ozone destruction in the lower stratosphere by solar protons and secondary electrons has been investigated.

A considerable part of the luminous emission of the upper atmosphere, known as airglow, is attributable to OH-emission. HUNT (1966) has recently presented calculations which indicate that the known features of this emission can be adequately explained by the reaction $H + O_3 \rightarrow OH' + O_2$

$$OH' \rightarrow OH + h\upsilon \; (\lambda \approx 6257 \text{ Å}).$$

The efficiency of hydrogen atoms in decomposing ozone was already know from laboratory experiments (CLYNE et al., 1963). In experiments to remove ozone by atomic oxygen according to the recombination process $O_3 + O \rightarrow 2\ O_2$, the authors

found that a contamination of the oxygen by hydrogen atoms in a concentration O : H = 300 : 1 provides a significant enhancement of the O_3 removal.

Furthermore, the hydroxyl molecules which are produced in the reaction H + O_3 will also react with ozone, a mechanism which has recently been elaborated by HAMPSON (1964) and RONEY (1965), discussing the influence of water vapour on the distribution of ozone in the stratosphere.

The mechanism works as follows:

Atomic oxygen will react with water vapour according to

$$O + H_2O \rightarrow 2\ OH,$$

whereas hydroxyl will propagate a reaction chain by which ozone is removed:

$$OH + O_3 \rightarrow HO_2 + O_2 \text{ and}$$
$$HO_2 + O_3 \rightarrow OH + 2\ O_2.$$

As a terminating reaction HAMPSON proposes

$$OH + HO_2 \rightarrow H_2O + O_2.$$

This mechanism has also been studied experimentally by NORRISH and WAYNE (1965), who conducted a laboratory experiment in which they found that the quantum yield of the photolysis of ozone by UV-radiation in the presence of water vapour was greater than that for pure ozone.

At first sight this mechanism looks very promising with regard to ozone destruction by solar protons. We therefore attempted to make an estimate of the amount of ozone removed by this mechanism in the lower stratosphere.

Assuming that all protons which enter the lower stratosphere react with ozone only (this assumption is certainly not true, but serves only to get an estimate of the maximum effect), we have to consider the reaction rates of the following reactions:

$$H + O_3 \xrightarrow{k_1} OH + O_2 \tag{1}$$

$$OH + O_3 \xrightarrow{k_2} HO_2 + O_2 \tag{2}$$

$$HO_2 + O_3 \xrightarrow{k_3} OH + 2\ O_2 \tag{3}$$

$$OH + HO_2 \xrightarrow{k_4} H_2O + O_2 \tag{4}$$

The rate of ozone removal according to reaction (1) is simply k_1 [H] [O_3], in which the symbol [ ] denotes the concentration of the relevant constituent. In order to compute the rate of removal due to OH and HO_2 we first have to know the equilibrium concentrations of these molecules. For the production of OH due to reactions (1) to (4) we may write

$$\frac{d[OH]}{dt} = k_1 [H] [O_3] + k_3 [HO_2] [O_3] - k_2 [OH] [O_3] - k_4 [HO_2] [OH]$$

The equilibrium concentration of OH will then be

$$[OH] = \frac{k_1 [H] [O_3] + k_3 [HO_2] [O_3]}{k_2 [O_3] + k_4 [HO_2]} = \frac{k_1 [H] + k_3 [HO_2]}{k_2 + k_4 [HO_2]/[O_3]} \qquad (I)$$

Since in the lower stratosphere certainly $[O_3] \gg [HO_2]$ and k_1 [H] is probably very small, equation (I) may be approximated to

$$[OH] \approx \frac{k_3}{k_2} [HO_2] \qquad (II)$$

Introducing (II) in (I) we easily obtain

$$[OH]^2 = \frac{k_1 k_3}{k_2 k_4} [H] [O_3] \qquad (III)$$

In order to get some quantitative results, it turns out to be necessary to make an estimate of the number density of the solar protons which enter the lower stratosphere. On the basis of the integral power law spectrum (see section IV.1.2) with exponent $n = 4$, we find for the flux J in the energy range 300—700 MeV a fraction of the order of 10^{-5} of the integral intensity J_0. Taking $J_0 = 10^4 \frac{\text{protons}}{\text{cm}^2\text{sec}}$ (section IV.2.1) we obtain for $J_{300-700\ \text{MeV}}$ a value of the order of 10^{-1} protons/cm^2 sec. This appears to be a rather conservative value, since in a number of cases it has been found that $J_{E > 300\ \text{MeV}} \approx 10^{0.5}$ cm^{-2}sec^{-1} (OBAYASHI, 1964b). With a velocity of the order of 10^{10} cm/sec a flux of 10^{-1} protons/cm^2 sec means a density of protons [H] equal to 10^{-11} per cm^3. According to HAMPSON (1964) very little is known about the values of the reaction constants. We shall adopt here the values quoted by HUNT (1966). These values are $k_1 = 2.6 \times 10^{-11}$, $k_2 = 5 \times 10^{-13}$, $k_3 = 10^{-14}$ and $k_4 = 10^{-11}$ cm^3 molec^{-1} sec^{-1}, respectively. HUNT admits that these values are rather uncertain, the value of k_3 being only an arbitrary assignment. With these values for [H] and k_1 and adopting for $[O_3]$ a value of 5.10^{12} cm^{-3} we find the rate of ozone removal due to protons only to be negligible, namely of the order of 10^{-9} molec cm^{-3} sec^{-1}.

From equation (III) we find an equilibrium concentration of hydroxyl molecules, $[OH] = 2.5$ molec cm^{-3}, which according to equation (II) means an equilibrium concentration of HO_2 equal to 125 molec cm^{-3}. Using these concentrations and the appropriate reaction constants the rate of ozone removal due to reactions (2) and (3) is found to amount to only 12.5 O_3 molec cm^{-3} sec^{-1}. This value, though many orders of magnitude greater than the ozone destruction by hydrogen only, is still far too small to account for the observed ozone decrease, which, as will be shown in the next section, is at least of the order of 10^6 molec cm^{-3} sec^{-1}.

Clearly the mechanism proposed above is ineffective in producing any great changes in the atmospheric ozone content. However, thus far we have only given attention to reactions initiated by the penetrating protons themselves. As is well-known, protons

stopping in air produce large showers of secondary electrons. Therefore, we shall now consider the possible interactions of secondary electrons with some atmospheric molecules, the ultimate result of which interactions might be the destruction of ozone.

The electrons once produced are involved mainly in two processes: electron-ion recombination and electron attachment to neutral species. However, most of the cross-sections for reactions occurring in the atmosphere are virtually unknown. This is for instance the case with the cross-section for dissociative attachment of electrons to ozone (WAGNER, 1966), which process perhaps may partly account for the observed ozone destruction.

In view of the hydroxyl reactions with ozone already discussed, one might envisage the possibility of H_2O-dissociation in the lower stratosphere by electrons produced by the penetrating protons. The energy of such electrons exceeds the thermal energy of atmospheric particles (≈ 0.03 eV) by several orders of magnitude; the energy of a photon of wave length 2390 Å, which is capable of dissociating H_2O, is equal to 5.2 eV.

The present state of knowledge concerning electron attachment to molecules, and more particularly electron attachment leading to dissociation of the molecule, has been described by PRASAD and CRAGGS (1962). With respect to dissociative attachment of electrons to water vapour molecules they refer to Russian measurements, which are the only ones available hitherto. Dissociative attachment to H_2O has been observed in two small regions of the electron energy spectrum, centred around 6.4 and 8.6 eV. Cross-sections measured for the two regions are 4.8×10^{-18} and 1.3×10^{-18} cm^2 respectively.

The rate of electron production must be known in order to compute the OH-production due to this mechanism.

The total electron-ion production by a proton is the sum of the primary ionization produced by the proton impact and the secondary ionization produced by electrons ejected during the primary ionization. According to DALGARNO (1962), the secondary ionization at high proton energies may be as large as the primary ionization.

The same author gives a formula of the (primary) production of electron-ion pairs per centimetre path as a function of the energy of a penetrating proton:

$$p = -\frac{dE}{dx} / \mathrm{W(E)}$$

where $\frac{dE}{dx}$ = the energy loss per cm path;

W(E) = mean energy per electron-ion pair produced.

It has been observed in laboratory experiments that W is nearly constant over a wide range of energies. The mean specific energy per electron-ion pair in air is 36 eV. With the simplest energy loss relation

$$\frac{dE}{d\rho} = -2 \text{ MeV/gcm}^{-2}$$

we can easily compute that in the layer between 250 and 125 mbar ($\approx 5.10^5$ cm) the number of electrons produced is 7.10^6 per proton. With a proton flux of the order of 10^{-1} cm^{-2} sec^{-1} the electron production in the lower stratosphere will be of the order of 10^6 cm^{-2} sec^{-1} in a column 5.10^5 cm in height.

However, since we do not know the energy spectrum of the electrons, an estimate of the fraction of the total number of electrons that will participate in the attachment process cannot easily be made. A reasonable assessment can be made, however, by using the electron spectrum observed at sea-level. (Electrons observed at sea-level are mainly secondary products of galactic cosmic radiation). The form of this spectrum is cited by CLAY (1948) as $N = N_0 E^{-1.3}$.

On the basis of this spectrum 7% of the electrons would have energies between 5 and 10 eV, which we assume to be the effective range for the H_2O-dissociation process.

Then, with a mean cross-section of 3.10^{-18} cm^2 and a water vapour concentration of 10^{14} H_2O molecules/cm^3 the OH (and H) production in the lower stratosphere will be:

$$0.07 \times 10^6 \times 10^{14} \times 3.10^{-18} = 20 \text{ molecules/cm}^3 \text{ sec.}$$

We can now compute the rate of ozone removal due to HAMPSON's mechanism; we calculate the equilibrium concentration of OH and HO_2 molecules in the same way as before.

Since the equilibrium concentration of H atoms will not reach high values due to the rapid reaction with ozone, the recombination of OH and H can be left out of consideration.

The equilibrium concentration of OH, taking into account reactions (1) to (4) and the OH production by dissociation of water vapour, now becomes

$$[OH]^2 = \frac{k_1 k_3}{k_2 k_4} [H] [O_3] + \frac{k_3}{k_2 k_4} \times 20 \qquad \text{(IV)}$$

The equilibrium concentration of hydrogen atoms which are produced by the dissociation process and removed by reaction (1) is found to be

$$[H] = \frac{20}{k_1 [O_3]} \qquad \text{(V)}$$

Introduction of (V) into (IV) gives

$$[OH]^2 = 40 \times \frac{k_3}{k_2 k_4} \qquad \text{(VI)}$$

With the values of the reaction constants already cited, we find $[OH] = 3 \times 10^5$ molec cm^{-3}. According to reaction (2) an OH-concentration of this nature will lead to an ozone removal of 0.75×10^6 O_3 molecules cm^{-3} sec^{-1}.

Even if we ignore any additional ozone destruction by HO_2 molecules and by H-atoms, we see that the observed ozone decrease after a flare can be fully explained by this mechanism.

Therefore, from the computations presented in this section, we may conclude that solar protons penetrating the lower stratosphere are capable of disturbing the ozone distribution. While the ozone removal by the protons themselves was found to be negligible, the interaction of the collisionally produced electrons with water vapour results in a production of OH-molecules high enough to account for an appreciable decomposition of ozone. Since in the latter mechanism the concentration of water vapour in the lower stratosphere plays a vital part, a few comments on the relation between the moisture conditions of the atmosphere and the occurrence of the solar flare effect will be made. (See section IV.2.4).

IV.2.3 Some findings concerning the statistical relationship between solar flares and variations in atmospheric ozone content are discussed in this section.

The influence of solar flares on total atmospheric ozone has been studied by SEKIHARI (1963). In his analysis the superposed epoch method was applied to ozone data from 5 low latitude stations. In the selection of key-dates a particular flare

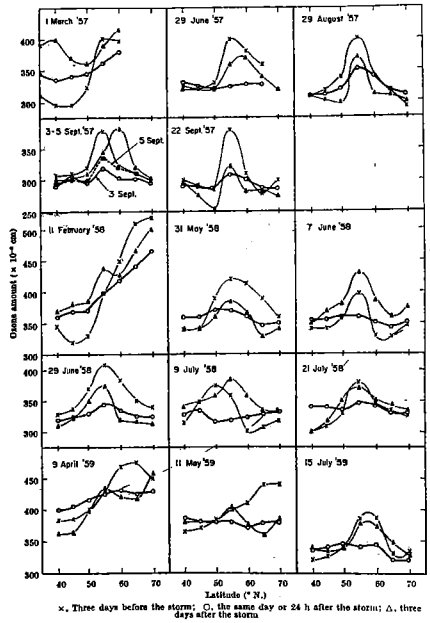

Fig. 27 Latitudinal mean amounts of total ozone at different latitudes on the third day before, the third day after and the day itself of the occurrence of a severe geomagnetic storm (after Kulkarni).

index was used instead of individual flare cases. No relation between the occurrence of a flare and total ozone amount could be established from the analysis.

SEKIHARI also applied the superposed epoch method to ozone data from 21 high latitude stations, using in this case an index of geomagnetic activity for the selection of key-dates. Here the results turned out to be positive in the sense that on the key-day itself (thus a day of high geomagnetic activity) total ozone amounts tended to be significantly less than on the days before and after the key-day.

This result confirms to some extent the investigations of KULKARNI (1963) on the mean meridional distribution of total ozone over European stations during severe magnetic storms. It is KULKARNI's work which we feel to be of particular importance in connection with the tropospheric flare effect presented here.

For fourteen days during the IGY/IGC period on which severe geomagnetic disturbances occurred, KULKARNI constructed latitudinal (38—70° N) profiles of the total ozone amount. Such profiles were also constructed for the third day before and after the geomagnetic storm. The result, which is reproduced here in Fig. 27, suggests a redistribution of total ozone content during or about the time of magnetic storm occurrence.

According to KULKARNI, the following points are of interest:

1 In all fourteen cases ozone decreased in the region 50—65° N; the magnitude of the decrease averages about 0.050 cm (= 50 D.U.).

2 South of 50° N, ozone increased in most cases (about 0.025 cm); on no occasion did it decrease in the region south of about 45° N.

3 The latitudinal distribution of total ozone three days after the storm usually seemed to return to about what it was before the storm.

Unfortunately, KULKARNI's profiles do not extend further poleward than 70° N. This restricts the possibility of comparing them with our latitudinal profile of $[\overline{\Delta H}]_{n=1}$ (500 mbar) (Fig. 9). For those latitudes for which the comparison can be made, an excellent negative correlation is found: a large positive value of $[\overline{\Delta H}]_{n=1}$ (500 mbar) in the latitude belt 50—65° N corresponds with a large decrease in ozone amount, whereas for latitudes below 45° N small negative height changes run parallel with small ozone increases.

The above result is in agreement with the observation that total ozone amounts tend to be large when atmospheric pressure (or height of constant pressure levels) in the upper troposphere is low, and vice versa (NORMAND, 1953). However, according to the annual report 1964—'65 of CSIRO, Melbourne, KULKARNI's result cannot be explained by advection processes, since, as is stated there, variations in ozone concentration are not related to systematic changes in upper level circulation patterns.

We have studied the flare-ozone relation* for our flare sample given in Table II.

During the IGY/IGC period 64 ozone stations were in operation throughout the world (53 in the northern and 11 in the southern hemisphere). Unfortunately, ozone observations are not made as regularly as aerological observations. In order to apply the same analysis method to ozone data as we have done to height data, we need observations on at least the day of the flare and the day before the flare outburst.

The change in total ozone amount between the first ozone observation after the flare and the ozone observation 24 hours earlier at a given station is denoted by ΔO_3. (Ozone observations are assumed to be made at 12h local time). At a large number of the 64 ozone stations only a small fraction of the 81 flare cases coincided with dates on which observations were available for the day itself and the day before. Nevertheless, we decided to evaluate the available data and computed mean 24-hour ozone changes after a flare ($\overline{\Delta O_3}$) for all stations.

In view of the relatively small number of stations covering the globe, the $\overline{\Delta O_3}$ values were not plotted on a geographic map, but on a one-dimensional graph as

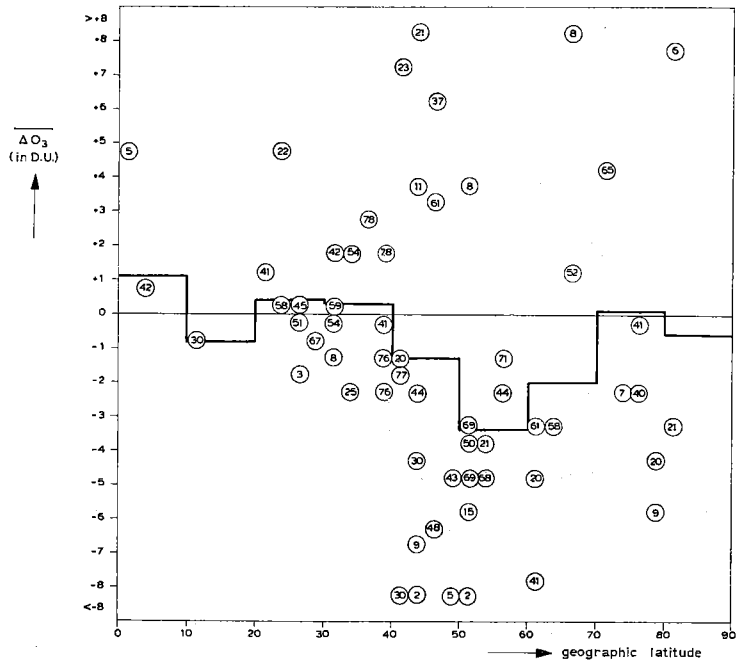

Fig. 28 Mean interdiurnal changes in total ozone amount after a flare. Circles indicate mean values for individual ozone stations, with inside the circles the number of cases. Horizontal lines indicate the mean of all available cases within 10° latitude zones.

* The data on total ozone for the period July 1957 through December 1959 were kindly supplied by J. LONDON, H. A. O., BOULDER, COL.

shown in Fig. 28. Small circles indicate values of $\overline{\Delta O_3}$ for each station; stations are arranged according to geographic latitude (no distinction is made between northern and southern latitudes). Inside each circle the number of available pairs of O_3 observations (at most 81) are indicated. (3 stations with zero available cases have been omitted).

At 40 of the remaining 61 stations $\overline{\Delta O_3}$ is negative; 19 out of the 24 stations at latitudes higher than 50° have a negative $\overline{\Delta O_3}$ value. Taking the mean of all available ΔO_3's in a zone of 10° latitude, we see that only a few of these means show low positive values, while high negative values occur especially in the 40—70° belt.

This result is in good accord with the effect discovered by KULKARNI (see foregoing sub-section). Actually, KULKARNI found the effect to occur on the day of a severe geomagnetic storm, whereas our result relates to the first ozone observation after a flare. Since geomagnetic storms mostly occur within a day or so after a flare, we are inclined to assume that the effect of ozone decrease in the 40—70° latitude belt lasts for some 24 hours, or at least is not reversed during the first 24 hours after a flare.

In view of the fact that the large ozone decreases are not apparently balanced by equally large ozone increases elsewhere, we draw the further conclusion that the ozone decreases are not the result of a redistribution through atmospheric motions, but may rather be considered due to destruction of ozone in the latitude belt concerned.

The maximum ozone decrease is found between 50 and 60°; the mean value of — 3.4 D.U. is found to be significant at the 1% level of statistical significance. Even if we consider all available ΔO_3's over all latitudes, the total number of ΔO_3's being 2282, then the mean is significantly negative beyond the 5% level. The differences between the mean values of $\overline{\Delta O_3}$ for the 10-degree latitude belts (tested by means of the analysis of variance) are found to be real, i.e. the hypothesis that the theoretical mean value of $\overline{\Delta O_3}$ is the same for all latitudes (north of 20° N) must be rejected at the 5% level.

A question of great importance is at what height in the atmosphere the ozone decrease takes place after a flare. Unfortunately, this point cannot be investigated thoroughly, due to the lack of data with respect to the vertical distribution of ozone during the IGY/IGC period. All available data on this subject have been published recently by H. U. DÜTSCH and C. L. MATEER in 'Uniform Evaluation of Umkehr Observations from the World Ozone Network', NCAR, Boulder, Col., August 1964.

Only at the ozone station Arosa (46°47′ N, 09°40′ E), where quite a large number of umkehr observations have been made, did some pairs of observations (observations on two successive days) coincide with flares from our sample. For only 20 flares (3 in 1957, 16 in 1958 and 1 in 1959) did we have the necessary data at our disposal (vertical ozone distribution shortly after the flare and on the preceding day).

In these 20 flare cases $\overline{\Delta O_3}$ was calculated for each of the nine standard ozone layers. The result is given in Fig. 29 together with the mean vertical distribution of ozone on the day preceding the flare. A general decrease of ozone content is found, as expected on the basis of Fig. 28 (mean decrease of total ozone for these 20 cases is 12.5 D.U.). The greatest decreases appear to be concentrated in the lower atmospheric layers, 500—250 mbar, 250—125 mbar and 125—62.5 mbar. The maximum decrease is found in the 250—125 mbar layer in which the tropopause layer is generally found. However, only the ozone decrease in the lowest layer (500—250 mbar), where the standard deviation of ΔO_3 is only half as great as in the first two layers above it, is statistically significant at the 5% level.

Though by means of Fig. 29 we have obtained an estimate of the ozone decrease in the lower stratosphere during the first 24 hours after a flare, the actual rate of ozone removal cannot easily be determined. Assuming that the ozone decrease in the lower stratosphere, being of the order of 5 D.U., has been established in 1 hour, the rate of ozone removal would be of the order of 10^6 molec cm^{-3} sec^{-1}. As we saw in section IV.2.2, a rate of removal of this order of magnitude can be explained by proton-produced electrons, through the intermediary of water vapour.

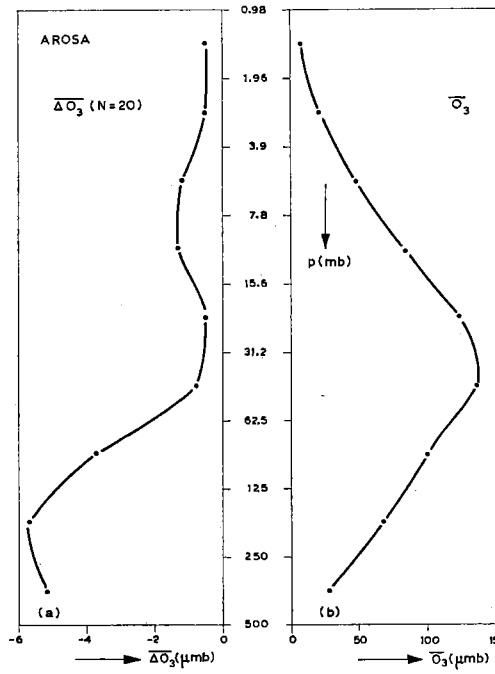

Fig. 29 Mean interdiurnal changes in ozone content of the indicated layers at Arosa, after a flare (a) and mean vertical distribution of ozone on the day preceding the flare (b).

IV.2.4 The effectiveness of the mechanism for ozone removal suggested above largely depends on the moisture conditions in the lower stratosphere. The relation is such that the greater the water vapour concentration, the higher the rate of ozone removal and, we expect, the greater the subsequent temperature and height changes in the troposphere. This link between the lower stratospheric water vapour concentration at a given location and the intensity of the atmospheric temperature and height changes after a flare, at the same place, is put forward here to explain some interesting features of the tropospheric flare effect. In turn, the fact that these features can be attributed to the influence of the initial water vapour distribution lends considerable support to the proposed mechanism of ozone removal by solar protons.

The first feature to be discussed is the maximum height rise of the 500 mbar level, which is located roughly at a latitude of 55 to 60 degrees (see Fig. 11). If it is true that the penetrating solar protons have to encounter a large concentration of water vapour in order to produce a strong solar flare effect, the location of the maximum of the effect may perhaps be explained as follows:

1 since the upper tropospheric region contains more water vapour than the region above the tropopause, the effect will be most marked when protons actually reach the tropopause;

2 in the polar regions where the tropopause is located at a low altitude (tropopause pressure about 300 mbar in the mean), only the very energetic tail of the proton spectrum which contains only a small number of protons will actually reach the tropopause;

3 moving in the direction of the equator, the tropopause, lying in a steeply inclined plane, is found at gradually lower pressures, so that protons of lower energies which, as we know, are more abundant than those of higher energies, can also reach the tropopause;

4 however, moving further equatorwards, the proton flux that actually reaches the tropopause will at the same time become smaller, due to the influence of the geomagnetic field; solar proton fluxes are negligible at latitudes lower than 50°.

According to these arguments an optimal latitude will occur where the proton influence is at maximum. An idealized diagram of the situation is given in Fig. 30.

A logical consequence of the foregoing discussion would be that the flare effect in the 55—60° latitude belt is stronger when the initial tropopause pressure is low (high tropopause) than when the initial tropopause pressure is high. This has been verified with the aid of the temperature data from Ship B.

The tropopause height (H_t) at Ship B for the epoch $n = -1$ was recorded in each of the flare cases.

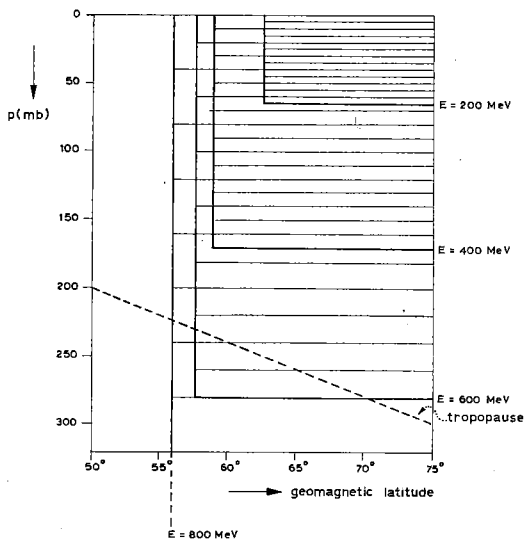

Fig. 30 Location of the tropopause (idealized) and solar proton flux as a function of geomagnetic latitude and height.

By dividing the original sample into two equal sub-samples according to this parameter, the tropopause height of the dividing line is found to be 252 mbar. The mean H_t of the sample with high tropopause is 187 mbar; for the sample with low tropopauses 287 mbar.

Though it is well known that the tropopause level is higher in summer than in winter, our sub-sample consisting of 40 cases with H_t above 250 mbar only slightly correlates with the 42 flares occurring in the summer season. $\overline{\Delta T}_{n=1}$ at Ship B was calculated for the two sub-samples. Fig. 31 shows the result.

The main point we observe in this figure is that the amplitude of the curve of $\overline{\Delta T}\,(p)$ is very much greater for the cases with high tropopause than for the cases with low tropopause. This is indeed what we expect. We have not applied any statistical test to these results. However, the result of a subdivision of the flare cases according to a different parameter, namely the 100 mbar temperature, will be shown for comparison (Fig. 31b). Since for this parameter the curves of $\overline{\Delta T}\,(p)$ are almost equal in amplitude, it seems to be reasonable to assume that the difference in the curves in Fig. 31a is really due to the influence of the initial tropopause height.

A second feature of the tropospheric flare effect that will be discussed here is the essentially cellular character of the effect in the 50—70° latitude belt; large cells of positive height changes of the 500 mbar level alternate with minor cells of negative height changes. In view of the foregoing remarks on a possible relation between the intensity of the positive height changes and the availability of water vapour, one

might inquire whether the location of the cells of great height rise can be connected with certain areas where the moisture content of the tropopause region is greater than in other areas.

In middle latitudes ascending air motions carrying moisture up to the high tropospheric levels are mainly found in frontal areas connected with the extra-tropical cyclones. In upper-air charts these areas may be roughly situated in or rather somewhat ahead of the troughs. In order to find out whether the relation anticipated above in fact exists, we constructed a map of the mean 500 mbar height for the epoch $n = -1$ and superimposed on it the pattern of $\overline{\Delta H_{n=1}}$. Actually this procedure has been followed separately for the flares occurring in both the winter season (October—March) and the summer season (April—September).

The coincidence of the cells of large height rises with troughs in the mean height pattern is clearly indicated in both maps.* Table IX demonstrates this coincidence, showing that the cells with $\overline{\Delta H_{n=1}} > 1.5$ gpdm (each of the two maps contains exactly 7 of these cells) are distributed according to the location of the permanent or semi-permanent upper-air troughs, in exactly the same way. Furthermore, it is found that the maximum values of $\overline{\Delta H_{n=1}}$ in the two deepest troughs (the Canadian trough and the Eastern-Asiatic trough) are nearly twice as high as the maximum values in the minor troughs. This appears to be true in both summer and winter.

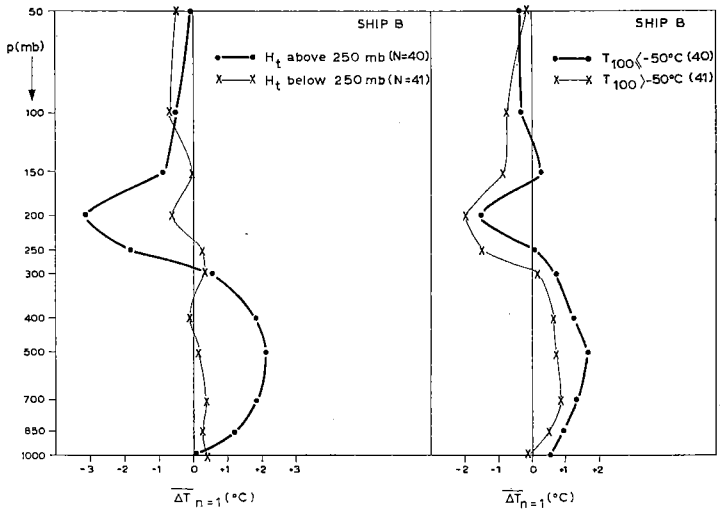

Fig. 31 Vertical distribution of mean temperature changes of the indicated pressure levels at Ship B, after a flare, for cases with initially high and low tropopause (a) and cases with initially high and low temperature at 100 mbar (b).

* The cells of height rises ($\overline{\Delta H_{n=1}} > 1$ gpdm) for the summer and winter season have already been shown in Figs. 6 and 7.

TABLE IX. *Positions and maxima of cells of mean height rise of the 500 mbar level ($\overline{\Delta H_{n=1}} > 1.5$ gpdm) and the associated upper-air troughs.*

season	position	maximum (gpdm)	associated trough
winter	54 N 01 W	2.2	Western-European low latitude trough
summer	52 N 05 E	1.7	
winter	60 N 55 E	1.7	Eastern-European trough
summer	55 N 46 E	1.5	
winter	48 N 110 E	1.9	Eastern-Asiatic trough (upstream)
summer	54 N 129 E	2.0	
winter	48 N 166 E	3.8	Eastern-Asiatic trough (centre)
summer	49 N 159 E	2.9	
winter	56 N 151 W	3.6	Eastern-Asiatic trough (downstream)
summer	46 N 152 W	3.4	
winter	50 N 118 W	1.9	Western-American low-latitude trough
summer	52 N 102 W	1.6	
winter	60 N 66 W	3.8	Canadian trough
summer	54 N 43 W	2.8	

These results seem to confirm the suggestion that the intensity of the tropospheric flare effect largely depends on moisture conditions in the upper troposphere.

In the light of these considerations the occurrence of a negative cell at $n = -3$ in Fig. 14 is not surprising, because negative height changes may be seen as an indication of the approach of a (moist) trough.

IV.3 Radiational temperature changes due to ozone removal in the lower stratosphere, especially during moist and cloudy conditions in the upper troposphere

IV.3.1 Our earlier suggestions that a radiational heat sink might be established due to a decreased ozone concentration in the lower stratosphere has been verified numerically.

In doing so two different amounts of ozone reduction have been used, both with a maximum in the lower stratosphere (see Fig. 32). As reference distribution a somewhat idealized curve has been assumed, which nevertheless represents quite well conditions occurring at middle latitudes in spring. The total amount of ozone defined by the curve is about 330 D.U. The amounts of ozone removed are $12\frac{1}{2}$ and 25 D.U. respectively.

Vertical distributions of temperature (ARDC Model Atmosphere) and water vapour used in the computations are given in Table X. The moisture distribution compares with the annual average conditions at middle latitudes, while for the third

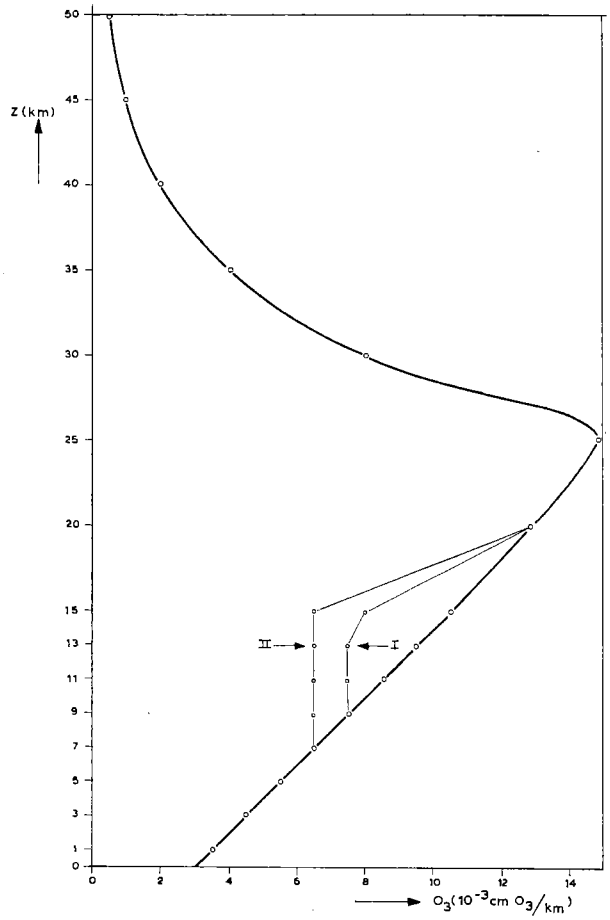

Fig. 32 Reference vertical distribution of ozone, with two different amounts of ozone removal indicated.

radiative constituent, carbon dioxyde, 0.0456 percent by weight has been taken, with uniform distribution in the vertical.

In the experiment the heating and cooling rates due to short wave absorption and long wave radiational heat loss for the given temperature distribution have been computed for the normal case in which no ozone has been removed, and for cases I and II. Furthermore, the differences have been computed in radiative equilibrium temperature as a function of height, between the normal state and any one of the states I and II.*

* The calculations were performed by computer at the Meteorological Institute of the University of Munich. The preparation and programming was carried out by R. GEBHART on the basis of a radiation model, which he used for the investigation of the diurnal variation of temperature (GEBHART, 1965). Details of the radiation model are given in the work by MANABE and MÖLLER (1961).

TABLE X. *Vertical distribution of temperature and water vapour mixing ratio used as initial conditions in the numerical experiment discussed in IV.3.1.*

altitude (km)	temperature (°K)	mixing ratio (g/g)
50	291	2×10^{-5}
45	276	2×10^{-5}
40	261	2×10^{-5}
35	246	1.6×10^{-5}
30	231	1×10^{-5}
25	216	6.5×10^{-6}
20	216	4.4×10^{-6}
15	216	5.5×10^{-6}
13	216	1×10^{-5}
11	216	3×10^{-5}
9	229	1×10^{-4}
7	242	4×10^{-4}
5	255	1×10^{-3}
3	268	2×10^{-3}
1	281	4×10^{-3}
0	287	6×10^{-3}

The results of the numerical experiment are given in Table XI. It is found that the ozone decrease leads to a cooling of the layer from which the ozone has been removed. The cooling is due to a decrease in short wave absorption as well as to an increase of the long wave divergence in the layer concerned.

TABLE XI. *Computed changes in heating rates and radiational equilibrium temperatures, for two different cases of removed ozone in the lower stratosphere.*

	Case I				Case II			
(km)	$\Delta(\delta Ts)$ (10^{-3} °C/min)	$\Delta(\delta TL)$	$\Delta(\delta TN)$	ΔTE (°C)	$\Delta(\delta Ts)$ (10^{-3} °C/min)	$\Delta(\delta TL)$	$\Delta(\delta TN)$	ΔTE (°C)
50	0	+ .003	+ .003	0	0	+ .006	+ .006	+ .1
45	0	+ .005	+ .005	0	0	+ .009	+ .009	+ .1
40	0	+ .006	+ .006	0	0	+ .011	+ .011	+ .1
35	0	+ .008	+ .008	0	0	+ .015	+ .015	+ .1
30	0	+ .011	+ .011	+ .1	0	+ .019	+ .019	+ .2
25	0	+ .013	+ .013	+ .1	0	+ .024	+ .024	+ .2
20	0	+ .011	+ .011	+ .2	0	+ .021	+ .021	+ .4
15	— .017	— .014	— .031	— 1.9	— .025	— .019	— .044	— 2.9
13	— .012	— .017	— .029	— 1.5	— .018	— .023	— .041	— 2.3
11	— .004	— .009	— .013	— .9	— .008	— .016	— .024	— 1.6
9	0	— .001	— .001	— .3	— .003	— .007	— .010	— .8
7	0	0	0	— .2	0	0	0	— .3
5	0	0	0	0	0	0	0	— .1
3	0	0	0	0	0	0	0	0
1	0	0	0	0	0	0	0	0

Δ = deviation from the normal
δTs = heating rate due to short wave radiation
δTL = heating rate due to long wave radiation
δTN = net rate of radiational change of temperature
TE = radiational equilibrium temperature

While the first contribution is trivial, the second may be explained by a diminished downward long wave flux from the relatively warm ozone layers above. Though the deviation from normal of the net rate of radiational temperature change is generally as expected, the absolute values appear to be far too small to account for the observed cooling related to the tropospheric flare effect. Only when radiative equilibrium is reached does the magnitude of the effect compare with the observed cooling, but due to the very slow rate at which the equilibrium is reached we cannot but conclude that the above cooling mechanism cannot account for any significant cooling during the first few hours after a flare.

IV.3.2 Though the cooling effect of a diminished ozone concentration seems to be small, one can envisage the possibility that under certain conditions such slight cooling might act as a starter for some other mechanism, which in its turn could amplify the cooling effect. There is the possibility for instance that slight cooling of an initially unsaturated tropopause layer might lead to the formation of a haze or cirrus layer.

The above idea seems promising for a number of reasons. In the first place such a mechanism would offer an additional argument for the observation that the intensity of the flare effect depends on the moisture conditions in the upper troposphere (see section IV.2.4). Second, the proposed mechanism would explain the observation by ARCHENHOLD (1938) that the frequency of occurrence of halos on the day of a solar flare and also on three subsequent days is higher than during six days preceding the flare. The result is based on halo observations made in Germany during the years 1935—1937. In theory too, an initially slight cooling effect near the tropopause may be regarded as favourable for the occurrence of condensation there. The Clausius-Clapeyron equation shows that a cooling of 5° C under tropopause conditions, e.g. a cooling from — 50 to — 55° C, will nearly halve the saturation vapour pressure. Besides, a cooling at the tropopause increases the vertical temperature gradient in the upper troposphere, which will cause an intensification of turbulent diffusion of water vapour from below towards the tropopause. Thus both conditions favourable for the occurrence of condensation, cooling and moisture supply, appear to be fulfilled.

The formation of high-level cirrus cloudiness as a result of solar corpuscular radiation has also been proposed by ROBERTS (1965). In the chain of events which he suggests a principal role is played by auroras, which are to be attributed to a slower component of solar particles than we have been envisaging here. For this reason ROBERTS' proposal will not further be discussed here, although the production of freezing nuclei at stratospheric levels, which he speculates on, might be of importance in our case too.

IV.3.3 In view of the possibility of haze or cloud formation near the tropopause as a result of an initial cooling mechanism, we shall now consider the radiative influence of a high-level cirrus or haze layer.

This problem was studied by MÖLLER in 1942. MÖLLER's calculations deal with the radiative temperature changes in a layer with discontinuous changes in water vapour and haze concentrations. For a layer 1.67 km deep, with a temperature of 10° C at the bottom and a lapse rate of 6° C/km, a relative humidity of 100% throughout the layer and 20% above the layer, and with a haze particle concentration proportional to the water vapour mixing ratio at 100% relative humidity, the calculations resulted in a cooling rate at the top of the layer of — 11.9° C/day. Such rapid cooling at the upper boundary is mainly the result of the discontinuity of the radiating constituents causing a strong outgoing radiation which cannot be compensated by the very small downward flux.

STALEY (1965), who studied radiation processes occurring at temperature inversions in the troposphere, also found that, in the case of rapidly decreasing water vapour mixing ratios upward from the inversion base, maximum cooling amounted to several degrees per day in the vicinity of the inversion base.

Besides these theoretical studies, two recently published observational studies give evidence of a strong cooling effect by cirrus layers and ice crystals suspended in the air.

Very strong cooling at 150 mbar, probably due to radiative heat loss from the anvil clouds of tall thunderstorms, was observed by LONG (1966) in a series of soundings at intervals of several hours. The rate of cooling was 5—7° C in 1½—2 hours, which can be shown to be unusually high in comparison with other temperature changes at 150 mbar (e.g. by advection).

According to GOTAAS and BENSON (1965) sharp decreases in air temperature in the interior of Alaska are associated with the occurrence of ice fog. A few of these cases were studied in detail. It was found that the observed cooling rates from the snow-covered surface up to 3 km were too high to be satisfactorily explained by advection and/or radiative heat loss from the snow and from the water vapour content of the air. The authors showed that the excess cooling could be accounted for by black body radiation from the ice crystals suspended in the air at a concentration of 1 crystal per cm^3.

From the above considerations it appears that a haze or cirrus layer or even a discontinuity in the vertical distribution of water vapour may be very effective in producing strong radiative cooling in a relatively thin layer of the atmosphere.

If therefore a high level cirrus deck were formed after a solar flare, the likelihood of the formation being discussed in the foregoing subsection, the creation of a radiative heat sink amounting to a cooling of several degrees per day would certainly be possible. Since a sharp discontinuity in the vertical distribution of water vapour near the tropopause would have the same cooling effect, there is also a possibility that the

destruction of water vapour involved in the ozone decomposition process (see IV.2.2) may be effective enough to produce a strong radiative heat loss from the tropopause region, without any cloud formation being present.

IV.4 Model of a heat sink at the tropopause as a possible explanation of the observed height changes in the troposphere

From the mainly theoretical arguments presented above the conclusion may be drawn that the creation of a radiational heat sink at the tropopause by the action of solar protons is at least plausible. Taking the suggested mechanisms into account the most likely characteristics of such a heat sink are the following:

a the horizontal extent of the heat sink is something of the order of the dimensions of a semi-permanent upper-air trough;

b the vertical extent is fairly limited, rapid cooling only occurring in a region as shallow as a few kilometres;

c the rate of cooling in the core of the heat sink may be of the order of 5—10° C per day in an individual case, but in the mean amounts to a few degrees per day;

d the core of the heat sink is located near the tropopause.

In this section we shall discuss, both qualitatively and quantitatively, the characteristics of the heat sink which can be deduced from the observed height and temperature changes after a solar flare. We shall see that these characteristics compare fairly well with those given above.

First some qualitative statements will be made about the influence of a heat sink on the pressure distribution. The effect in the first instance will be a rapid re-establishment of the hydrostatic equilibrium, mainly consisting of a shrinking of the column of air above the heat sink. This in turn causes a lowering of pressure levels with respect to the environment in the layer above the heat sink, followed by an inflow of air in the direction of the pressure gradient force. In this process, known as the isallobaric convergence process, the pressure gradient force is not balanced by the coriolis force; the isallobaric wind will therefore blow towards the region of the greatest negative pressure tendency. The process as outlined above has already been discussed in the literature on the subject, mostly in connection with the problem of a stratospheric influence on tropospheric circulation changes (e.g. THOMAS (1935)).

The isallobaric convergence in the upper layers will give rise to isallobaric divergence below the heat sink, which as a secondary effect will lag behind the inflow of air above. We may therefore expect that below the heat sink the pressure will increase. The development of a circulation system, as sketched in Fig. 33, may be expected in the case of a heat sink in the lower stratosphere with a maximum near the tropopause.

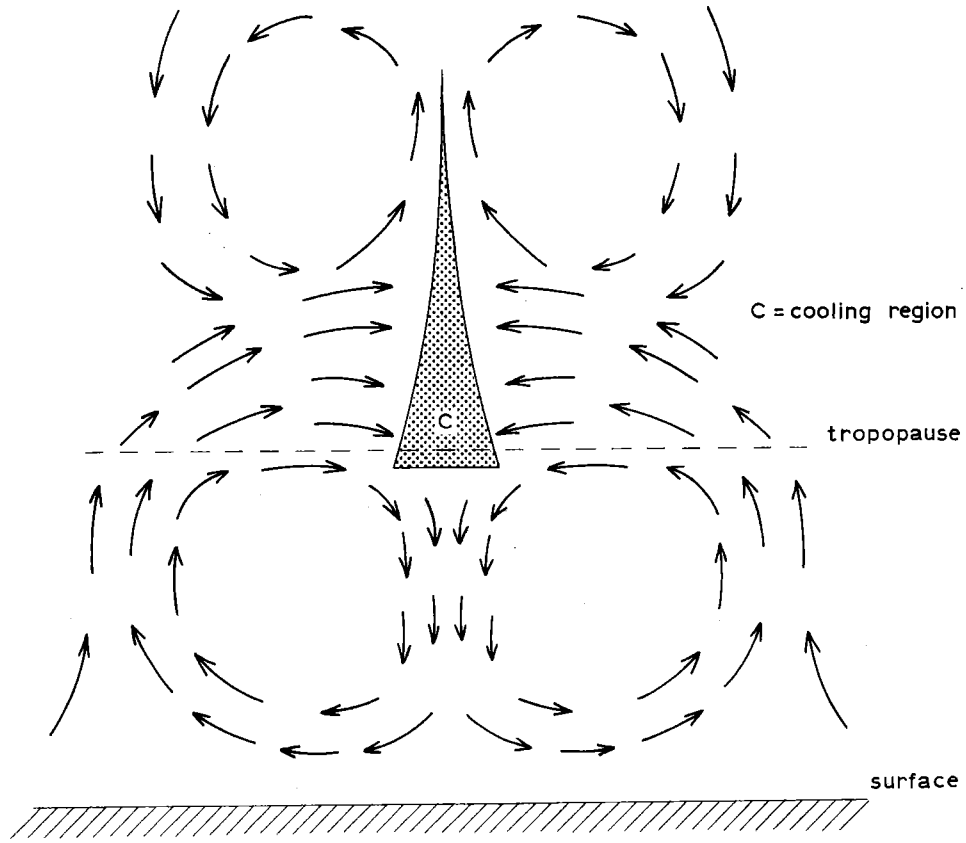

Fig. 33 Sketch of the proposed circulation system initiated and maintained by a heat sink at the tropopause.

The downdraft in the troposphere, which will lead to adiabatic heating of the air, is thought to be responsible for the large temperature rise in the middle and lower troposphere (see Fig. 17). The updraft in the stratosphere is probably small, if not fully compensated by the downward motion due to shrinking of the column of air above the heat sink. Therefore, the original vertical distribution of the cooling in the lower stratosphere will be only slightly modified by adiabatic temperature changes, so that the observed profile represents the shape of the heat sink fairly well.

We shall now elaborate the above considerations quantitatively.

On the basis of the model of convergence and divergence outlined above we shall try to find an analytical expression describing the pressure variations in the troposphere due to a heat sink near the tropopause. A more general expression relating pressure variations in the atmosphere to local heating or cooling has been given by SCHMIDT (1946):

$$\frac{\partial p}{\partial t}(x, y, z) = g \int_z^\infty \frac{\partial \rho}{\partial t}\, dz + \frac{g}{f^2} \int_0^\infty \left(\frac{\partial^2}{\partial x^2} + \frac{\partial^2}{\partial y^2}\right) \frac{\partial p}{\partial t}\, dz\, e^{-k_\pi z} \tag{1}$$

where x, y, z are the Cartesian coordinates, $\frac{\partial p}{\partial t}$ and $\frac{\partial \rho}{\partial t}$ are the local changes of pressure and density respectively, g is the acceleration of gravity, f is the coriolis parameter and k_π is a constant relating to the compressibility of the atmosphere.

In order to solve the integral equation we assume the vertical variation of $\frac{\partial p}{\partial t}$ and $\frac{\partial \rho}{\partial t}$ to be independent of the horizontal coordinates, so that we may write

$$\frac{\partial p}{\partial t}(x, y, z) = A(x, y) \frac{\partial p}{\partial t}(z) \text{ and } \int_z^\infty \frac{\partial \rho}{\partial t}\, dz = D(x, y)\, R(z) \tag{2}$$

Substitution in (1) gives:

$$\frac{\partial p}{\partial t}(z) = g \frac{D(x, y)}{A(x, y)} R(z) + \frac{g}{f^2} \frac{\left(\frac{\partial^2}{\partial x^2} + \frac{\partial^2}{\partial y^2}\right) A(x, y)}{A(x, y)} \int_0^\infty \frac{\partial p}{\partial t}(z)\, dz\, e^{-k_\pi z} \tag{3}$$

Equation (3) can be solved by integration according to z. Re-substitution in (3) gives

$$\frac{\partial p}{\partial t}(z) = g \frac{D(x, y)}{A(x, y)} R(z) + \frac{\frac{g^2}{f^2} R_1 \frac{\left(\frac{\partial^2}{\partial x^2} + \frac{\partial^2}{\partial y^2}\right) A(x, y)}{A(x, y)} \cdot D(x, y)\, e^{-k_\pi z}}{1 - \frac{g}{f^2 k_\pi} \cdot \frac{\left(\frac{\partial^2}{\partial x^2} + \frac{\partial^2}{\partial y^2}\right) A(x, y)}{A(x, y)}} \tag{4}$$

where $R_1 = \int_0^\infty R(z)\, dz$.

Equation (4) will be used to deduce from the observed height (pressure) changes the shape of the original heat sink. First we write the equation in a simpler form,

$$\frac{\partial p}{\partial t}(x, y, z) = g\, D(x, y)\, R(z) + \alpha\, D(x, y)\, R_1\, e^{-k_\pi z} \tag{5}$$

where

$$\alpha = \frac{\frac{g^2}{f^2} \left(\frac{\partial^2}{\partial x^2} + \frac{\partial^2}{\partial y^2}\right) A(x, y)}{1 - \frac{g}{f^2 k_\pi} \frac{\left(\frac{\partial^2}{\partial x^2} + \frac{\partial^2}{\partial y^2}\right) A(x, y)}{A(x, y)}}$$

For our purpose equation (5) can be interpreted as follows:

$\frac{\partial p}{\partial t}(x, y, z) = \frac{\partial p}{\partial t}(z)\, A(x, y)$ is the observed pressure variation,

$\frac{\partial p}{\partial t}(z)$ giving the vertical profile and $A(x, y)$ giving the horizontal distribution.

The first term on the right hand side is the pressure variation due to the re-establishment of the hydrostatic equilibrium after the initial disturbance of the heat balance. The horizontal distribution $D(x, y)$ of this part of the pressure variation will be essentially equal to the horizontal distribution of the heat sink. The function $R(z)$, which of course is closely related to the vertical structure of the heat sink, will be discussed later on. For the moment we shall only use the condition that $R(z)$ vanishes at the surface, since density variations occurring as a result of the re-establishment of the hydrostatic equilibrium in themselves cannot lead to pressure variations at the ground. Thus for $z = 0$ the observed pressure variation is equal to the second term on the right hand side of equation (5), which term describes the pressure variation due to isallobaric divergence. For $z = 0$ we may thus write

$$\frac{\partial p}{\partial t}(x, y) = \alpha D(x, y)\, R_1 \tag{6}$$

Equation (6) will now be applied to the observed pressure variation at Ship B and at the centre of the cell of pressure rise in which Ship B is located, in order to solve the unknown expressions $D(x, y)$ and R_1. At the centre of the cell of pressure rise $D(x, y)$ and $A(x, y)$ are equal to one. If we denote α at Ship B by α_B and α in the centre by α_C, then by using equation (6) we get

$$\frac{\partial p}{\partial t}(\text{Ship B}) = \alpha_B\, D(\text{Ship B})\, R_1 \tag{7a}$$

$$\frac{\partial p}{\partial t}(\text{centre}) = \alpha_C\, R_1 \tag{7b}$$

Since $\frac{\partial p}{\partial t}(\text{Ship B}) = A(\text{Ship B})\, \frac{\partial p}{\partial t}(\text{centre})$, we find

$$D(\text{Ship B}) = A(\text{Ship B})\, \frac{\alpha_C}{\alpha_B} \tag{8}$$

A (Ship B), α_C and α_B have been evaluated on the map of mean 500 mbar height changes given in Fig. 3.

With the following values for the constants appearing in the expression for α:

$g = 981$ cm/sec^2

$f = 1.1 \times 10^{-4}$ sec^{-1}

$k_\pi = 9.1 \times 10^{-7}$ cm^{-1}

we find

$$D(\text{Ship B}) = 0.73 \times \frac{0.878}{0.647} = 0.990$$

Assuming a radial symmetric distribution of the form $D(r) = e^{-\frac{r^2}{b^2}}$ and using the fact that the distance r between Ship B and the centre is about 380 km, we find that the width of the distribution function b is 3800 km. Since the semi-permanent upper-air troughs in the mid-latitude belt are of the same dimensions, this implies that the heat sink must be distributed fairly uniformly over the trough area, the intensity at the boundaries of the trough still being nearly one half of the intensity in the centre. In view of the suggested mechanism by which the heat sink is created, such a uniform distribution within the trough region seems to be fairly plausible especially since the influx of protons will not show great longitudinal differences.

From the computed values of D (Ship B) and α_B, and using the observed value of $\frac{\partial p}{\partial t}$ (Ship B), R_1 may be evaluated from equation 7a. The pressure variations at Ship B have been computed from the observed height variations $\overline{\Delta H}_{n=1}$ (see Fig. 13). The equivalent pressure variation of $\overline{\Delta H}_{n=1}$ at 1000 mbar has been taken for $\frac{\partial p}{\partial t}$ at the ground; it was found to be 1.2 mbar. This results in a value of $R_1 = -1.88 \times 10^6$ mbar sec^2, which will be used later on to compute the other characteristics of the heat sink.

The next step will be to evaluate the height of the core of the heat sink. So far the maximum of the heat sink has been positioned tentatively at the tropopause level. If we now only assume that the sink has a sharp lower boundary at some level z_t, with the maximum of the sink coincident with this lower boundary, z_t may be easily deduced from equation (5) in conjunction with the profile of the observed pressure changes at Ship B. Since at all levels below z_t, $R(z)$ will be zero, equation (5) for the location Ship B reduces to

$$\frac{\partial p}{\partial t}(z) = \alpha_B \, D \text{ (Ship B) } R_1 \, e^{-k_\pi z} \tag{9}$$

Since in particular $\frac{\partial p}{\partial t}(z_t) = \alpha_B \, D\text{(Ship B) } R_1 \, e^{-k_\pi z_t}$, z_t can be found as the height of the point of intersection between the observed $\frac{\partial p}{\partial t}(z)$ curve and the function $\alpha_B \, D$ (Ship B) $R_1 \, e^{-k_\pi z}$.

In this way it is found that $z_t = 12.5$ km, which is indeed quite close to the tropopause at Ship B, especially in cases where the tropopause is relatively high. In these cases, as we have seen, the flare effect is more pronounced than in cases of a relatively low tropopause. Furthermore, it is very interesting to observe that the computed z_t perfectly coincides with the height of the observed maximum cooling, which is found at 200 mbar ($\sim$ 12 km) (see Fig. 17). This may be seen as a first indication that the

initially established heat sink is only slightly modified by the dynamic motion afterwards.

As we have already seen, $R(z)$ will be zero at z_t and all levels below. If furthermore, as we have assumed, the heat sink has its maximum at z_t, we can try to specify the vertical distribution $f(z)$ of the heat sink. A cooling $\frac{\partial T}{\partial t}$ will initiate a density variation $\frac{\partial \rho}{\partial t}$, at constant pressure, which may be written as

$$\frac{\partial \rho}{\partial t} = -\frac{\rho}{T}\frac{\partial T}{\partial t} \tag{10}$$

Since the cooling takes place in the lower stratosphere, we may assume isothermal conditions, so that

$$\frac{\partial \rho}{\partial t}(z) = -\frac{\rho_t}{T} e^{-\frac{z}{H}} \frac{\partial T}{\partial t}(z) \tag{11}$$

where ρ_t is the density at the lower boundary and H is the scale height, while z now refers to the vertical distance of a certain level with respect to z_t. If $\frac{\partial T}{\partial t}(z)$ is written as $\Delta T \,.\, f(z)$, then we find

$$R(z) = \int_z^\infty \frac{\partial \rho}{\partial t}\, dz = -\frac{\Delta T}{T}\rho_t \int_z^\infty e^{-\frac{z}{H}} \cdot f(z)\, dz \tag{12}$$

It can be shown that the conditions: $R(0) = 0$ and $f(z)$ has a maximum where $z = 0$, are fulfilled if $f(z)$ is given by the following function:

$$f(z) = e^{-\frac{z}{a}} \left[1 - \left(\frac{1}{H} + \frac{1}{a}\right) z\right] \tag{13}$$

Integration of (12) gives

$$R(z) = \frac{\Delta T}{T}\rho_t\, e^{-\gamma z} \,.\, z \tag{14}$$

where $\gamma = \frac{1}{H} + \frac{1}{a}$.

From (14) we proceed to calculate R_1

$$R_1 = \int_0^\infty R(z)\, dz = \frac{\Delta T}{T}\rho_t \int_0^\infty e^{-\gamma z} \,.\, z\, dz = \frac{\Delta T}{T}\frac{\rho_t}{\gamma^2} \tag{15}$$

Combining (14) and (15) gives

$$R(z) = \gamma^2 \, e^{-\gamma z} \, . \, z \, R_1 \tag{16}$$

Introduction of (16) in equation (5) then gives an expression from which γ can be evaluated.

Applied to Ship B, this expression is as follows:

$$\frac{\partial p}{\partial t}(z) = g \, D \text{ (Ship B) } R_1 \, \gamma^2 \, e^{-\gamma(z - z_t)} \, (z - z_t) + \\ + \alpha_B \, D \text{ (Ship B) } R_1 \, e^{-k_\pi z} \tag{17}$$

At $z = 13.5$ km ($z - z_t = 1$ km), i.e. at 150 mbar, the observed pressure variation is 0.16 mbar. Inserting this value and all other known values in equation (17) we find $\gamma = 1.07 \times 10^{-6}\text{cm}^{-1}$. With $\frac{1}{H} = 1.57 \times 10^{-6}\text{cm}^{-1}$, which means a stratospheric temperature of 220° K, the resulting value for $\frac{1}{a}$ is $-0.5 \times 10^{-6}\text{cm}^{-1}$.

The vertical distribution of the heat sink $f(z)$ then takes the form:

$$f(z) = e^{0.05(z - z_t)} \, [1 - 0.11 \, (z - z_t)] \tag{18}$$

As may be seen in Fig. 34, this distribution function shows some similarities to the observed profile of lower stratospheric cooling, again suggesting that the initial cooling is relatively unchanged by adiabatic processes. Furthermore, the prognosis made from theoretical arguments that the vertical extent of the sink is fairly limited is substantially confirmed.

Finally, ΔT has been computed from the formula for R_1 given in (15). With a value of $-1.7°$ C, it almost exactly equalled the observed maximum cooling, which was $-1.8°$ C.

Our conclusions are as follows:

1 The model of the heat sink which, by means of SCHMIDT's equation for the local pressure variation, can be derived from the observed pressure variations, is largely compatible with the model which has been deduced from the considerations concerning the mechanism by which the heat sink is created. This implies that the suggested mechanism is probably right.

2 As a by-product of our calculations, we have found that in the lower stratosphere adiabatic processes modifying the diabatic heat sink are probably of low intensity, since the observed cooling has the same characteristics as the computed heat sink.

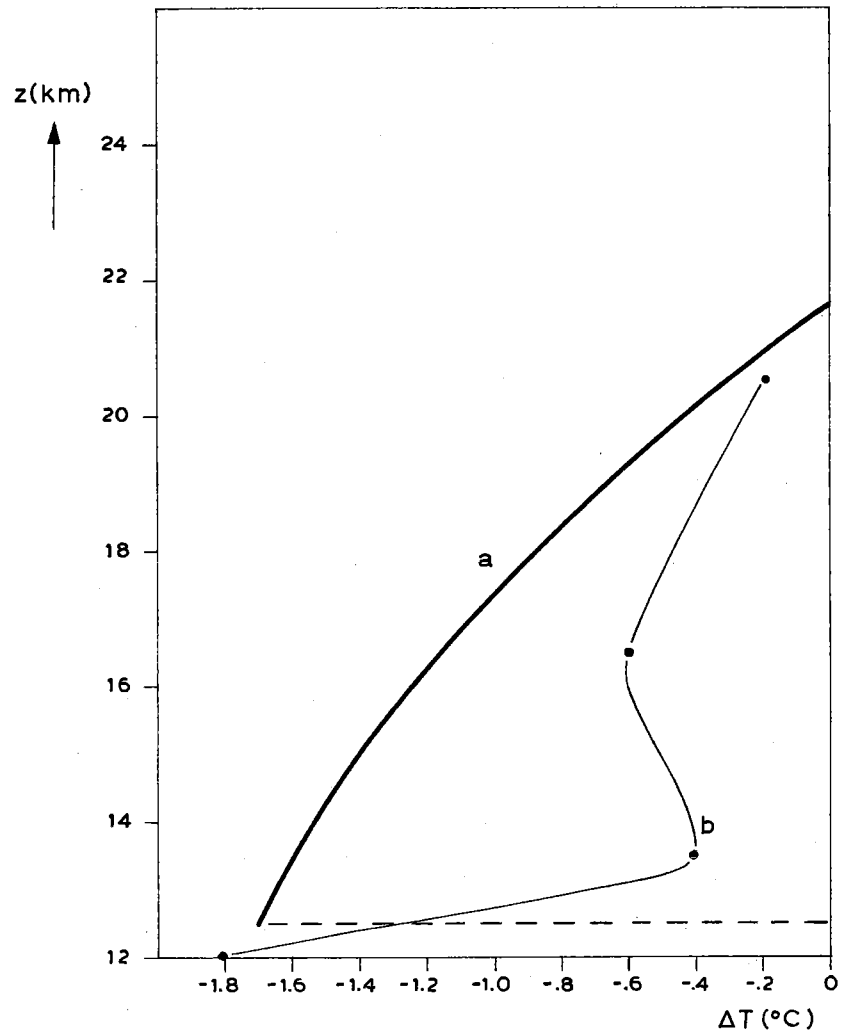

Fig. 34 Vertical distribution of observed mean temperature changes after a flare (b), compared with the vertical distribution of the computed heat sink.

V. THE TROPOSPHERIC FLARE EFFECT AS A POSSIBLE FACTOR IN THE OCCURRENCE OF LONG-TERM WEATHER ANOMALIES

V.1 The flare effect in an individual case

Before discussing the consequences of the flare effect on the weather, in both the short and the long term, we should first like to find out whether the effect discovered as a mean of 81 flare cases manifests itself in an individual flare case. Two flares, both occurring in 1960, have been examined for their tropospheric effect.*

The first flare taken was the one that occurred on June 1, 1960, 09.00 GMT, being of importance 3^+. The reason for selecting this flare was the fact that HARTMANN (see Table I) attributed to it a general increase in the northern hemisphere 500 mbar temperatures from June 1 to June 2. We constructed a cross-section of $\Delta H(p, t)$ and a graph of $\Delta T_{n=1}(p)$ for this particular flare at our test station Ship B. As is clearly shown by the Figs. 35a, b, the tropospheric reaction to this flare was generally the same as the mean reaction derived from the original flare sample (e.g. compare Fig. 35a with Fig. 14 and Fig. 35b with Fig. 17). The drop in temperature at the tropopause level and the height rise of constant pressure levels in the upper troposphere were about 5 times as great as the corresponding changes in the mean effect over 81 cases.

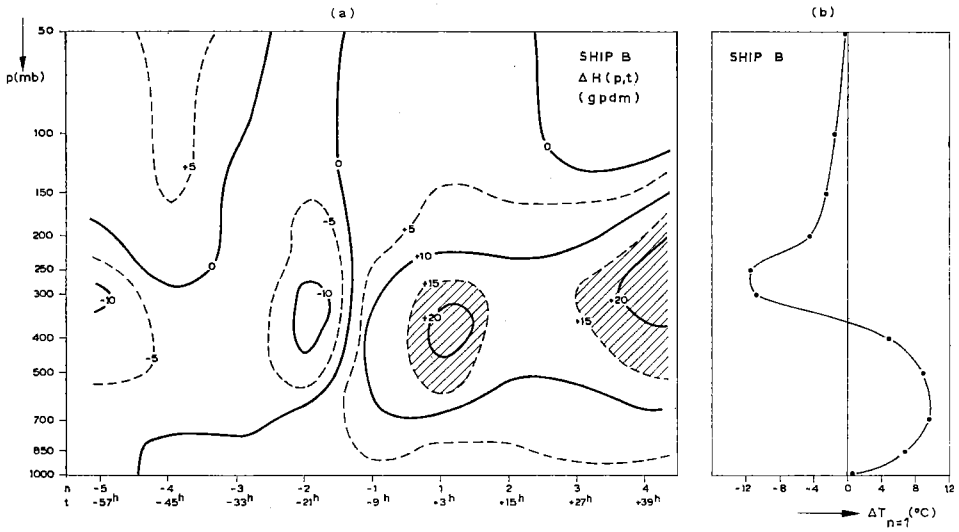

Fig. 35 Height and temperature changes at Ship B, related to the solar flare of June 1, 1960.

* Since these two flares are not contained in the original flare sample, the results at the same time form a verification of the proposed effect on independent data.

The second flare, the 2+ flare of March 29, 07.10 GMT, was chosen because of its presumed effect on the earth's rotation rate (DANJON, 1960). According to this author a temporary increase of the length of the day of about one half millisecond was observed after the occurrence of the flare. Effects of this order of magnitude have been observed several times after the eruption of strong flares. Since it has been shown that the yearly variation of the length of the day, being of the order of about 1 msec, can be explained by the seasonal variation of the atmospheric circulation (MUNK and MILLER, 1950), it seems probable that a variation in the length of the day as reported by DANJON can be accounted for by the tropospheric flare effect, which essentially means a latitudinal shift in atmospheric air masses. However, the question will not be discussed in further detail here. We shall return instead to the main point of this section, namely the representativeness of the mean tropospheric flare effect in individual cases.

$\Delta H(p, t)$ and $\Delta T_{n=1}(p)$ at Ship B have been computed for the flare of March, 29 in the same way as before. The cross-section and the graph (not shown here) exhibit the expected features. In addition, we computed the latitudinal profile of $[\Delta H_{n=1}]$ (500 mbar) for this flare in both the northern and the southern hemispheres. The similarity of these profiles to the mean curve based on the 81 flares is striking (compare Fig. 36 with Fig. 9).

Although only two individual flare cases have been examined in this section, it seems reasonable to conclude that the tropospheric effect of an individual flare is very similar in character to the mean tropospheric flare effect.

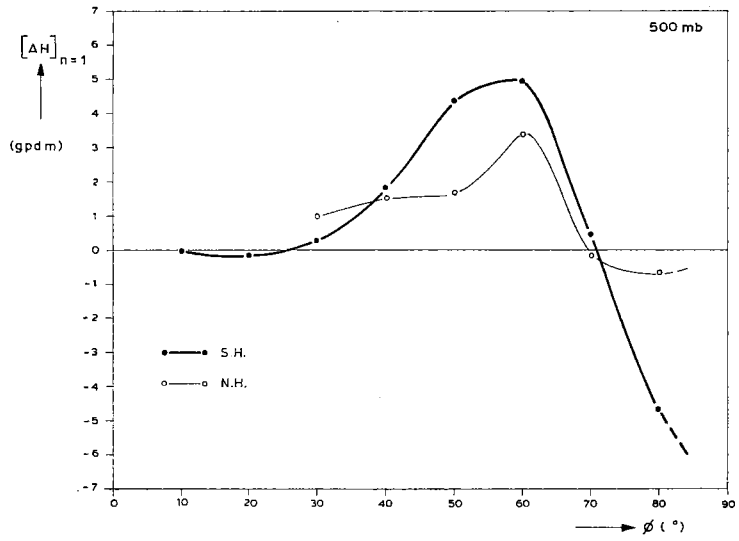

Fig. 36 Zonal averaged height changes of the 500 mbar level for the northern and southern hemisphere, related to the flare of March 29, 1960.

V.2 Increased frequency of meridional circulation types over Western Europe as a result of the flare effect

V.2.1 From the synoptician's point of view one feature of the tropospheric flare effect deserves particular attention, namely the cellular character of the latitudinal shift in air mass. As has been anticipated (see section III.3.3), this feature might well favour an increased meridionality of the atmospheric circulation. In this section we shall consider this point in more detail, especially as far as the western European area is concerned.

German meteorologists have developed a scheme to classify circulation types for the European-Atlantic region. These 'Grosswetterlagen' were introduced in 1952, when HESS and BREZOWSKY published their 'Katalog der Grosswetterlagen Europas'. A daily record of circulation types given in this catalogue goes back as far as 1881. 28 distinct circulation types are defined. The basic idea of isolating so many different types is the changing location of the steering anticyclone in the region concerned. The 28 circulation types can be subdivided into three principal circulation types:
zonal circulations (*Z*), in which the subtropical high is situated at about its normal position; half-meridional (H), in which the subtropical anticyclone shows a north, northeast or northwestward displacement to about 50° N; and meridional circulation (M) or blocking, in which a quasi-stationary high is located between 50° and 70° N.

We have investigated the mean frequency of Z, H and M types for each day during the first week after a flare. The original sample of 81 flares given in Table II has been used. The overall mean frequency of Z, H and M types is 29.6, 26.6 and 43.8% respectively. The deviations in mean frequency from the overall mean for each day are given in Table XII. As is clearly indicated by the figures, the half-meridional and meridional types increase in frequency from the day of the flare onwards at the expense of the zonal type circulations. A maximum of meridional circulation types is reached on the third day. The table as a whole suggests a gradual northward displacement of the subtropical anticyclone in the first three days after a flare, with subsequent southward movement during the fourth and fifth days. Though this course of events is evident in the mean of the 81 flares and also in the means of two subsamples consisting of 40 and 41 flares, the effect is not statistically significant. Nevertheless, it seems worth while taking this effect into consideration in studies of blocking development

TABLE XII. *Deviations in mean frequency of Z, H and M circulation types from the overall mean, for the day of a flare and the first 7 days thereafter.*

	0	1	2	3	4	5	6	7
M	−0.6	−1.8	+5.6	+5.6	−3.1	−6.7	+1.9	−0.6
H	−3.2	+3.0	+0.6	−0.6	+3.0	+4.3	−4.4	−3.1
Z	+3.8	−1.2	−6.2	−5.0	+0.1	+2.4	+2.5	+3.7

in the western European area. The use of the above relationship in extended range forecasting is probably of little advantage, since the sequence of the circulation does not take place after every flare.

V.2.2 In view of the above it seems reasonable to expect that in periods of many flare outbursts the frequency of meridional type circulations in the western European area will be higher than in periods of little flare activity. To investigate this point we first have to find out which periods may be considered to be 'flare-active'. In the 11-year cycle strong flares are observed especially during the years of the maximum phase and they are virtually absent in the minimum phase of the cycle.

As a first approximation, therefore, a subdivision of the available data into years of maximum solar activity and years of minimum solar activity would seem to be sufficient. However, any new study on the difference in pressure distribution between solar maximum and solar minimum would be entirely superfluous, since numerous papers on the subject already exist. We shall give here a brief review of the results.*

WEXLER (1950) examined the 40-year (1899—1939) historical series of northern hemisphere sea-level charts for evidence of the effect. Furthermore, in his paper, he made a comparison with earlier work done by CLAYTON. CLAYTON used data from 200 stations all over the world; his investigation covered the period from 1858—1919 (5 sunspot cycles). In the work of WEXLER the maxima and minima were determined objectively by taking for each cycle the group of three consecutive years showing the highest mean sunspot numbers and the group of three consecutive years having the lowest numbers. Without entering into further details, we reproduce CLAYTON's and WEXLER's curves here. (Fig. 37).

Though the two curves are rather dissimilar in shape, both show a positive pressure difference in mid to high latitudes and negative differences in the sub-tropical to tropical belt.

WEXLER has also shown that, for the 1899—1939 period, separation into winter and summer observations results in almost identical curves. However, curves for individual sunspot cycles were not very consistent from cycle to cycle, so that WEXLER considers the results to be inconclusive.

The Clayton curve in fact extends to approximately 60° southern latitude. In the southern hemisphere positive pressure differences are found southwards of 40° S, and negative pressure differences equatorwards of 40° S. A further study on southern hemisphere fluctuations of sea-level pressure related to sunspots was made by RAMAMURTI (1953). The study was based on pressure data from 19 South-American stations, lying between 5° and 60° S. All available data from the period before 1940 were used.

* Papers only discussing the difference in sea-level pressure between opposite extremes of solar activity for one particular station are disregarded.

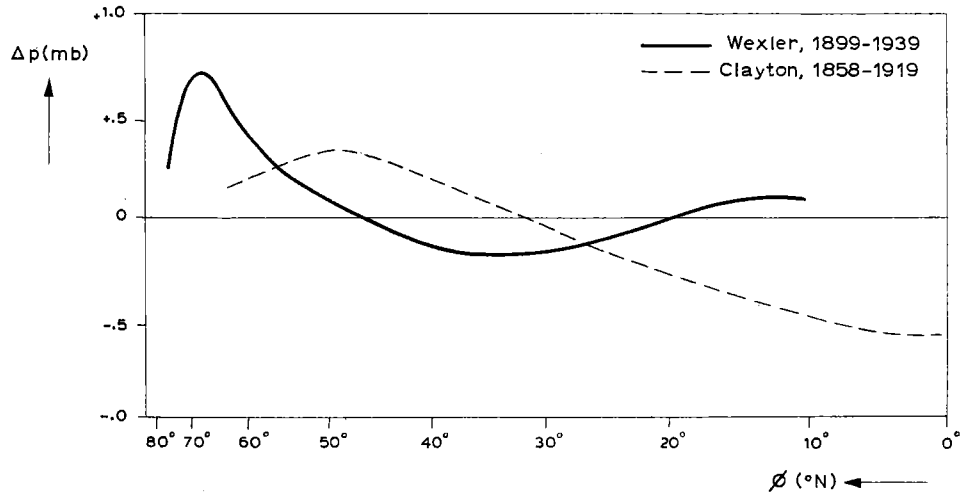

Fig. 37 Mean difference of pressure at sunspot maximum from that at sunspot minimum (after Wexler).

It was shown by RAMAMURTI that functions describing the latitudinal deviation of monthly mean pressure from the normal curve are significantly correlated with sunspot numbers. As an example, derived from his formulas, he gives the distribution curves of pressure during April—May of the years 1913 (minimum sunspots) and 1938 (maximum sunspots). Comparing these curves we observe a positive pressure difference (1938 minus 1913) between 45° and 60° S with a maximum of about 4 mbar at 60° S and similar negative differences between 10° and 45° S.

The question of differences in pressure distribution at opposite extremes of solar activity has been extensively discussed by WILLETT. From his numerous papers on the subject we will mention only the last (1965). In this paper WILLETT presents mean pressure difference profiles for the four meteorological seasons separately. The study is based upon data on sea-level pressure for the period 1899—1962, available in the form of seasonal mean maps covering the northern hemisphere north of 20° N. The period 1899—1962 contains 6 solar cycles, thus six solar maxima could be compared with six solar minima. The seasonal curves give the mean difference in pressure for the six opposite extremes. (See Fig. 38). (Actually, WILLETT gives seasonal pressure difference curves for several indices, indicating extreme states of solar activity, e.g. umbra to spot ratio, geomagnetic character figure; only the curves based on sunspot numbers are reproduced here). WILLETT's own comments on the figure are: 'the four seasonal difference profiles are consistent in showing at maximum solar spottedness compared with the minimum a significant relative displacement of atmospheric mass from lower to higher latitudes. The latitudinal belt most affected by this displacement

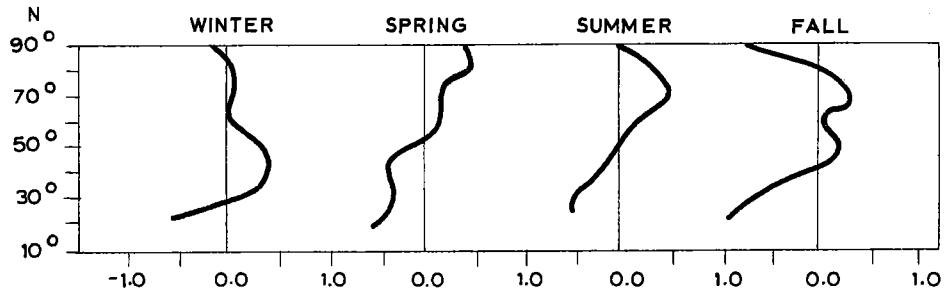

Fig. 38 Mean difference between pressure in sunspot maximum years and that in sunspot minimum years, expressed in standard deviations of mean pressure (after Willett).

shifts polewards in a manner that might be expected with the poleward movement of the sun from the winter to the summer season, and moves equatorwards again by autumn. The consistency of the effect from season to season is the more surprising in view of the fact that by no means the same calendar years are included in the 6 maximum and minimum groups for each season.'

To sum up the evidence offered by the papers reviewed in this sub-section, relationships seem to be indicated between the zonal distribution of sea-level pressure and opposite extremes of solar activity, generally in the sense anticipated from experience of the tropospheric flare effect.

So far only profiles of zonal average pressure differences have been discussed. However, the problem stated at the beginning of this section mainly concerns changes in the frequency of circulation types. A study of this type was performed by CAPPEL (1957), who investigated the frequency of Grosswetterlagen as a function of the phase of the solar activity cycle. The author admits that the use of the solar cycle according to phase is somewhat unrealistic, since it does not allow for the considerable differences in amplitude of the various solar cycles. In spite of this drawback Cappel was able to show that the frequency of certain Grosswetterlagen varies systematically during a solar cycle. The most interesting of his conclusions regarding the flare effect are that anticyclonic conditions over Central Europe most frequently occur during a solar maximum and for some years thereafter and that blocking type circulations, especially those in which the anticyclone is situated over Scandinavia, are much more persistent in the half cycle of the solar maximum than in the opposite half cycle.

Finally, we should like to mention a paper by WEXLER (1956), in which northern hemisphere maps of the average differences in sea-level pressure between years of maximum and minimum solar activity for January and July were published. Pressure data from the period 1899—1939 were used.

The pressure difference pattern for January is much stronger in amplitude than the one for July. The former shows a wave number-two-to-three configuration, especially in the latitudes higher than 50° N. On the 60° N latitude circle centres of positive pressure difference (sunspot maximum minus minimum) are found at 40° W, 140° W and 80° E; centres of negative differences at 80° W, 160° E and 10° E. (The wave with maximum at 40° W and minimum at 80° W, however, is not very pronounced). On the basis of the monthly mean maps of sea-level pressure published by the Deutscher Wetterdienst in its publication 'Grosswetterlagen Mitteleuropas' we have computed the mean difference in sea-level pressure for January 1957, 1958 and 1959 (latest sunspot maximum) and January 1963, 1964 and 1965 (latest solar minimum). The large scale features of the map of these mean pressure differences are the same as shown by WEXLER's January map: a pronounced wave number-two pattern with positive centres at 140° W and 80° E and negative ones at 160° E and on the Greenwich meridian. The profiles of the mean sea-level pressure difference along 60° N latitude circles in WEXLER's and our map, compared at 18 gridpoints, show a statistically significant correlation (correlation-coefficient $r = +0.62 \pm 0.49$).

In conclusion we may say that the results of these first approximation studies confirm our ideas about the relation between the frequency of flare occurrence and the frequency of development of high pressure at middle to high latitudes.

V.2.3 In trying to make a more detailed study of the above relationship for individual years we need a more specific relationship between the frequency of flare occurrence and solar activity. From solar physics it is well-known that flare outbursts are strongly related to the location and development of individual sunspot groups. The greatest flare activity is concentrated in the phases of rapid development or decline of a sunspot group. During the long lasting phase of slow decay of the group, flare activity is negligible (WALDMEIER, 1959).

A statistical study of the relation between sunspot size and flare occurrence has been made by several authors, e.g. GREATRIX (1963) and most recently ENGER et al. (1966).

In the latter study in which solar data covering the 10 year period 1955—1964 were investigated by an objective technique, earlier views are confirmed, notably that the probability of flare occurrence depends markedly on the size of the spot group and depends also, to a lesser but significant extent, on the change in group size from one day to the next. Negative as well as positive changes in spot group size contribute to the increase of flare probability, though the effect of positive changes appears to be much greater.

In this thesis on sunspot models, ZWAAN (1965) has attempted to develop a physical relation between the spasmodic evolution of sunspots and the origin of flares.

Solar activity appears to be spasmodic in nature not only with regard to the evolution of single spots or spot groups. If we look at a long series of daily sunspot numbers we observe very wide variations, irregular in magnitude and duration. Not only are the rising and declining phases of the 11-years cycle characterized by alternating periods of high and low activity, but also the maximum of the cycle. Even a series of monthly numbers and sometimes yearly sunspot numbers shows such irregularities.

The growth in sunspot number of, say, 50 units in a few days is frequently referred to by German authors as 'solarer Stosz', and the influence of such solar pulses on the atmospheric circulation has been investigated (TRENKLE, 1957). In view of the discussion on the relation between the evolution of individual sunspots and flare outbursts, substantial increases in sunspot number in a few days may well be regarded as an enhancement of flare activity.

On may wonder, however, whether substantial increases or decreases in monthly or yearly sunspot number can also be identified with a greater probability of flare occurrence. As far as we know such relation has not been investigated as yet. However, assuming the relation indicated to be valid, we might investigate the possible relationship between solar flares and climatological data through the intermediary of the variation in yearly sunspot number. For this purpose the variation, denoted by ΔR_y, will be arbitrarily defined as

$$\Delta R_y = \frac{|R_{y+1} - R_y| + |R_y - R_{y-1}|}{2}$$

where R_y denotes the sunspot number of year y.

In order to verify the conclusion stated at the end of the previous sub-section, the frequency of occurrence of the three classes of circulation types (classes of Grosswetterlagen) for the years 1881—1964 (84 years) have been compared with the variation of the yearly sunspot number (ΔR_y) for these years. This was done by dividing the years into three classes of 28 years each: class I ($\Delta R_y < 11$), class II ($11 \leqslant \Delta R_y < 20$) and class III ($\Delta R_y \geqslant 20$). The investigation was performed for each season separately. In Table XIII the mean yearly and seasonal frequency (%) of occurrence of zonal (Z), half-meridional (H) and meridional (M) circulation types are given for the three different solar activity classes, along with the overall mean frequency.

The table shows that in all seasons meridional circulation types most frequently occur in the highest solar activity class. Furthermore, in the intermediate solar activity class the frequency is higher than in the lowest class, except for the summer season. From this investigation we may conclude that the assumed relationship — a higher level of solar activity corresponds to a more frequent occurrence of meridional circulation types — is confirmed. The 2.7% difference in annual mean frequency of meridio-

nal circulation types in the highest solar activity class, as compared with the overall mean, is significant beyond the 5% level. This has been tested by means of the standard deviation of the annual occurrence of meridional circulation types, which is 24.7 days. The standard deviation of a sub-sample mean is $\frac{\sigma}{\sqrt{N}}$, which in our case is equal to $\frac{24.7}{\sqrt{28}} = 4.66$. The above-mentioned 2.7% difference is equivalent to a difference of 10 days, which is more than twice the standard deviation.

The results have been tested also by means of the χ^2-test. It was found that the distribution of the number of days with meridional circulation over the three solar activity classes significantly deviates from the expected (uniform) distribution, for the year and for the seasons winter and spring, but not for summer and autumn. The distributions of the number of days with half-meridional and zonal circulations have not been tested statistically, since from Table XIII it is obvious that the increase in M types with increasing solar activity goes at the expense of a decreasing frequency of both Z and H types. In order to find out whether the observed changes in relative frequency of Z, H and M types with changing solar activity conditions are due to changes in the relative frequency of Z, H and M type spells or to changes in the length of the spells, the following investigation has been performed.

TABLE XIII.

	Winter				Spring		
	Z	H	M		Z	H	M
I	32.7	29.0	38.3	I	24.5	20.7	54.9
II	28.1	28.1	43.8	II	24.5	18.6	56.8
III	31.7	22.9	45.4	III	21.0	17.7	61.4
T	30.8	26.6	42.5	T	23.3	19.0	57.7
	Summer				Autumn		
	Z	H	M		Z	H	M
I	34.2	27.1	38.7	I	34.3	23.5	42.3
II	35.7	27.7	36.6	II	31.1	24.5	44.4
III	33.5	25.8	40.7	III	30.2	23.3	46.5
T	34.5	26.9	38.7	T	31.8	23.8	44.4

	Year		
	Z	H	M
I	31.4	25.0	43.6
II	29.9	24.7	45.4
III	29.1	22.4	48.5
T	30.1	24.1	45.8

One representative member has been chosen from each of the three classes of circulation types. The representative types are denoted by the symbol Wz (zonal circulation, mean yearly frequency 15.0%), HM (half-meridional, 10.9%) and HFa (meridional, 3.7%).

In Table XIV the mean yearly percentual frequency of occurrence of Wz, HM and HFa and mean duration of spells of Wz, HM and HFa are given for the three different solar activity classes, along with the mean values of frequency and duration over all 84 years.

TABLE XIV.

	Frequency of occurrence (%)				Duration (days)			
	I	II	III	all	I	II	III	all
Wz	17.0	14.7	13,4	14.9	5.1	4.8	4.7	4.9
HM	11.9	11.6	9.4	10.9	4.5	4.3	4.2	4.3
HFa	3.6	3.4	4.1	3.7	3.5	3.7	4.4	3.9

In accordance with the tendency shown by Table XIII, the first part of this table indicates a gradual decrease in the frequency of occurrence of Wz and HM with a higher class of solar activity. This decrease is partly offset by an increase in the frequency of occurrence of HFa, which may be considered a blocking type circulation. Since we now also have at our disposal some numbers indicating the mean duration of a circulation type for each solar activity class, the question posed above can be answered. As is shown by the second part of the table, the mean duration behaves in the same way with respect to solar activity as the mean frequency does, suggesting that the changes in mean frequency partly originate from changes in the mean duration of circulation types and not only from changes in the frequency of initiation of the various types. Therefore, we might say that increased solar activity, apart from having an influence on the development from meridional type circulations, strengthens the persistence (i.e. continuation tendency) of meridional or blocking type circulations, while on the other hand it interrupts spells of westerly zonal circulation, which are normally quite long.

V.3 Some indications of a relationship between the yearly amplitude and the month-to-month persistence of monthly mean temperatures at De Bilt and sunspot variability

V.3.1 Increased blocking action changes the climate of the Netherlands from the normal maritime to a more continental type. The change could be traced by means of several climatological parameters. For our purpose we have taken quite a simple index of continentality, namely the yearly amplitude of monthly mean temperature.

We have defined this quantity as the difference between the mean temperature of the warmest month of the summer season (June, July or August) and the coldest month of the preceding winter season (December, January or February). The quantity is denoted by ΔT_m.

In the Netherlands we are fortunate in possessing records of monthly mean temperatures covering nearly two and a half centuries (LABRIJN, 1945). The earliest observations were made at Zwanenburg and district (1736—1849). LABRIJN has reduced these figures to Utrecht—De Bilt, where observations have been made since 1849. The whole series of temperature data is cited here as the records of De Bilt.

Accurate values of monthly mean sunspot numbers are available only from 1749 onwards.

We have therefore chosen the period 1749—1964 (216 years) for investigating the possible relation between ΔT_m at De Bilt and ΔR_y. First, mean values of ΔT_m have been calculated for the years $\Delta R_y < 10$, ΔR_y 10—20, ΔR_y 20—30, ΔR_y 30—40 and $\Delta R_y \geqslant 40$ (here the subdivision is more precise than in the previous section because of the longer data record). Since these mean values suggested a gradual increase of ΔT_m with increasing solar activity class, the linear regression equation between ΔT_m and ΔR_y was computed. For the period 1749—1964 this equation takes the form:

$$\Delta T_m = 0.025\ \Delta R_y + 16.85^\circ\ C$$

This corresponds to a correlation coefficient $r = +0.12$, which according to the t-test is not significant at the 5% level, though it comes close.

As a further test of the significance of this result, the period was sub-divided into two equal parts of 108 years each and the following regression equations were found:

$$1749—1856: \Delta T_m = 0.01\ \Delta R_y + 17.45^\circ\ C$$

$$1857—1964: \Delta T_m = 0.04\ \Delta R_y + 16.17^\circ\ C$$

The results are shown in Fig. 39, both for the whole period and the two sub-samples; the values between brackets indicate the number of years in each solar activity class.

Ignoring probably insignificant details, the general trend is clear: the yearly amplitude of monthly mean temperatures at De Bilt increases with increasing variation of the yearly sunspot number. (A similar analysis of ΔT_m with respect to the yearly sunspot number R_y itself failed to show any clear correlation). The above result fits beautifully into the pattern outlined in the preceding section of enhanced solar activity favouring high-latitude blocking in the European-Atlantic sector, incidentally causing the climate of the Netherlands to change from a maritime to a more continental type.

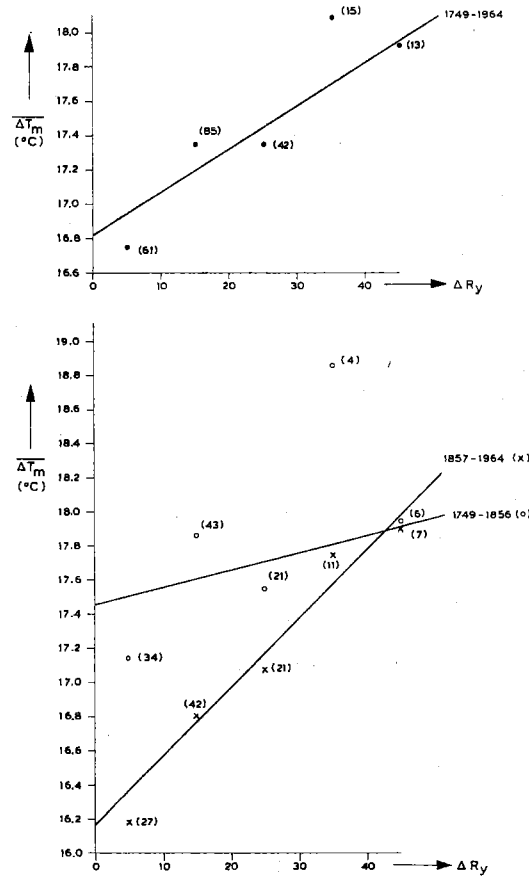

Fig. 39 Mean yearly amplitude of monthly mean temperatures at De Bilt for years in different classes of solar activity. Solar activity is classified by the variation in yearly sunspot number. The number of years in each class is given between brackets. Regression lines, according to regression equations given in the text, are indicated for the period 1749-1964 and the subperiods 1749-1856 and 1857-1964.

V.3.2 In section V.2 it was pointed out that persistence of circulation types probably has something to do with solar activity. Persistence in circulation type will cause persistence of weather type end eventually persistence of monthly mean temperatures.

By persistence of monthly mean temperatures we mean that the temperature of a given month shows the same deviation from normal as the temperature of the preceding month.

Deviations from normal are quantitatively defined as anomaly classes, by dividing the frequency distribution of monthly mean temperatures into a certain number of parts. In our case the frequency distribution is divided into 3 parts, each containing

$33\frac{1}{3}\%$ of all cases. The classes are designated by the usual names: below (B), normal (N) and above (A).

The existence of month-to-month persistence in temperature and precipitation anomalies has long been recognized and this parameter has been used in numerous methods of long-range weather forecasting. The annual course of month-to-month persistence in the United States was investigated by NAMIAS (1952). In general it was found that any high degree of persistence only exists in the winter and summer season; there is little if any persistence in spring and autumn, especially April—May and October—November.

In the United States the annual course of persistence in temperature and precipitation anomalies is generally the same. According to NAMIAS this annual course may well be related to the annual course of persistence in tropospheric circulation patterns. The periods of least persistence during spring and autumn are ascribed to the normal changeability at these times of year, when continents and oceans reverse their thermal roles and the prevailing westerly circulation in middle latitudes is most varied.

The periods of high persistence during summer and winter are ascribed to the low normal changeability of the inactive summer circulation and the vigorous winter circulation. In a later paper (1959) NAMIAS tries to explain the reason for long-period persistence of circulation regimes in prolonged anomalous surface conditions and also in the natural hydrodynamic stability of certain anomalous forms of the general circulation.

The possibility that solar activity could play a role in persistence has sometimes been entertained, but according to NAMIAS, opinions in this respect are still conflicting.

In section V.2 we expressed the view that in the European-Atlantic area solar activity might strengthen persistence of high-latitude blocking. Persistent blocking would favour mont-to-month persistence of above normal temperatures in the Netherlands in summer and persistence of below normal temperatures in winter.

We have verified this by an investigation of mont-to-month persistence of mean monthly temperatures at De Bilt.

The De Bilt series of monthly mean temperatures for the period 1749—1964 was used.

The annual course of persistence, which was first studied, is found to be the same as in the United States: high persistence in the winter and summer season, with distinct minima in spring and autumn. The same result had already been established by VAN DER BIJL (1954), who studied the persistence of monthly mean temperatures at De Bilt by means of correlation calculus.

We next computed the percentage of cases in which successive summer months (June—July, July—August and August—September) and successive winter months (December—January, January—February and February—March) showed persistence

of monthly mean temperatures. The percentages were computed for the years in the various solar activity classes, as well as for the total number of years.

The difference in degree of persistence* in the various solar activity classes turned out to be slight, except for the class ΔR_y 20—30, which both for summer and winter temperatures shows a persistence considerably above normal (see Table XV).

TABLE XV.

	All years N = 216	$\Delta R_y < 10$ N = 61	ΔR_y 10 — 20 N = 85	ΔR_y 20 — 30 N = 42	$\Delta R_y \geqslant 30$ N = 28
Summer	42.1	42.7	40.0	47.6	39.4
Winter	39.4	38.3	36.9	45.2	36.8

However, the values in this table cannot answer our question fully, since we have not yet distinguished between persistence of below, normal and above temperature anomalies.

Considering persistence per anomaly class it is interesting to observe that persistence normal-to-normal (NN) is practically non-existent.

Reduced to persistence per anomaly class the winter and summer values for all 216 years become (in %):

TABLE XVI

	Summer	Winter
AA	16.2	13.2
NN	10.6	11.1
BB	15.3	15.3

AA (above-to-above), BB (below-to-below)

Since we are mostly interested in AA and BB persistence, NN has been ignored in the considerations below. AA and BB persistence deviations from normal have been computed for each solar activity class, and for summer and winter.

In order to get an idea of the significance of the results the computations have also been performed separately for the first part (1749—1856) and the second part (1857—1964) of the period.

* By degree of persistence we mean the difference between the actual percentages and the $33\frac{1}{3}\%$ accounted for by chance.

The results are given in Table XVII. Considering first the values for the summer season, we find an increased tendency to AA persistence in the two highest solar activity classes, exactly as we had anticipated. Strong persistence of above normal June temperatures in Central Europa during the rising phase of the 11-year cycle, as reported by DINIES (1965), also agrees with the above finding.

With respect to BB persistence in summer the relation with solar activity is exactly the opposite: high persistence occurring at low solar activity (more maritime conditions) and low persistence when solar activity is high. Here, however, the two subsamples are not in agreement.

Looking at the values for the winter season we do not observe the expected increase of BB persistence with increasing solar activity class. In class ΔR_y 20—30 we even find a diminished degree of BB persistence, along with strongly enhanced AA persistence.

WILLETT's view (see section V.2) that the latitude belt most affected by solar activity induced pressure rise moves with the sun could be offered by way of explanation of this. This would mean that in summer this belt is nearer to the pole than in winter. Hence for the region of The Netherlands the situation could arise that during winter high pressure is favoured just south of 50° N, which would maintain a continuous westerly circulation, giving rise to persistence of above normal temperatures. The long record (1755—1965) of pressure data for Basel (47°35′ N, 7°35′ E) gives at least some support to this suggestion. For 21 years with ΔR_y 20—30, occurring in the period 1749—1856, and for 21 years with ΔR_y 20—30, occurring in the period 1857—1964, the mean deviations of the surface pressure in the winter season from the long-term normal (1755—1960) are + 0.2 mbar and + 0.3 mbar respectively.

Only when solar activity is extremely high ($\Delta R_y > 30$) will real high latitude blocking perhaps occur, causing persistence of sub-normal temperatures in winter.

The general conclusion from the foregoing section is that the flare effect on the troposphere is a factor of some importance in the initiation and maintenance of long-term weather anomalies. The main effect at ground level, at least in the western European area, is the poleward shift of air masses, reaching its maximum at about three days after each individual flare. The effectiveness of this influence certainly depends on the initial atmospheric conditions, while the latitude belt most affected by the air mass displacements seems to vary with the seasonal position of the sun. Though in view of the above the effect of an individual flare may well be negligible in some cases, the cumulative effect of a large number of flares during intervals of enhanced solar activity may be very marked. During such intervals in summer the zonal circulation, bringing maritime air masses into the European continent, may be more frequently interrupted than usual, while the normal tendency to blocking may be increased to such an extent that blocking periods of very long duration may occur. This situation will give rise to a marked persistence of above normal temperatures and a very slight persistence of below normal temperatures in western European summers.

TABLE XVII. *Deviations (in %) from normal AA and BB persistence in summer and winter temperatures (normals are given in Table XVI) for different solar activity classes.*
Deviations are given for the whole period 1749—1964 and for the sub-periods 1749—1856 and 1857—1964. (For the number of years in each solar activity class, for the whole period as well as for the sub-periods, see Fig. 39).

	WINTER				SUMMER			
	AA-persistence				AA-persistence			
	$\Delta R_y < 10$	ΔR_y 10—20	ΔR_y 20—30	$\Delta R_y > 30$	$\Delta R_y < 10$	ΔR_y 10—20	ΔR_y 20—30	$\Delta R_y > 30$
1749—1964	— 0.6	— 3.4	+ 9.0	— 1.3	— 0.9	— 5.2	+ 5.2	+ 10.0
1749—1856	— 1.4	+ 1.5	+ 10.6	— 3.2	— 0.5	— 3.8	+ 6.0	+ 7.2
1857—1964	+ 0.4	— 8.4	+ 7.4	— 0.3	— 1.4	— 6.7	+ 4.4	+ 11.6

	BB-persistence				BB-persistence			
	$\Delta R_y < 10$	ΔR_y 10—20	ΔR_y 20—30	$\Delta R_y > 30$	$\Delta R_y < 10$	ΔR_y 10—20	ΔR_y 20—30	$\Delta R_y > 30$
1749—1964	0.0	+ 1.2	— 5.0	+ 3.7	+ 4.4	+ 0.8	— 1.0	— 8.1
1749—1856	+4.3	+ 1.7	— 4.2	+ 1.4	+ 7.3	— 3.7	— 5.8	— 5.3
1857—1964	— 5.4	+ 0.6	— 5.8	+ 5.1	— 1.7	+ 5.3	+ 3.7	— 9.7

In winter, moderately high flare activity will result in a subtropical high pressure belt, displaced somewhat northward, giving rise to an intensified zonal circulation at the middle latitudes. Persistence of above normal temperatures will be favoured by this situation. As has been suggested in the previous section, only at a very high level of solar activity may the flare influence give rise to more frequent blockings than usual in the relevant area.

In conclusion, we may tentatively say that solar flares play quite an important role in the development of warm and dry summers at the mid-latitudes of western Europe, while their role in the establishment of cold and severe winters is probably small. It is more likely that flare activity to a certain extent prevents winters from becoming severe.

V.4 The 80—90 year period in sunspot variability and its related climatic cycle

V.4.1 Finally, a few remarks will be made on the possible relation between variations in solar activity and climatic changes.

The curve of the yearly means of sunspot numbers, from the year 1700 to the present time, gives evidence that low and high maxima of sunspot activity alternate in a not entirely irregular way. Low maxima are followed by high ones, with a period of about 90 years. The astronomer WOLF first drew attention to this long cycle in 1861. In a recent article WALDMEIER (1966) has shown that there are several other statistical aspects of sunspots, besides the height of the maxima, which vary over a period of 80—90 years. Among these are the length of the 11-year cycle and the ratio between the sunspot activity on the northern and southern hemispheres of the sun. The index of solar activity ΔR_y, which we have introduced, is also found to vary in a secular way. The 10-year overlapping means of ΔR_y are shown in Fig. 40 merely as an illustration of this feature. Ten year overlapping means have been chosen to filter out, to a certain extent, the variation of ΔR_y within the 11-year cycle.

In search for physical characteristics of the long solar cycle, WALDMEIER brings up the important question of what quantity is responsible for the high and low 11-year maxima. Are there more spot groups originating at the maximum stage of the long cycle or is their life longer than at the minimum stage? In answering this question WALDMEIER refers to the work of KOPECKÝ, who showed that the mean life of sunspot groups does not substantially participate in the 11-year cycle, but closely follows the 80—90 year cycle. On the other hand, the 11-year cycle of solar activity results from the number of sunspot groups originated, which number does not participate significantly in the long cycle. Since the life of a spot group largely depends on its size, the conclusion may be drawn that the size or importance of sunspot groups varies in a long period of 80—90 years, without much variation of this quantity in the 11-year cycle. With reference to section V.2, we may then state that the number of important

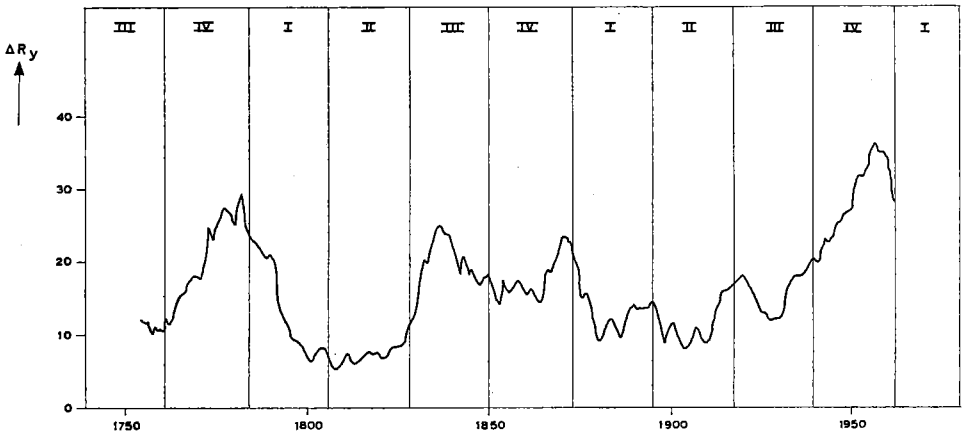

Fig. 40 Curve of 10-year overlapping means of the variation in yearly sunspot number, showing a quasi-periodic behaviour with a period of 80-90 years. Roman numbers refer to quarters of an 89-year cycle, characterizing phases of declining (I), low (II), rising (III) and peak (IV) solar activity conditions.

flares produced on the sun will show a large variation in phase with the 80—90 year cycle, although, as we have seen, the variation in the number of flares with respect to the 11-year cycle is far from negligible.

Opinions among the investigators differ as to the exact length of the long solar cycle. CLAYTON (1947) writes about an 80-year cycle, comprising 7 11-year cycles. VISSER (1957; 1959) refutes the idea of a period of 7 cycles and is in favour of an 89-year cycle, encompassing 8 primary cycles. In the most recent investigations (1964), however, LINK, who traced the long solar cycle back to 800 A.D. on the basis of historical observations of auroras, again estimates the length of the cycle at 80 years.

V.4.2 The existence of a long cycle in terrestrial climate parallel to the long solar cycle has been studied for several years. From the climatological records of pressure, temperature and precipitation it has been recognized for some time that longterm variations of the order of several decades or even a century do occur. Many important studies in this field have been performed by LAMB (1965; 1966), who was able to show, with regard to the frequency of weather types in Britain, that variations which have taken place this century are greater than can be explained by chance.

As in the case of long-term weather anomalies (cold winters, wet summers), discussed in I.2, several explanations for the long-term climatic anomalies have been suggested:

1 solar variations;
2 surface-atmospheric interactions;
3 combinations of 1 and 2.

A solar cause of the long-term climatic anomalies was proposed by WILLETT (1961). In his numerous papers on the subject, much emphasis is laid on the 80—90 year solar-climatic cycle. A concise description of the characteristics of this long cycle appeared in one of his recent papers (1965). The long cycle is divided into four parts, according to solar activity: low, rising, peak and decline (see Fig. 40). According to WILLETT, during the declining phase the general circulation changes abruptly from a low index blocking pattern during the peak quarter of solar activity to a low latitude zonal circulation pattern. The low latitude zonal circulation results in cool maritime conditions in middle latitudes. During the low and rising phase of the solar cycle the zonal climatic pattern tends to shift poleward, becoming markedly high-latitude zonal. This will cause a warming trend in most latitudes north of 50° N, while equatorwards of 50° N an intensification of continental-maritime contrasts is observed due to the weakening of the westerlies there. The poleward shift of atmospheric mass is at a maximum during the peak quarter of solar activity, causing pronounced high latitude blocking.

Among the investigators of long-term climatic anomalies, EASTON (1917) was probably the first to draw attention to the 80—90 year climatic cycle. On the basis of the character figures of winter cold in western Europe for the period 760 A.D.—1916, he was able to show that 13 temperature waves of 89 years length occurred during this period. Choosing the beginning of each 89-year cycle to coincide with the beginning of the rising phase of the solar cycle, EASTON found a strong variation in frequency of occurrence of severe and very severe winters, in phase with the solar cycle. EASTON'S results as far as the mean frequencies over all 13 cycles are concerned are reproduced in Table XVIII.

TABLE XVIII. *Mean frequency of occurrence of severe and very severe winters in western Europe, corresponding to a cycle of 89 years, for the period 760—1916.*

Quarter of cycle (according to Fig. 40)	I (decline)	II (low)	III (rise)	IV (peak)
severe	2.4	0.8	2.3	1.7
very severe	1.3	0.2	0.9	0.5

VISSER (1950) later investigated this accumulation of extremes by means of the standard deviation of the winter character figures. He considered only the period 1205—1949, since there were some breaks in the series from 760—1205. As was to be expected, intervals of high standard deviations alternate with intervals of low standard deviations during the whole period. By superposing individual periods of 89 years (8 cycles between 1205 and 1916) and taking the mean of the 8 cycles for each of the 89-year cycle, VISSER found that in the first and third quarters the standard

deviations were high, in the second and fourth quarters standard deviations of winter character figures tended to be low.

Very recently VALNÍČEK (1965) has shown that an 80—90 year cycle in the frequency of occurrence of severe winters can also be deduced from the long series (200 years) of recorded winter temperatures in Prague. The long cycle at this location is in phase with the 89-year cycle suggested by EASTON's data for Western Europe.

V.4.3 Applying our own views on the relation between variations in solar activity and circulation anomalies to the problem of the 80—90 year solar-climatic cycle, we find that the conclusions are generally in agreement with the characteristics outlined in the preceding section. This will be illustrated here by discussing the characteristics of the first (I) quarter of the long cycle. According to EASTON's grouping of years, during the last three centuries the following years belong to the first quarter: 1695—1717; 1784—1806; 1873—1895 and 1962 (—1984).

For those years ΔR_y generally proves to be in the solar activity classes $\Delta R_y < 20$, with most of the years in the class ΔR_y 10—20. From the discussions in section V.2 (Table XIII), we find that the summer circulation in this solar activity class may be characterized by a normal to above normal frequency of zonal type circulations. Along with a moderately low yearly amplitude of temperature (Fig. 39), this is compatible with the characteristics of the first quarter given by WILLETT (low latitude zonal circulation causing cool, maritime conditions at middle latitudes). From Table XVII we may infer that the conditions of persistence in the first quarter are such that the degree of persistence of above normal summer temperatures is quite low, while persistence of 'below' summer temperatures is slightly above normal. This inference is also in accordance with the assumed maritime conditions.

In winter, however, the maritime character is possibly less pronounced. The winter circulation in solar activity class II (see Table XIII) shows a diminished frequency of zonal type circulations, while in Table XVII we observe that for ΔR_y 10—20 above normal winter temperatures are less persistent and below normal temperatures more persistent than normal. This tendency corresponds to the increased frequency of severe and very severe winters in the first quarter, as suggested by the work of EASTON and VISSER.

It thus appears that a tendency to lower temperatures occurs in the first quarter of the 80—90 year cycle, both in winter and in summer. A suggestion that during the first quarter sub-normal temperatures should prevail in each season of the year is given by Table XIX, in which the mean deviation of seasonal temperatures from the normal over the relevant 89-year period is given from the temperature records at De Bilt.

TABLE XIX. *Mean deviations of seasonal temperatures during the first quarter of the 89-year solar-climatic cycle, from the seasonal mean of the relevant cycle (in °C).*

	Winter	Spring	Summer	Autumn
I_A (1695 — 1717)	— 0.45	+ 0.07	— 0.28	— 0.31
I_B (1784 — 1806)	— 0.67	— 0.39	— 0.31	— 0.30
I_C (1873 — 1895)	— 0.27	— 0.13	— 0.02	— 0.14

From the above it may be concluded that the climatological consequences of solar flare activity are far from negligible. Rather than giving rise to an 11-year cycle in terrestrial climate, a feature looked for by several authors without any conclusive results, solar activity probably causes a much longer climatic cycle of 80—90 years, which as far as winter temperatures in Western Europe are concerned, may be regarded as a double cycle of about 40—45 years.

In 1962 we entered the coolest quarter of the long cycle. Temperatures are lower in this quarter in all seasons of the year* than the long-term normal. As a tentative explanation for this we suggest that in the summer half year temperatures are lower because of infrequent blocking as a result of the very low level of solar activity; in the winter half year the lack of flare activity prevents the subtropical high pressure cells from moving northward. The very low latitude circulation then gives rise to more frequent dispersion of cold arctic anticyclones over the middle latitudes.

* For the six years 1962 — 1968, mean seasonal temperatures have indeed been lower than the long-term average, in all seasons.

SUMMARY

This study is concerned with the age-old problem of the influence of solar activity on the weather. Though a vast number of papers on the subject have been published during the last century, the problem is still unsolved. The situation at the present time is that there are no generally accepted widespread conclusions, nor has a working mechanism been proposed that can be considered complete and physically sound. The often conflicting and confusing results of the various studies have made many people, especially meteorologists, suspicious of the subject. Nevertheless, the problem is of interest to meteorologists, and will remain so as long as there is no proper explanation for the occurrence of long-term weather anomalies (severe winters, dry summers) and climatic fluctuations.

The present study starts (Chapter II) with a survey of the essential features of solar activity and a short review of previous research on solar-weather relationships. Next, a more detailed description is given of the activity phenomenon known as solar flare, the influence of which on the earth's lower atmosphere forms the specific subject of this study.

The various components of the flare radiation and their influence on the upper layers of the atmosphere, are relatively well known. However, our knowledge about reactions of the flare radiation, both short-wave electromagnetic and corpuscular, with atmospheric constituents in the deeper layers is extremely poor. Moreover, the various ways in which the upper and lower layers of the atmosphere interact are insufficiently understood. For these reasons nobody has been able to deduce theoretically the influence of a solar eruption on the lower layers of the atmosphere.

During the past two decades a number of statistical studies have been performed on the subject, the results of which are summarized in Table I of this study. No general conclusion can be drawn from these, because of the diversity of the atmospheric elements used.

In the present treatise the problem is also approached through a statistical investigation (Chapter III). The number of flares used in the statistics is 81, which is a much larger sample than in all but one of the previous studies. The atmospheric element considered here is the height of the atmospheric constant pressure levels, from the ground up to 50 mbar (20 km). For one level (500 mbar) the study covers the whole globe, except for the tropical belt, for which no data were available. In all of the previous investigations atmospheric elements for only a few stations or small geographic regions were taken into account. A great effort has been made to test the various results of our analysis for their statistical significance, a question which has been completely disregarded in all but two of the earlier studies.

The results of our statistical investigation can be summarized as follows:

1 The mean change in height of atmospheric constant pressure levels (mean of 81 cases) during the first 24 hours after a flare is greater than may be expected from mere random fluctuations in height.

2 At some locations the mean change in height is positive, at other locations negative. However, when averaged over latitude circles, mean positive height changes are found to occur in the mid-latitude belts 45—65°, with a maximum of about 5 gpm per day at 55° latitude, whereas mean negative height changes prevail poleward of 70° latitude, with a maximum of about 10 gpm per day at the pole. Equatorward of 45° latitude the mean height changes are generally between 0 and 2 gpm per day.

3 In the vertical the maximum mean height rises are found to occur at about the 300 mbar level (± 10 km), just below the tropopause. Mean height drop does not show any vertical variation.

4 Mean temperature changes related to mean height rises are positive throughout the troposphere and strongly negative just above the tropopause.

5 Significant mean height changes are found to occur only during the first 24 hours after a flare, except for ground level (1000 mbar), where significant mean height changes do not appear until the third day after a flare.

6 The flare effect appears to be stronger in winter than in the other seasons of the year, a fact which seems to be related to the stronger atmospheric circulation during the winter months.

At the end of the relevant sections in Chapter III the results summarized above are individually discussed. The most important conclusions drawn are:

a Our results are in agreement with those of the comparable, though much less extensive, studies mentioned in Table I.

b The rise of pressure levels in middle to high latitudes may very probably be identified as the effect which explains the characteristic difference in the distribution of sea-level pressure between years of maximum solar activity and years of minimum solar activity. (WEXLER (1950); WILLETT (1965)).

c The vertical distribution of the atmospheric reaction suggests that this effect, which shows a maximum at the tropopause, is not propagated downward from higher levels in the stratosphere but is initiated in situ, most likely through a cooling mechanism near the tropopause level.

d In the troposphere the reaction is probably propagated downward, causing the circulation of the lower layers to become more meridional after a few days.

e The intensity of the reaction seems to be dependent on initial atmospheric conditions.

In Chapter IV a physical theory is described by which it is possible to give a reasonable explanation of the observed reaction. First, it is shown that the causing agent is to be sought in the corpuscular radiation of the flare rather than in the UV-radiation. It has been possible to estimate the energy range of the relevant flare particles, which are assumed to be protons, as 100—1000 MeV. It has also been shown that these high energy protons can penetrate to levels between 30 km and the ground. In view of the likelihood of the reaction of the tropospheric layers being initiated by a cooling mechanism near the tropopause, the possibility that the penetrating protons might create a heat sink has been investigated.

The most effective diabatic cooling or heating mechanism in the lower stratosphere is undoubtedly the radiation process. Therefore the interaction of the protons with ozone, one of the radiative constituents, has been studied. Another argument for studying the interaction with ozone is that in the sample of flares used in Chapter III a reduction of the ozone content of the atmosphere was found during the first 24 hours after a flare, the reduction being greatest in the lower stratosphere.

Various reactions involving protons and ozone are discussed. The reaction chain eventually proposed, which is capable of explaining quantitatively the observed ozone removal after a flare, is as follows: in entering the lower stratosphere, protons produce electrons by numerous collisions with air molecules. Some of these electrons have energies just sufficient to dissociate water vapour through the process of attachment to the vapour molecules. In this process OH-molecules are produced which strongly react with ozone according to a reaction chain proposed by HAMPSON (1964).

Since the availability of water vapour is a vital factor in the proposed effective mechanism, it becomes much more likely that the tropopause region is the seat of the initial effect. This led us to examine the material used in the statistical investigation (Chapter III) in more detail. As was to be expected from the important part played by water vapour, it was found that the tropospheric flare effect is larger in case of a high tropopause than in case of a low tropopause. Furthermore, regions of height rise of mid-latitude tropospheric pressure levels proved to be associated with the semi-permanent troughs in the hemispheric circulation, which are usually moist up to the tropopause.

The amount and especially the vertical distribution of water vapour near the tropopause also play an extremely important role in the radiative temperature changes which take place after the ozone has been removed. As has been found by performing a numerical investigation, the influence of a certain reduction of the ozone content of the lower stratosphere on the radiative temperature changes at these levels is very slight; though there was some cooling, it was found to be only a few tenths of a degree per day at the base of the layer from which ozone had been taken away. Since it could safely be assumed that the diabatic cooling would be at least of the order of magnitude of the observed cooling, being 1.8° C per day in the mean of 81 cases, an additional cooling mechanism had to be found. According to several publications

on radiational cooling in the atmosphere, such a mechanism may be provided by the strong cooling effects, of the order of several degrees per day, occurring at the base of an inversion, where there is a certain discontinuity in the vertical distribution of water vapour and/or haze.

Since the tropopause is a kind of permanent inversion, and since the decomposition of water vapour in the dissociative attachment process just above the tropopause may create some discontinuity in the water vapour distribution, a cooling of a few degrees per day by the above mechanism seems at least a tenable theory.

Finally, the characteristics of the heat sink inferred from the proposed mechanism have been compared with the properties of the heat sink computed from the observed horizontal and vertical distribution of the height changes. An analytical expression given by SCHMIDT (1946) for the local change of pressure due to local density variations and density variations caused by isallobaric effect was used for the latter computation. The only assumptions made were that the heat sink must have a maximum ΔT at some level z_t, must be zero below z_t, must decrease above z_t and must have a radial symmetric horizontal distribution. The results were as follows:

$z_t = 12.5$ km

$\Delta T = 1.7°$ C/day

$z_{1/e} = 19$ km (height at which the cooling is $1/e\ \Delta$T)

$r_{1/e} = 3800$ km (distance at which the cooling is $1/e\ \Delta$T)

As is pointed out in Chapter IV, the fact that the observations or quantities derived from the observations agree so closely with the results of the theoretical considerations warrants some confidence in the proposed explanation.

The last chapter (Chapter V) of this study may be considered as an attempt to find applications of the observed relationship between flares and the tropospheric pressure distribution in the field of long-range weather forecasting. The tropospheric reaction was traced for two individual flares not contained in the original sample. It was found to be generally of the kind expected from the study of the sample of 81 flares, which seems promising for forecasting purposes. However, in weather forecasting one is naturally more concerned with changes in circulation at ground level than in the upper air. For this reason, an earlier statement that at the ground the circulation might become more meridional a few days after the occurrence of a flare was examined in more detail. It was found that indeed on the second and third day after a flare the frequency of occurrence of meridional circulation types in Western Europe was higher than on other days. However, the relation is not significant and certainly too weak to be used as a forecasting rule.

The subject has therefore been considered from a more general point of view. A tendency of the circulation in the lower layers to become meridional a few days after a flare, however slight, would mean that during periods of many flares the circulation would tend to be more often meridional than during periods of no flares. This prognosis was further investigated using data relating to daily circulation types for Western Europe from the period 1881—1964. As a measure of the number of flare outbursts per year, which especially for the earliest years is completely unknown, we used an index of year to year sunspot variability, which for this purpose seems to be a better index than the yearly sunspot number itself. The results confirm the expectation that in years of high sunspot variability the frequency of occurrence of meridional circulation types is significantly higher than in years of slight variability.

To investigate this point still further, use was made of the long-period record of monthly mean temperatures at De Bilt (1749—1964). Since in years of higher frequency of meridional circulation types anomalies of monthly mean temperatures tend to be great, the difference between the highest mean temperature of a given summer month and the lowest monthly mean temperature of a preceding winter month may be expected to be larger in years of high sunspot variability than in years of low variability. This suggestion was also found to be true: the yearly amplitude of monthly mean temperatures increases nearly linearly with the increasing solar variability index. Although the above results indicate that the cumulative effect of solar flare influence does exist, there is probably no proper way to use the relevant relationships in long-range weather forecasting.

There might well, however, be a way to use two other results which have been discussed in connection with the index of sunspot variability. The first is the month-to-month persistence in monthly mean temperatures at De Bilt; it was found that above normal temperatures in summer months are much more persistent in years of large sunspot variability than in other years; the opposite is true for below normal temperatures in summer. For winter months the relation is less clear, although there seems to be an indication that persistence of above normal temperatures is enhanced in years of moderate sunspot variability, whereas persistence of below normal temperatures is favoured in years of high variability.

The last subject discussed is the very long period of fluctuation in the activity of the sun (80—90 years), which period seems to be paralleled by a climatic fluctuation of the same length. It is shown that the characteristics of this climatic cycle, as indicated by WILLETT (1965), are compatible with the changes in the atmospheric circulation which may be expected on the basis of a variation in the frequency of occurrence of the tropospheric flare effect. Extrapolation of the long-period cycle would mean that in the quarter of a century which started in 1962, the atmospheric circulation will behave in such a way that in Western Europe north of about 50° N mean monthly temperatures throughout the year will generally be lower than during the quarter of a century immediately preceding it.

REFERENCES

ALLEN, C. W. (1964). The influence of the sunspot cycle on phenomena at the bottom of the atmosphere. Plan. space sci., *12*, 327.

ATTMANNSPACHER, W. (1955). Chromosphärische Eruptionen und Temperaturen. Met. Rundschau, *8*, 12.

ARCHENHOLD, G. (1938). Untersuchungen über den Zusammenhang der Haloerscheinungen mit der Sonnentätigkeit. Gerl. Beitr. z. Geoph., *53*, 395.

BAILEY, D. K. (1957). Disturbances in the lower ionosphere observed at VHF. Journ. geoph. res., *62*, 431.

BAILEY, D. K. (1964). Polar Cap Absorption. Plan. space sci., *12*, 495.

BARBAS, W. H. and BERGER, M. J. (1964). Tables of energy losses and ranges of heavy charged particles. NASA SP-3013.

BASLER, R. P. and OWREN, L. (1964). Ionospheric radio wave absorption events and their relation to solar phenomena. Scient. report Geoph. Inst. Univ. of Alaska, UAG-R 152.

BATES, D. R. and GRIFFING, G. (1953). Scale height determination and auroras. Journ. atm. & terr. phys., *3*, 212.

BAUR, F. (1967). Meteorologische Beziehungen zu solaren Vorgänge. Met. Abh. Inst. f. Met. & Geoph., Fr. Univ. Berlin, Bd. 50, Heft 4.

BERKOFSKY, L. and SHAPIRO, R. (1964). Some numerical results of a model investigation of the atmospheric response to upper level heating. Plan. space sci., *12*, 219.

BORISOVA, L. G. and KHESINA, B. G. (1963). Influence of solar activity on the formation of synoptic processes. Proc. Central Inst. of Weather Forecasting, Moscow, nr. 124, p. 28.

BROOKS, C. E. P. and CARRUTHERS, N. (1953). Statistical Methods in Climatology, London.

BIJL, W. VAN DER (1954). Ten research papers issued at the centenary of the Royal Netherlands Meteorological Institute. Med. & verh. K.N.M.I., 102 - no. 59.

CAPPEL, A. (1957). Die Häufigkeit der Grosswetterlagen im Sonnenfleckenzyklus. Met. Rundschau, *10*, 189.

CLAY, J. (1948). Kosmische stralen. Servire's Encyclopedie, Den Haag.

CLAYTON, H. H. (1947). Solar cycles. Smiths. misc. coll., *106*, nr. 22.

CLYNE, M. A. A. et al. (1963). Some reactions of ozone in discharge flow experiments. Nature, *199*, 1057.

CRADDOCK, J. M. (1957). An analysis of the slower temperature variations at Kew Observatory by means of mutually exclusive band pass filters. Journ. Roy. Stat. Soc., Ser. A, *120*, 387.

DALGARNO, A. (1961). Charged particles in the upper atmosphere. Ann. de géoph., *17*, 16.

DALGARNO, A. (1962). Range and energy loss. Chapt. 15 in Atomic and molecular processes, ed. D. R. BATES, Acad. Press, New York.

DANJON, A. (1960). l'Eruption solaire du 29 mars 1960 et la rotation de la terre. C. R. Acad. Sci. de Paris, *251*, 308.

DINIES, E. (1965). Über die Erhaltungstendenz übernormaler Temperaturen des Juni im 11-jährigen Sonnenfleckenzyklus. Met. Rundschau, *18*, 102.

DUDEL, H. (1961). Über Schwankungen der zonalen Windkomponente 500 mb nach Anstiegen der solaren Aktivität. Ber. Deutschen Wetterd., *11*, nr. 78.

DUELL, B. and DUELL, G. (1948). The behaviour of barometric pressure during and after solar particle invasions and solar ultraviolet invasions. Smiths. misc. coll., *110*, nr. 8.

EASTON,C. (1917). Klimaatschommeling en weersvoorspelling. Tds. Kon. Ned. Aardr. Genootschap, *34*, nr. 5.

ELLISON, M. A. (1963). Energy releases in solar flares. Quart. journ. Roy. Astron. Soc., *4*, 62.

ENGER, I. et al. (1966). Solar flare occurrence as a function of sunspot size. Air Force Surveys in geoph., nr. 178.

GEBHART, R. (1965). Ein theoretisches Modell für den Tagesgang der Atmosphärentemperaturen. Beitr. Phys. Atm., *38*, 2.

GNEVYSHEW, M. N. and SAZONOV, B. I. (1964). The influence of solar activity on processes in the earth's lower atmosphere. Astron. journ. Acad. Sci. USSR, *41*, 937.

GOTAAS, I. and BENSON, C. S. (1965). The effect of suspended ice crystals on radiative cooling. Journ. appl. met., *4*, 446.
GREATRIX, G. R. (1963). Statistical relation between sunspots and flares. Monthly notices Roy. Astron. Soc., *126*, 123.
HAKURA, Y. (1964). Patterns of polar cap blackouts drawn in geomagnetic coordinates corrected by the higher terms of spherical harmonic development. Rep. of ionosph. and space res. Japan, *18*, 345.
HAMPSON, J. (1964). Photochemical behavior of the ozone layer. Canadian Armament Research and Development Establishment, Techn. note 1627/64.
HARTMANN, W. (1963). Einfluss einer Sonneneruption auf die Flächenmitteltemperatur der Nordhalbkugel in 500 mb. Met. Rundschau, *16*, 150.
HUNT, B. G. (1966). Photochemistry of ozone in a moist atmosphere. Journ. geoph. res., *71*, 1385.
KRAUS, E. B. (1965). Models of atmospheric circulation. Proc. of Seminar on possible responses of weather phenomena to variable extra-terrestrial influences. NCAR techn. note TN-8.
KUBISHKIN, V. V. (1966). The distribution of solar-tropospheric disturbances on the earth's surface. Astron. journ. Acad. Sci. USSR, *43*, 374.
KULKARNI, R. N. (1963). Relation between atmospheric ozone and geomagnetic disturbances. Nature, *198*, 1189.
LABRIJN, A. (1945). The climate of the Netherlands during the last two and a half centuries. Med. & verh. K.N.M.I., 102 - no. 49.
LAMB, H. H. (1965). Frequency of weather types. Weather, *20*, 9.
LAMB, H. H. (1966). The changing climate. Methuen & co., London.
LAWRENCE, E. N. (1965). Terrestrial climate and the solar cycle. Weather, *20*, 334.
LINGENFELTER, R. E. and FLAMM, F. J. (1964). Production of carbon-14 by solar protons. Journ. atm. sci., *21*, 134.
LINK, F. (1964). Manifestation de l'activité solaire dans le passé historique. Plan. space sci., *12*, 333.
LONG, M. J. (1966). A case of rapid cooling in the vicinity of the tropopause near a line of tall thunderstorms. Journ. appl. met., *5*, 851.
MANABE, S. and MÖLLER, F. (1961). On the radiative equilibrium and heat balance of the atmosphere. Monthly Weather Rev., *89*, 503.
MÖLLER, F. (1942). Die Wärmestrahlung des Wasserdampfes in der Atmosphäre. Beitr. z. Geoph., *58*, 11.
MUNK, W. H. and MILLER, R. L. (1950). Variations in the earth's angular velocity resulting from fluctuations in atmospheric and oceanic circulation. Tellus, *2*, 93.
MUSTEL, E. R. (1966). Manifestations of solar activity in the troposphere and the stratosphere. The Astron. Council of the USSR Acad. Sci., Hydrometeorological Center of the USSR, Moscow.
NAMIAS, J. (1952). The annual course of month-to-month persistence in climatic anomalies. Bull. Amer. Met. Soc., *32*, 279.
NAMIAS, J. (1953). Thirty-day forecasting: a review of a ten-year experiment. Met. monogr. Amer. Met. Soc., *2*, nr. 6.
NAMIAS, J. (1959). Persistence of mid-tropospheric circulations between adjacent months and seasons. The Rossby Memorial Volume, Oxford Univ. Press, New York.
NORDØ, J. (1953). A statistical discussion of a possible connection between solar activity and sea-level pressure. Inst. for Weather and Climate Research, the Norwegian Acad. Sci. & Letters, Publication no. 2.
NORRISH, R. G. W. and WAYNE, R. P. (1965). The photolysis of ozone by UV-radiation. Proc. Roy. Soc., London, Ser. A., *288*, 361.
OBAYASHI, T. (1964a). Streaming of solar particles between sun and earth. Plan. space sci., *12*, 463.
OBAYASHI, T. (1964b). The streamings of solar flare particles and plasma in interplanetary space. Space sci. rev., *3*, 79.
PALMER, C. E. (1953). The impulsive generation of certain changes in the tropospheric circulation. Journ. met., *10*, 1.
PRASAD, A. N. and CRAGGS, J. D. (1962). Attachment and ionisation coefficients. Chapt. 6 in Atomic and molecular processes, ed. D. R. BATES, Acad. Press, New York.
RAMAMURTI, K. S. (1953). On fluctuations of the atmospheric circulation in the vicinity of South America, and their relation to sunspots. Journ. met., *10*, 474.

RIEHL, H. (1956). On the atmospheric circulation in the auroral belt at 500 mb. Journ. geoph. res. *61*, 525.
ROBERTS, W. O. and MACDONALD, N. (1960). Further evidence of a solar corpuscular influence on the large-scale circulation at 300 mb. Journ. geoph. res., *65*, 529.
ROBERTS, W. O. (1965). Stratospheric circulation and auroral activity. Proc. of Seminar on possible responses of weather phenomena to variable extra-terrestrial influences. NCAR techn. note TN-8.
RONEY, P. L. (1965). On the influence of water vapour on the distribution of atmospheric ozone. Journ. atm. & terr. phys., *27*, 1177.
SCHIØTT, H. E. (1966). Range-energy relations for low-energy ions. Mat.-fys. medd. Danske Vid. Selsk., *35*, nr. 9.
SCHMIDT, F. H. (1946). On the causes of pressure variations at the ground. Med. & verh. K.N.M.I., Ser. B, I, nr. 4.
SCHUURMANS, C. J. E. and OORT, A. H. (1969). A statistical study of the height changes of constant pressure levels in the troposphere and lower stratosphere after strong solar flares. Pure and appl. geoph., 73, 30.
SEKIHARI, K. (1963). A superposed epoch study on solar activity and ozone. Rep. ionosph. space res. Japan, *17*, 137.
SHAPIRO, R. (1956). Further evidence of a solar-weather effect. Journ. met., *13*, 335.
SMITH, H. and SMITH, E. (1963). Solar flares. Macmillan, New York.
STALEY, D. O. (1966). Radiative cooling in the vicinity of inversions and the tropopause. Arch. f. Met., Geoph. & Bioklim., Ser. A, *10*, 1.
STOLOV, H. L. and SPAR, J. (1968). Search for tropospheric responses to chromospheric flares. Journ. atm. sci., *25*, 126.
ŠVESTKA, Z. and FRITZOVA-ŠVESTKOVÁ, L. (1966). Type IV bursts. II. In association with PCA events. Bull. Astron. Inst. of Czechoslowakia, *17*, 249.
TALJAARD, J. J. and LOON, H. VAN (1964). Southern Hemisphere weather maps for the IGY. Bull. Amer. Met. Soc., *45*, 88.
THOMAS, H. (1935). Zum Mechanismus stratospärisch bedingten Druckänderungen. Met. Zts., *52*, 41.
TRENKLE, H. (1957). The zonal wind component in the Atlantic-European sector as influenced by short-scale fluctuations in solar activity. Forschungsabt. des Deutschen Wetterdienstes, scient. rep. no. 2, Contr. no. AF 61(514)-954-C.
TWITCHELL, P. F. (1963). Geomagnetic storms and 500 mb trough behaviour. Bull. de géoph., College Jean-de-Brébeuf, Montréal, nr. 13, 69.
VALNÍČEK, B. (1952). Les éruptions chromosphériques et le temps. Bull. Astron. Inst. of Czechoslowakia, *3*, 71.
VALNÍČEK, B. (1953). Les éruptions chromosphériques et le temps. Bull. Astron. Inst. of Czechoslowakia, *4*, 179.
VALNÍČEK, B. (1965). The 80-year period of solar activity and winter temperatures in Prague. Bull. Astron. Inst. of Czechoslowakia, *16*, 368.
VISSER, S. W. (1946). De invloed van zonnevlekken op het weer. Inaugurale rede, Rijksuniversiteit Utrecht.
VISSER, S. W. (1950). On Easton's period of 89 years. Proc. Kon. Ned. Acad. v. Wet., Amsterdam, *53*, nr. 2.
VISSER, S. W. (1957). De elfjarige zonnevlekkencyclus. Tds. Kon. Ned. Aardr. Genootschap, *74*, nr. 3.
VISSER, S. W. (1959). A new analysis of some features of the 11-year and 27-day cycles in solar activity and their reflection in geophysical phenomena. Med. & verh. K.N.M.I., 102 - no. 75.
WAGNER, CHR. U. (1966). Die Entstehung der niederen Ionosphäre im Lichte der Aeronomie. Vorträge der Sommerschule Untere Ionosphäre, Kühlingsborn/Heiligendamm, 1964. Nationalkomitee f. Geod. & Geoph. DDR bei der Deutschen Akad. der Wiss. zu Berlin, Reihe II, H.2, 127.
WALDMEIER, M. (1959). Sonne und Erde. Buchergilde Gutenberg, Zürich.
WALDMEIER, M. (1966). Statistics and evolution of sunspots. Astron. Mitt. Eidgen. Sternw. Zürich, nr. 274.
WARWICK, C. S. and WOOD, M. (1961). A study of solar activity associated with PCA. Arch. f. Geoph., *3*, 457.

WEXLER, H. (1950). Possible effects of ozone heating on sea-level pressure. Journ. met., *7*, 370.
WEXLER, H. (1956). Variations in insolation, general circulation and climate. Tellus, *8*, 480.
WHITTEN, R. C. and POPPOFF, I. G. (1965). Physics of the lower ionosphere. Prentice Hall, Inc., Englewood Cliffs, N.Y..
WILLIAMSON, C. F. et al. (1966). Tables of range and stopping power of chemical elements for charged particles of energy 0.05 to 500 MeV. Rapport CEA-R 3042, Centre d'Etudes Nucléaires de Saclay (France).
WILLETT, H. C. (1952). Atmospheric reactions to solar corpuscular emissions. Bull. Amer. Met. Soc., *33*, 255.
WILLETT, H. C. and PROHASKA, J. T. (1964). Reactions of the general circulation to sudden solar disturbance. M.I.T., final report, Contr. no. AF 19(604)-7996.
WILLETT, H. C. (1965). Solar-climatic relationships in the light of standardized climatic data. Journ. atm. sci., *22*, 120.
ZWAAN, C. (1965). Sunspot models, a study of sunspot spectra. Dissertatie, Rijksuniversiteit Utrecht.

Van de reeks MEDEDELINGEN EN VERHANDELINGEN *zijn bij het Staatsdrukkerij- en Uitgeverijbedrijf nog verkrijgbaar de volgende nummers:*

23, 25, 26, 27, 29*b*, 30, 31, 34*b*, 35, 36, 37, 38, 39, 40, 42, 43, 44, 45, 46, 47, 48, 49, 50, 51, 52 53, 54, 55, 56, 57, 58, 59.

alsmede

60. C. Kramer, J. J. Post en J. P. M. Woudenberg. Nauwkeurigheid en betrouwbaarheid van temperatuur- en vochtigheidsbepalingen in buitenlucht met behulp van kwikthermometers. 1954. (60 blz. met 11 fig.) 3,60

62. C. Levert. Regens. Een statistische studie. 1954. (246 blz. met 67 fig. en 143 tab.) 10,30

63. P. Groen. On the behaviour of gravity waves in a turbulent medium, with application to the decay and apparent period increase of swell. 1954. (23 blz.) 1,55

64. H. M. de Jong. Theoretical aspects of aeronavigation and its application in aviation meteorology. 1956. (124 blz. met 80 fig., 9 krt. en 3 tab.) 4,60

65. J. G. J. Scholte. On seismic waves in a spherical earth. 1956. (55 blz. met 24 fig.) 5,15

66. G. Verploegh. The equivalent velocities for the Beaufort estimates of the wind force at sea. 1956. (38 blz. met 17 tab.) 1,80

67. G. Verploegh. Klimatologische gegevens van de Nederlandse lichtschepen over de periode 1910—1940.

Deel I: Stormstatistieken. — Climatological data of the Netherlands light-vessels over the period 1920—1940. P. I.: Statistics of gales. 1956. (68 blz. met tabellen) 3,60

Deel II: Luchtdruk en wind; zeegang. — Climatological data of the Netherlands light-vessels over the period 1910—1940. P. II: Air pressure and wind; state of the sea. 1958. (91 blz. met tabellen.) 7,70

Deel III: Temperaturen en hydrometeoren; onweer. — Climatological data of the Netherlands light-vessels over the period 1910—1940. P. III: temperatures and hydrometeors; thunderstorms. 1959. (146 blz. met tabellen.) 8,25

68. F. H. Schmidt. On the diffusion of stack gases in the atmosphere. 1957. (60 blz., 12 fig. en tab.) 5,15

69. H. P. Berlage. Fluctuations of the general atmospheric circulation of more than one year; their nature and prognostic values. 1957 7,70

70. C. Kramer. Berekening van de gemiddelde grootte van de verdamping voor verschillende delen van Nederland volgens de methode van Penman. 1957. (85 blz., fig. en tab.) 7,20

71. H. C. Bijvoet. A new overlay for the determination of the surface wind over sea from surface weather charts. 1957. (35 blz., fig. en tab.) 2,60

72. J. G. J. Scholte. Rayleigh waves in isotropic and anisotropic elastic media. 1958. (43 blz., fig. en tab.) 3,10

73. M. P. H. Weenink. A theory and method of calculation of wind effects on sea levels in a partly-enclosed sea, with special application to the southern coast of the North Sea. 1958. (111 blz. met 28 fig. en tab.) 8,25

74. H. M. de Jong. Geostrophic flow. Geostrophic approximation in the upper air flow with application to aeronavigation and air trajectories. 1959. (100 blz. met 17 fig., 14 krt. en 2 tab.) 5,15

75. S. W. Visser. A new analysis of some features of the 11-year and 27-day cycles in solar activity and their reflection in geophysical phenomena. 1959. (65 blz. met 16 fig. en 12 tab.) 3,60

76. A. R. Ritsema and J. Veldkamp. Fault plane mechanisms of South East Asian earthquakes. 1960. (63 blz. met 26 fig. en 11 tab.) 4,10

77. G. Verploegh. On the annual variation of climatic elements of the Indian Ocean. P. I.: text. P. II: charts. 1960. (64 blz., 15 fig., 28 krt.) 6,15

78. J. A. As. Instruments and measuring methods in paleomagnetic research. 1960. (56 blz., 20 fig.) 2,55

79. D. J. Bouman. Consistency of approximations in discontinuous fields of motion in the atmosphere with an introduction to the use of generalized functions or distributions in meteorology. 1961. (94 blz., 6 fig.) 6,70

80. H. Timmerman. The influence of topography and orography on the precipitation patterns in the Netherlands. 1963. (49 blz., 37 fig. en 5 tab.) 6,70

81. A. W. Hanssen & W. J. A. Kuipers: On the relationship between the frequency of rain and various meteorological parameters (with reference to the problem of objective forecasting). 1965. (77 blz., 18 fig. en 12 tab.) 10,25

82. G. A. de Weille: Forecasting crop infection by the potato blight fungus. A fundamental approach to the ecology of a parasite — host relationship. 1964. (144 blz., 37 fig. en 37 tab.) 14,90

83. H. J. de Fluiter, P. H. van de Pol, J. P. M. Woudenberg (redactie) e.a. Fenologisch en faunistisch onderzoek over boomgaardinsekten. Phenological and faunistic investigations on orchard insects. 1964. (226 blz., 84 fig. en 59 tab.) 9,50

84. D. J. Bouman & H. M. de Jong: Generalized theory of adjustment of observations with applications in meteorology. 1964. (89 blz., 8 fig. en 1 tab.) 11,30

85. L. Otto: Results of current observations at the Netherlands lightvessels over the period 1910—1939. P. 1. Tidal analysis and the mean residual currents. 1964. (56 blz. en 8 tab.) 6,40

86. F. H. Schmidt: An analysis of dust measurements in three cities in the Netherlands. 1964. (68 blz., 14 fig. en 22 tab.) 5,65

87 Commissie Meteorologische Voorlichting van Straalvliegtuigen: Climatology of Amsterdam Airport (Schiphol). 1966. (145 blz., 6 fign., 10 tab.) 17,00

88. H. P. Berlage: The southern oscillation and world weather. 1966. (152 blz. 46 fig., 34 tab.) 15,95

89. G. Verploegh: Observation and analysis of the surface wind over the ocean. 1967. (67 blz., 14 tab., 4 krt.) 6,70

90. R. Dorrestein: Wind and wave data of Netherlands lightvessels since 1949. 1967. (123 blz., 22 tab.) 15,95

91. P. J. Rijkoort: The increase of mean wind speed with height in the surface friction layer. 1968. (115 blz., fig., tab.) 15,95

825366*-316